uOttawa

L'Université canadienne
Canada's university

FACULTÉ DES ÉTUDES SUPÉRIEURES ET POSTOCTORALES

uOttawa

L'Université canadienne
Canada's university

FACULTY OF GRADUATE AND POSDOCTORAL STUDIES

Mehmet Cevat Catana
AUTEUR DE LA THÈSE / AUTHOR OF THESIS

M.A.Sc. (Civil Engineering)
GRADE / DEGREE

Department of Civil Engineering
FACULTÉ, ÉCOLE, DÉPARTEMENT / FACULTY, SCHOOL, DEPARTMENT

Compaction and Water Retention Characteristics of Champlain Sea Clay

TITRE DE LA THÈSE / TITLE OF THESIS

Dr. V. Garga and S. Vanapalli
DIRECTEUR (DIRECTRICE) DE LA THÈSE / THESIS SUPERVISOR

CO-DIRECTEUR (CO-DIRECTRICE) DE LA THÈSE / THESIS CO-SUPERVISOR

EXAMINATEURS (EXAMINATRICES) DE LA THÈSE / THESIS EXAMINERS

Dr. M. Fall

Dr. P. Simms

Gary W. Slater
Le Doyen de la Faculté des études supérieures et postdoctorales / Dean of the Faculty of Graduate and Postdoctoral Studies

Compaction and Water Retention Characteristics of Champlain Sea Clay

by

M. Cevat Catana

A thesis
submitted under the supervision of
Dr. Sai K. Vanapalli
Dr. Vinod K. Garga

In partial fulfillment of the
requirements for the degree of
Master of Applied Science
in
Civil Engineering

Department of Civil Engineering
University of Ottawa
Ottawa, Canada
K1N 6N5

May 2006

Your file Votre référence
ISBN: 978-0-494-25750-0
Our file Notre référence
ISBN: 978-0-494-25750-0

Abstract

Several engineering structures for geotechnical engineering applications are constructed using compacted fine-grained soils (i.e., dams, road embankments, pavements, canals, and waste containment structures such as soil covers and liners). The compacted fine-grained soils are typically in a state of unsaturated condition and plastic in nature. There is a growing interest in recent years to apply the mechanics of unsaturated soils in the design of geotechnical structures constructed with compacted fine-grained soils. The soil-water retention curve (SWRC) is being used as a key tool in extending the mechanics of unsaturated soils into engineering practice. Conventionally, SWRC is determined in the laboratory without taking account the volume changes with respect to soil suction. The water retention characteristics of plastic soils depend on the pore-size distribution, compressibility characteristics and the volume change behavior. For this reason, the conventional procedures that are used in the measurement of the SWRC may not provide reliable information. Therefore, the engineering behavior of compacted fine-grained soils cannot be reliably estimated or predicted if the volume change behavior with respect to suction is not considered while measuring the water retention curves for compacted fine-grained soils.

In this thesis, a comprehensive experimental program is undertaken to determine the water retention characteristics of a local plastic soil, Champlain sea clay. This soil is commonly used in the construction of several structures in Ottawa and Quebec region. The SWRCs of Champlain sea clay were measured on specimens that were statically or dynamically compacted at different water contents and densities using different compaction energies. The suction measurements of the individually compacted specimens were determined using axis-translation technique and thermocouple psychrometers. The volume changes of the specimens were measured at each value of suction while determining the SWRC. In light of the experimental results, the parameters that influence the SWRC behavior such as compaction type (i.e., static or dynamic) and effort, initial compaction water content and void ratio on the water retention behavior of compacted fine-grained soils were investigated. In addition, a database of 16 compacted plastic soils with measured SWRCs and their conventional properties from the published literature was summarized.

Relationships between the parameters of the SWRC, namely, the rate of desorption and the conventional soil properties were studied using the results of the present experimental program and the information from the database. This study shows that liquid limit coupled with clay fraction can be a useful tool to correlate with the rate of desorption for compacted soils. Based on this information, a new technique is proposed for the estimation of the entire SWRC of compacted fine-grained soils following the drying path. The required information for using this technique includes one point measurement of suction versus water content in the suction range of 0-500 kPa, along with data on the liquid limit and the clay fraction. The proposed technique provides good comparison between the measured and estimated SWRCs for the data studied in this research program. This technique can be used in the preliminary design stages of a project when detailed information about the soil is no available.

In addition a state-of-art literature review on the devices presently available for the measurement of soil suction is summarized.

Acknowledgements

The author would like to express his most sincere appreciation to his supervisors, Dr. Sai K. Vanapalli and Dr. Vinod K. Garga, for their encouragement and continuous support throughout the research program. The author also wishes to thank his friends and fellow graduate students Jules A. I. Sedano, Kenton Power and Elizabeth Garven.

The author also would like to acknowledge the financial support received from the University of Ottawa and the Natural Sciences and Engineering Research Council of Canada (NSERC).

Page v missing.

Contents

List of Tables

List of Figures

Chapter 1

Introduction

1.1 Statement of the Problem

Significant advances were made to our present understanding of the engineering behavior of unsaturated soils with respect to the development of theoretical frameworks, experimental methods and numerical techniques since the extension of Terzaghi's effective stress principle for unsaturated soils by Bishop in 1959. (Jennings, 1961; Lambe & Whitman; 1979, Allam & Sridharan 1987; Alonso *et al.*, 1990; Fredlund & Rahardjo, 1993; Lu & Likos, 2004). However, implementation of these advancements into engineering practice is rather slow. The key reason for this slow advancement is associated with the excessive costs of the direct measurements of unsaturated soil properties both in laboratory and in the field. In spite of several recent developments in devices for the measurement of matric suction, there is still a need to develop reliable and inexpensive equipment that can be used to measure soil suction in the field.

Fredlund & Morgenstern (1977) presented an approach for explaining the unsaturated soil behavior in terms of two stress state variables, namely; net normal stress, $(\sigma - u_a)$ and matric suction, $(u_a - u_w)$. This approach provided was considered to be a rational interpretation technique for the engineering behavior of unsaturated soils (Wheeler & Sivakumar, 1995; Gallipoli *et al.* , 2003). Alonso *et al.* (1987) were among the first researchers to propose an integrated framework based on the theory of elasto-plasticity to interpret the unsaturated soils behavior in a qualitative way. A constitutive model that unifies the principles of a critical state type of framework to couple strength and volumetric response in unsaturated soils was presented by Alonso *et al.* (1990). Subsequent research works supported the main features of this framework

(Wheeler & Karube, 1995; Maatouk *et al.* , 1995; Cui & Delage, 1996). More recently, Wheeler *et al.* (2003) have proposed coupling of mechanical behaviour and hydraulic hysteresis. The recent research focus has been shifted to the coupled hydro-mechanical behavior of unsaturated soils, and critical state soil mechanics (Tarantino & Tombolato, 2005; Infante Sedano *et al.*, 2006).

During the last two decades, researchers focused on the development of indirect estimation or prediction methods to obtain the engineering behavior of unsaturated soils to alleviate some expensive and time consuming testing (Meerdink *et al.* , 1996; **?**; Benson & Gribb, 1997; Barbour, 1998; Fredlund, 2004). The relationship between the amount of soil water (which can be expressed in terms of degree of saturation or volumetric or gravimetric water content) and soil suction played a central role in the development of these methods. This relationship has been referred to in the literature using several terms; the widely used terms in geotechnical and geo-environmental engineering fields are the soil-water characteristic curve (SWCC), the soil-water retention curve (SWRC) and soil moisture curve (SMC). The term SWRC was used through remainder of this thesis.

Several investigators have proposed techniques to predict or estimate the key parameters of SWRC for coarse-grained soils and as well as fine-grained soils using easy to obtain parameters from conventional laboratory tests such as the grain size distribution curve, void ratio, and Atterberg limits (Jucá, 1993; Tinjum *et al.* , 1997; Fredlund *et al.* , 1997; Aubertin *et al.* , 2003; Vanapalli & Catana, 2005). The estimation techniques are attractive to the practicing engineers as they reduce the costs and time associated with the direct measurement of the SWRC. However, there are limited comparisons between the estimated SWRC and the field SWRC (Meerdink *et al.* , 1996). In addition, studies exploring the influence of volume change on the SWRC is also limited for unsaturated compacted fine-grained soils. Limited studies have shown that the engineering behavior is significantly different when volume change is substantial (Dineen, 1999). These observations are more applicable to fine-grained compacted soils which are abundantly used in engineering practice. The practical applications associated with unsaturated compacted fine-grained soils covers a broad spectrum ranging from embankments used for roads and culverts, to barriers used for nuclear waste disposals (Delage & Lefebvre, 1983; Meerdink *et al.* , 1996; Blatz & Graham, 2000).

Several parameters such as soil structure, stress state, mineralogy, specific surface, chemical composition, initial compaction water content, void ratio or porosity, surface activity, soil chemistry, interstitial water and pore-size distribution influence the engineering properties of compacted, fine-grained unsaturated soils (Cui & Delage, 1996; Vanapalli *et al.* , 1999; Vanapalli *et al.* , 2001; Aubertin *et al.* , 2003). In addition, the size of the soil specimen, the method used for specimen saturation, the type of compaction procedure and the method used for compacting the specimen, can influence the soil structure regardless of the initial homogeneity of the specimen or the applied stress (Fleureau *et al.* , 2002; Vanapalli *et al.* , 2004).

In this thesis, an experimental study was carried out to investigate the water retention characteristics of compacted Champlain sea clay. This type of clay is abundantly found and used in several geotechnical studies in Ottawa and many parts of Quebec region (Quigley, 1980; Torrance, 1999). The focus of this research was to study the influence of initial water content, compaction type and energy, and volume change on the water retention characteristics of compacted Champlain sea clay. A total of 34 statically compacted and 3 dynamically compacted specimens were prepared, using normal stresses of 1000, 2000 and 4000 kPa and water contents ranging from 15% to 29% (ranging from dry of optimum water content to wet of optimum water content). The compaction stress of 1000 kPa provides similar results as compared to the standard Proctor test in terms of dry unit weight and initial compaction water content. As a result, it was possible to understand whether it was the compaction induced conditions or fundamentally different soil structure that causes differences associated with the engineering behavior. The volume change properties were also determined. In addition, a technique has been proposed to predict the SWRC of compacted fine-grained soils by using easy to obtain parameters; compaction curve, Atterberg limits, shrinkage limit, volume-mass properties along with one point measurement of suction versus water content. This technique was tested using several published data which includes 18 measured SWRC and related parameters of compacted fine-grained soils.

1.2 Research Objectives

The objectives of this research were:

1. To determine the SWRCs of statically and dynamically compacted Champlain sea clay specimens.

2. To investigate the influence of different compaction types (static and dynamic) and effort on the post-compaction suction of compacted Champlain sea clay specimens.

3. To investigate the influence of initial compaction water content on the water retention characteristics of compacted Champlain sea clay specimens.

4. To determine the volume change (i.e., shrinkage) of the compacted specimens during drying and compare the water content *vs.* suction relationship with the degree of saturation *vs.* suction relationship.

5. To propose a technique for estimating the drying portion of soil-water retention curves of compacted fine-grained soils using the information on compaction curve, volume mass properties and Atterberg limits along with one point measurement (i.e., water content versus suction).

6. To compare suction measurements in the suction range 0-500 kPa using the axis-translation technique and psychrometer.

1.3 Scope of Research

The experimental studies to address the research objectives listed in the earlier section were undertaken at the Geotechnical Laboratory of the University of Ottawa. The suction measurements of individually compacted specimens were determined using both axis-translation technique and thermocouple psychrometers. In addition, data on the SWRCs of compacted fine-grained soils along with their conventional soil properties from published literature has been summarized. This database was used to estimate the relationship between the key parameters of the SWRC (i.e., air-entry value (AEV), rate of desorption, residual water content) and conventional soil properties. Finally, a technique is proposed to estimate the SWRC of compacted fine-grained soils with only one point measurement (i.e., suction versus water content). There is a good comparison between the measured and the estimated SWRCs of compacted fine-grained soils studied in this research program.

The outcome of this research program is expected to reduce laboratory testing and result in savings of resources and time. The approach presented through this research should encourage the practicing geotechnical engineers to extend the unsaturated soil mechanics into practice.

1.4 Thesis Organization

The second chapter, "Literature Review", is a brief summary on topics related to the research objectives. The key topics summarized were related to the direct and indirect techniques of measuring suction and the soil-water retention curves and their applications in unsaturated soil mechanics. The parameters that influence the engineering behavior of compacted fine-grained soils is also detailed.

The third chapter, "Equipment Details", provides related information of the equipments used in the experimental study, presented in this thesis, along with the modification introduced to some of the equipments. The calibration, precision and the discussion on the design principles of the equipments are also briefly discussed.

The fourth chapter, "Experimental Results and Discussions", provides the details of the undertaken experimental program and laboratory procedures. The soil properties used in the study along with the sample preparation are reported. In addition, the problems encountered during the experimental program are also discussed along with the discussion on the test results.

The fifth chapter, "A Technique for Estimating the SWRC", provides the relationships between the parameters obtained from conventional laboratory tests and the parameters of SWRC. A step-by-step procedure is summarized for estimating the SWRC of compacted fine-grained soils.

The sixth chapter provides the summary and conclusions of the research program. Recommendations useful for further research work are also summarized.

Chapter 2

Literature Review

2.1 Introduction

This chapter starts with a brief review of extending the effective stress principle conventionally used for saturated soils to the interpretation of unsaturated soils. The text goes on to describe the role of suction in unsaturated soil mechanics and present a review of the direct and indirect suction measurement techniques. Finally, the use of soil-water retention curve to estimate the engineering properties of unsaturated soils and a summary of some important aspects associated with the compacted soils are presented.

The literature review focus is towards providing background information that is necessary for interpreting of soil-water retention curve behavior with volume change data for compacted plastic soils.

2.2 Background for Saturated & Unsaturated Soil Mechanics From Continuum Mechanics

In 1936, Terzaghi explained the effective stress principle valid for saturated soils as (Fig. 2.2):

> *"All the measurable effects of a change of stress, such as compression, distortion and a change in the shearing resistance are exclusively due to changes in effective stress. Every investigation of the stability of a saturated body of earth requires the knowledge of both the total and the neutral stresses"*

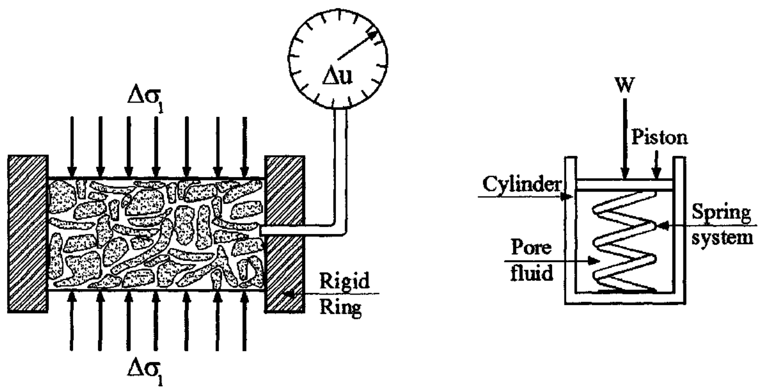

Figure 2.1: Terzaghi's effective stress analogy

A similar observation has also been made in "Theoretical Essay on the Equilibrium of Elasticity of Pulverulent Masses and on the Pressure of Earths without Cohesion" (Boussinesq, 1876):

> "*One can ignore the atmospheric pressure, for this acts in all directions within the sand and all around each grain... It therefore has no influence on their mutual action and consequently will not modify the supplementary pressure that acts at the contact between the grains... Only this supplementary pressure has to be considered.*"

The stress state of a saturated soil can be expressed in a matrix form using the effective stress principle as given below:

$$|\sigma'| = \begin{vmatrix} (\sigma_x - u_w) & \tau_{yx} & \tau_{zx} \\ \tau_{xy} & (\sigma_y - u_w) & \tau_{zy} \\ \tau_{xz} & \tau_{yz} & (\sigma_z - u_w) \end{vmatrix} \qquad (2.1)$$

where:

σ' : effective normal stress

$\sigma_x, \sigma_y, \sigma_z$: total normal stresses in x,y, and z directions, respectively

Terzaghi's effective stress equation not only satisfies the conceptual framwork of continuum mechanics but also has proven to be useful to interpret the engineering behavior of saturated soils. Several instruments are available to determine the pore water pressure reliably both in the laboratory and in the field when the soil is in a saturated conditions.

However, if the soil is not fully saturated, a part of the voids are filled with water and remainder space is occupied with air, hence a different approach is required for explaining the unsaturated soil behavior (Fig. 2.2).

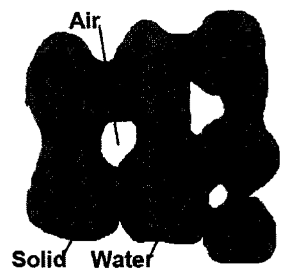

Figure 2.2: The unsaturated soil media

The success in implementing the Terzaghi's effective stress principle for saturated soils into the conventional engineering practice has prompted numerous investigators to extend the same effective stress principle to unsaturated soils. Table 5.1 summarizes some of the important equations suggested for interpretation of unsaturated soil behavior in terms of single stress state variable.

Of all these equations, the original equation, proposed by Bishop (1959) is still popular and more commonly used. In their research, Bishop & Donald (1961) conducted triaxial tests on silt specimens prepared from saturated slurries and desaturated with varying combinations of $(\sigma_3 - u_a)$ and $(u_a - u_w)$. The minor principal stress, σ_3, u_a and u_w were varied to keep $(\sigma_3 - u_a)$ and $(u_a - u_w)$ constant. The monotonic shape of stress strain curve did not change under these combinations, giving credibility to the equation proposed by Bishop (1959).

Subsequent studies (Jennings, 1961; Blight, 1967; Abramento & Carvalho, 1989) proved that single stress-state equations given given by Bishop (1959) did not provide reliable results for the interpretation of the mechanical behavior of unsaturated soils (shear strength and volume change properties) (Fig. 2.3). Jennings (1961) pointed out that it is necessary to prove that the soil behavior is unaffected by changes in $(\sigma - u_a)$ and $\chi(u_a - u_w)$ such that their sum remains constant for total validity of Bishop's equation (1959). He also demonstrated that the shortcomings in the method proposed by Bishop for determining the χ, which resulted in values less than zero. In addition, Blight's (1967) theoretical analysis has shown that χ values can be greater than unity at low suction values. Abramento & Carvalho (1989) have also reported experimental values

Table 2.1: Proposed effective stress equations for unsaturated soils

Equation	Author	Parameters
$\sigma' = \sigma + p''$	(Donald, 1956)	p'':pressure deficiency of the pore water
$\sigma' = \sigma - (u_a + u_c)$	(Hilf, 1956)	u_c:capillary pressure
$\sigma' = \sigma - \beta' u_w$	(Croney *et al.* , 1958)	β':bonding factor which is a measure of the number of bonds ender tension, effective in contributing to the shear strength σ: Total normal stress
$\sigma' = (\sigma - u_a) - \chi(u_a - u_w)$	(Bishop, 1959)	χ:parameter related to the degree of soil saturation
$\sigma' = \sigma - \psi p''$	(Aitchison, 1961)	ψ:parameter with the values ranging from zero to one p":pore-water pressure deficiency
$\sigma' = \sigma - \beta p''$	(Jennings, 1961)	β:a statistical factor of the same type as the contact area p":negative pore-water pressure
$\sigma' = \sigma_i - (u_a - u_w) + \chi(\sigma - u_a)$	(Newland, 1965)	σ_i:intrinsic stress arising from interparticle forces χ:a parameter related to the degree of soil saturation
$\sigma' = \sigma + \chi_m p''_m + \chi_s p''_s$	(Aitchison, 1973)	p''_m:matric suction p''_s:solute suction
$\sigma' = (\sigma - u_a) + a_w(u_a - u_w)$	(Lambe & Whitman, 1979)	a_w:ratio of area of water-mineral and water-water contact of total area of "wavy" plane
$\sigma' = (\sigma - u_a) + \chi(u_a - u_w)$ $-R - \zeta T_s$	(Allam & Sridharan, 1987)	χ:a parameter representing the proportion of the total void area occupied by the water on a reference plane R:osmotic suction ζ:interface parameter on the reference plane
$\sigma' = (\sigma - u_a) + \left[\frac{(u_a-u_w)_f}{(u_a-u_w)_b}\right]^{-0.55}(u_a - u_w)$	(Khalili & Khabbaz, 1998)	$(u_a - u_w)_f$:matric suction in the specimen at failure condition $(u_a - u_w)_b$:air entry value

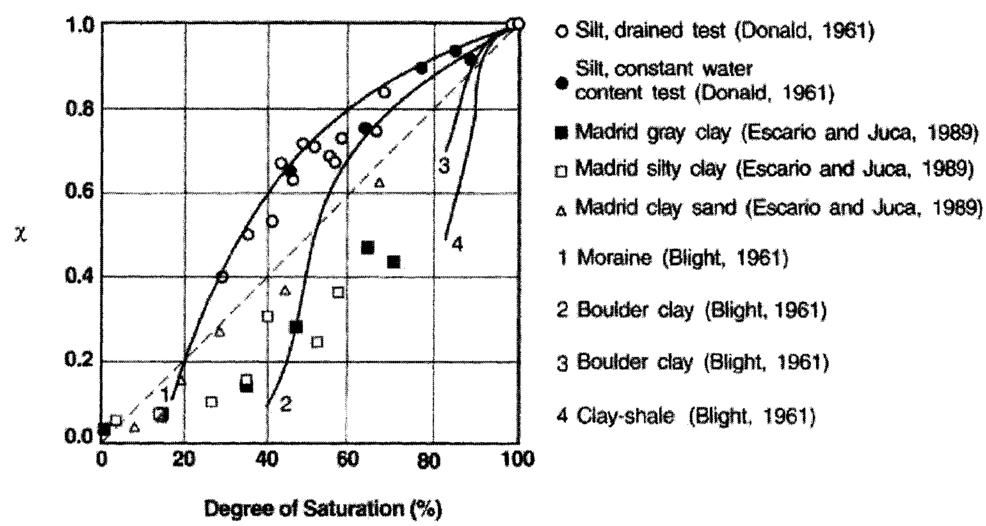

Figure 2.3: Experimental results showing the dependency of Bishop's effective stress parameter χ on degree of saturation

of χ greater than unity making the proposed equation incompatible with the proposed theoretical behavior.

In 1977, Fredlund and Morgenstern proposed a framework for unsaturated soils showing that any of the following two stress state variables can be used to define the stress state of an unsaturated soil: net normal stress,(σ_n - u_a) and matric suction, (u_a-u_w), (σ_n - u_w) and (u_a-u_w), (σ_n - u_a) and (σ-u_w).

The stress state variables more often used in the formulation of interpreting unsaturated soils behavior extending continuum mechanics principles can be shown in matrix form as follows (Fredlund 1997b):

$$\begin{vmatrix} (\sigma_x - u_a) & \tau_{yx} & \tau_{zx} \\ \tau_{xy} & (\sigma_y - u_a) & \tau_{zy} \\ \tau_{xz} & \tau_{yz} & (\sigma_z - u_a) \end{vmatrix} \tag{2.2}$$

$$\begin{vmatrix} (u_a - u_w) & 0 & 0 \\ 0 & (u_a - u_w) & 0 \\ 0 & 0 & (u_a - u_w) \end{vmatrix} \tag{2.3}$$

Fredlund et al. (1978), suggested that the above combination; net normal stress,(σ_n - u_a) and matric suction, (u_a-u_w), was more appropriate because only one stress state variable is affected when the pore water pressure changes.

The role of soil suction and its influence on engineering properties of unsaturated soils is well recognized. Several models that incorporate its effect on the soil properties, have been developed and new models are still being proposed (Brady, 1988; Rahardjo *et al.* , 1995; Blatz & Graham, 2000).

2.3 Soil Suction

The first group to recognize the importance of suction in civil engineering application was Croney *et al.* (1954) at the Road Research Laboratory in London. They used the terminology from soil science and observed the effect of soil moisture deficiency on soil behavior (Krahn & Fredlund, 1972). Soil suction is essentially a stress state which can also be defined as the energy per unit volume. The thermodynamic potential of soil pore water may aid to fully understand the energy state of soil pore water:

$$\psi = \psi_c + \psi_o + \psi_g + \psi_z \tag{2.4}$$

where;
ψ : total potential
ψ_c : matric (capillary) potential
ψ_o : osmotic potential
ψ_g : air pressure potential
ψ_z : gravimetric potential

Neglecting the gravimetric and air pressure potentials, total soil suction quantifies the thermodynamic potential of soil pore water relative to a reference potential of free water, which is equal to the sum of matric and osmotic suction:

$$-\psi = (u_a - u_w) + \pi = s + \pi \tag{2.5}$$

where;
$s = -\psi_c = (u_a - u_w)$: matric suction
$\pi = -\psi_o$: osmotic suction

Free water in this regard is defined as water containing no dissolved solutes, having no interactions with other phases that impact curvature to the air-water interface, and having no external forces other than gravity. The physical and physicochemical mechanisms responsible for total suction are those that decrease the potential of the pore water relative to this reference state (Buckingham, 1907).

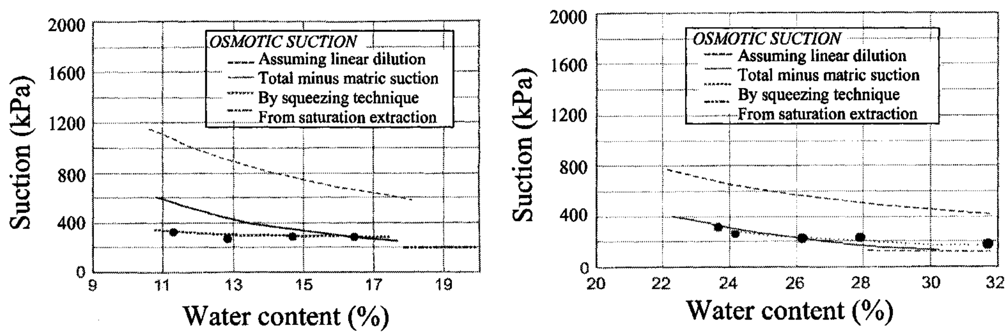

(a) Glacial till (b) Regina clay

Figure 2.4: Comparison of suction components (Krahn & Fredlund, 1972)

Krahn & Fredlund (1972) measured total, matric and osmotic suction, independently, on a low plasticity glacial till and high plasticity clay and verified the assertion that total suction is equal to the sum of the matric and osmotic suction (Fig. 2.4). They used psychrometer to measure total suction. A modified consolidometer operating on the same principle as the pressure plate was used to measure matric suction. The osmotic suction was measured using a high pressure hydraulic squeezer.

2.3.1 Physical Representation of Capillary Suction

The air-water interface that forms in between the adjacent soil particles of an unsaturated soil is similar to the water rise in a capillary tube due to the surface tension phenomena, as shown in Fig. 2.5.

The curved shape of the air-water interface is the result of the upward force, which exists at the boundary due to the wetting of the surface. The upward force that holds the column of water in a capillary tube can be mathematically expressed as a relationship shown below:

$$\mathbf{u_a \pi r^2} = u_w \pi r^2 + 2\pi r T_s cos\alpha \tag{2.6}$$

where; T_s: surface tension at the boundary
u_a, u_w: air and water pressure, respectively

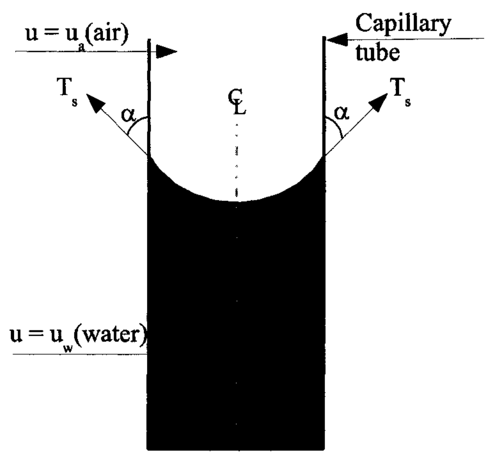

Figure 2.5: Capillary rise phenomena

r: the radius of the capillary tube
α: angle of contact between water and the boundary surface

For perfectly spherical meniscus the angle of contact will be 90^0 and the above equation will reduce to:

$$(\mathbf{u_a} - \mathbf{u_w}) = \frac{2T_s}{r} \tag{2.7}$$

The spherical interface model developed for capillary tubes provides a conceptual model to describe the pressure change across an air-water interface and a physical explanation for an important component of suction in unsaturated soil. In a real soil, however, a spherical interface does not occur as the soil particles with various shapes and sizes contribute to a complex pore fabric. Therefore, assumptions and limitations must be spelled out about the complex pore geometry in order to extend the simple capillary tube model in analyses of unsaturated soil behavior (Lu & Likos, 2004). However, discussion on these models are out of the scope of the present study.

2.3.2 Measurement Units

The units of suction are same as pressure. The commonly used units for suction measurement are: (pF, cm (H_20), psi, $kPa/$ MPa, Bar, atm)

'*atm*' (meaning Atmosphere) has been adopted to replace the term '*Bar*'. The 'Atmosphere' is a barometric term and as such is dependent on altitude. The unit pF can be defined as "the common logarithm of the height in centimeters of the water column needed to provide the suction "(Schofield, 1935).

$1\ cB = 1\ kPa$ and $1\ pF = log_{10}$h.

where; h is the height of the water column in cm.

$1\ Bar = 1\ atm = 100\ kPa = 3\ pF$

2.4 Soil Suction Measurement Techniques

The soil suction is determined using; (i) Direct methods or (ii) Indirect methods. In direct methods the pore water energy which is the relevant quantity under scrutiny is directly measured. Whereas in indirect methods, another parameter such as; relative humidity, resistivity, conductivity and moisture content is measured and related to the suction through a calibration with a known values of suction (Ridley & Wray, 1995).

2.4.1 Direct Measurement Techniques

Direct methods include tensiometers, pressure plates, pressure membranes and suction plates. These methods directly measure the pore pressure in the soil or impose a known pressure to the soil and allow the pore pressure to come to equilibrium with the applied pressure.

- **Tensiometers**: Tensiometers are devices that directly measure the negative pore-water pressure (Fig. 2.6). They are more commonly used in the field, although recently some researchers have started using them on instananeous profile type laboratory experiments, oedometer cells and direct shear tests (Tadepalli & Fredlund 1991; Plagge *et al.*, 1992; Caruso & Tarantino, 2004; Tarantino & Tombolato, 2005). Tensiometers consist of a porous ceramic and a high air-entry cup connected to a device that measures the pressure using a mercury manometer, a vacuum gauge, or an electronic pressure transducer. The column of tensiometer is filled with de-aired water. The water in the tensiometer communicates with the soil fluid through the ceramic cup, tends to bring the cup water into hydraulic equilibrium with the soil water (Richards, 1965). Standard tensiometers have a limitation for the range they can measure suction. This limitation is attributed to the phenomenon called cavitation, and it is about 100 kPa. Galileo Galilei was believed to be the one who first observed that water cannot rise indefinitely. He

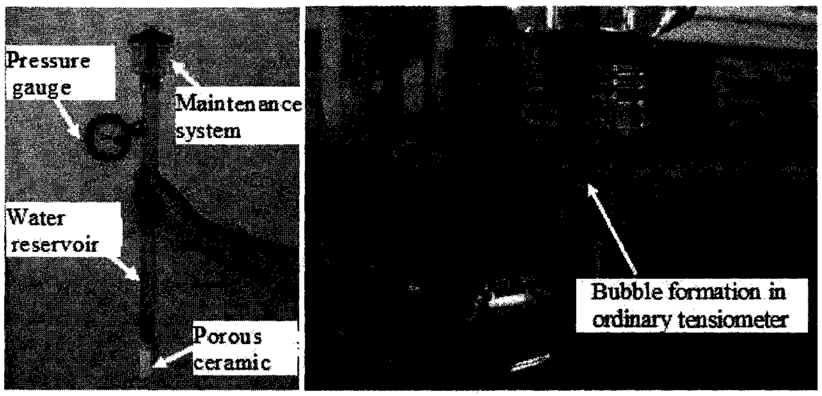

Figure 2.6: A conventional tensiometer

found out that 10 m was the limit to which the water could rise in a suction pump (http://www.experus2005.ing.unitn.it/1MarinhoTakeTarantino.pdf).

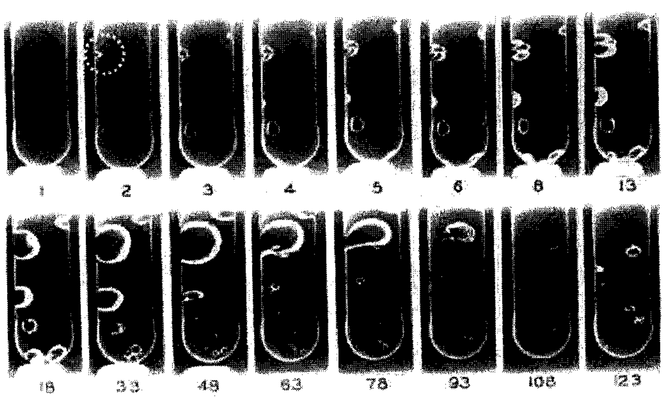

Figure 2.7: Air bubbles in a glass tube (Harvey *et al.* , 1944)

An experimental verification for the formation of cavitation is provided by Harvey *et al.* (1944) using glass tubes in which he applied increasing suction values in stages and monitor the formation of air bubbles (Fig. 2.7). Marinho & Chandler (1995) provided the stages of the bubble formation during cavitation (Fig. 2.8). In the first stage the meniscus sustains the positive water pressure and hinder air-cavity dissolution. As the water pressure reaches negative values, the cavity expands and air pressure drops. In addition, air diffuses towards the cavity to restore atmospheric air pressure and cavity further expands. Eventually, the air cavity detaches from the surface and triggers cavitation.

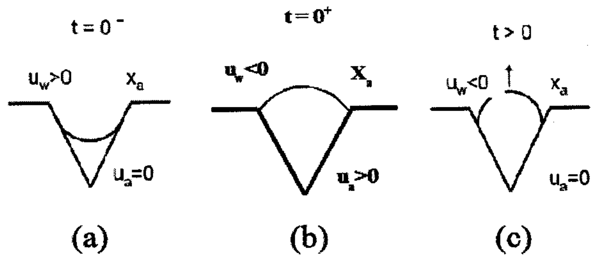

Figure 2.8: Cavitation phenomenon (Marinho & Chandler, 1995)

Some attempts have been made to overcome cavitation and extend the range of the tensiometer. Peck and Rabbidge (1969) used a smaller tensiometer, replaced the water with polyethylene glycol (PEG), and placed a membrane, which is permeable to water but impermeable to large PEG molecules. This type of tensiometers were referred to as osmotic tensiometer. In osmotic tensiometers, a positive pressure is developed into the reservoir, placing the device in a bath of pure water at atmospheric pressure. However, subsequent studies conducted by Dineen & Burland (1995) suggested that a small percentage of the PEG molecules could pass through the membrane decreasing the concentration of the solution and lowering the suction, hence undermining the accuracy of the instrument.

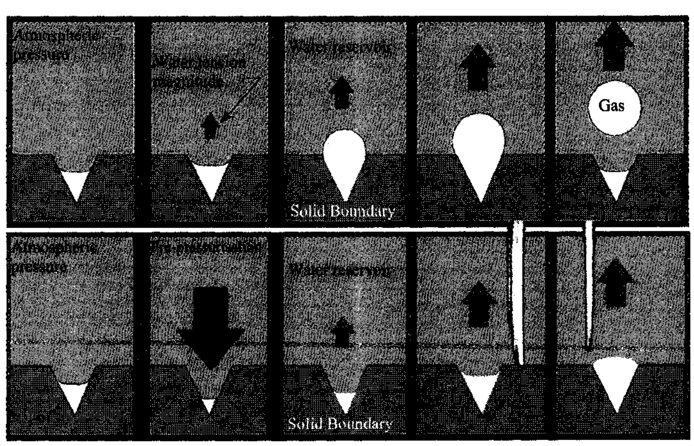

Figure 2.9: The effect of pre-pressurization (Ridley & Wray, 1995)

In another attempt, Ridley & Burland (1995), Tarantino & Mongiovi (2003) pre-

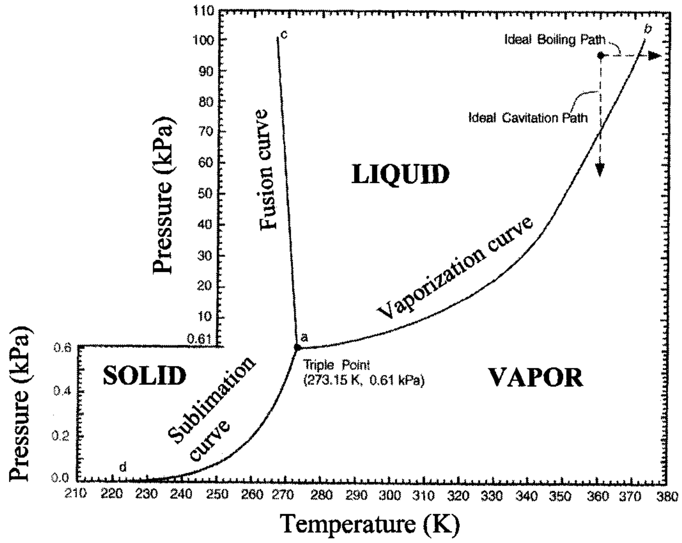

Figure 2.10: Thermodynamic phase diagram of pure water (Lu & Likos, 2004)

pressurized the water in the reservoir, inhibiting the formation of air within the tensiometer (Figure 2.9). They alleged that little crevices that exist in the tensiometers provide a trap for tiny amounts of air that are released when the tensiometer is placed in a state of tension, forming bubbles in the reservoir. In other words, the pore water pressure can actually drop beyond 100 kPa, which is defined as metastability (Fig. 2.10) (Marinho & Chandler, 1995). These type of tensiometers are called high capacity tensiometers (HCT) (Fig. 2.11).

This innovation has provided new research possibilities for the experimental investigations of the engineering behaviour of unsaturated soils. However, the widespread exploitation of this technology has been limited by the lack of a commercially available tensiometer capable of measuring high suctions, and by the complex and highly experience-driven nature of the filter saturation process (Take & Bolton, 2003). Problems arise from the high air-entry interface, which prevents air from entering the instrument and enables water to sustain high tensile stresses. If not adequately saturated, the porous ceramic may lead to inaccurate results that might be difficult to detect (Tarantino & Mongiovi, 2003). Nevertheless, the technology of the high capacity tensiometer (HCT) is maturing and becoming more widely used (Take & Bolton, 2003).

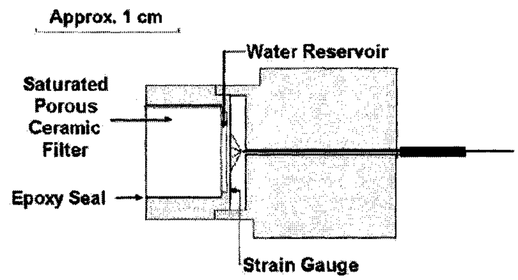

Figure 2.11: High capacity tensiometers (Ridley & Wray, 1995)

- **Pressure Plate**: Hilf (1956) was the first one who provided a setup to measure matric suction with axis-translation measurement technique as shown in Fig. 2.12. This technique is used to measure suctions higher than 100 kPa. In this technique, the soil specimen is placed on a previously saturated porous plate and sealed in a the pressure chamber. Under the influence of the applied pressure, the "atmospheric pressure" of a specimen is raised until a condition of equilibrium is reached between the soil specimen and the applied air pressure (Fig. 2.13). At equilibrium, the matric suction of the soil equals the applied pressure (Lee & Wray, 1995). The

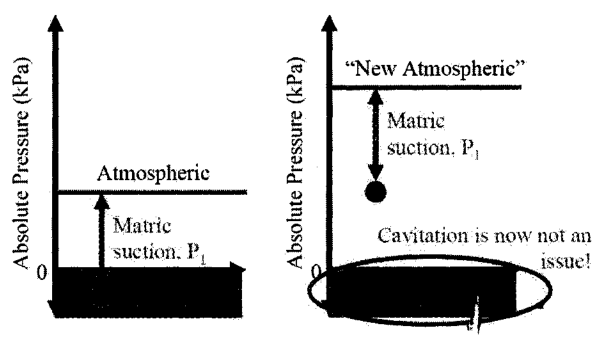

Figure 2.12: A schematic explanation for axis-translation technique

soil suction measurement range of the pressure plate is limited to the air-entry value of the plate. Typically, the highest limit used is 700 kPa (i.e., 100 psi) in conventional laboratories and 1500 kPa (i.e., 200 psi) in strong rooms with special safety provisions.

A pressure differential is measured across a high air-entry ceramic disc using tensiometers and pressure plate apparatus. In addition, expansion of air cavities in

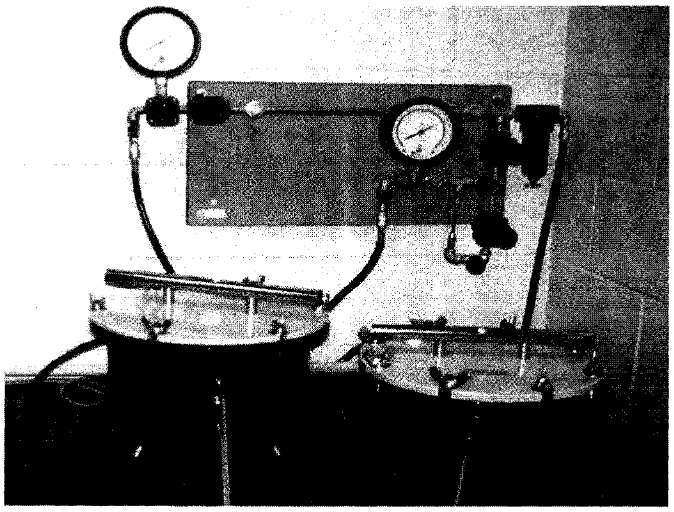

Figure 2.13: Null pressure plate apparatus

the ceramic disc may take place in both cases, if the ceramic disc is not fully saturated. The water pressure in the water reservoir may also differ from the pore water pressure if the ceramic disc is not fully saturated.

On the contrary, there are two main differences between the tensiometers and pressure plate apparatus. In the case of high capacity tensiometers, the water in the reservoir of tensiometer is in metastable conditions. Whereas in pressure plate apparatus, the water is either in atmoshperic pressure or under the cavitation pressure. However, it is not beyond the vaporization point in the phase diagram, in other words, metastable conditions. Due to the air diffusion, relatively large cavities in the ceramic disc may slowly expand in axis translation technique. However, there is no rapid expansion of cavitation nuclei as in the case of tensiometers.

The validity of axis-translation technique was verified by several researchers in different soil specimens compacted to different degrees of saturation values (Bishop, 1959; Olson & Langfelder, 1965; Vanapalli *et al.* , 1999; Tarantino *et al.* , 2000; Power, 2005). In the light of these experimental results, it was shown that at high degree of saturation (i.e., $S_r > 0.85$-0.9), the increase in air pressure causes an increase in the boundary of compacted meniscus curvature and, hence, the difference $(u_a - u_w)$. Therefore matric suction measured using axis-translation might overestimate suction at high degrees of saturation (Fig. 2.14).

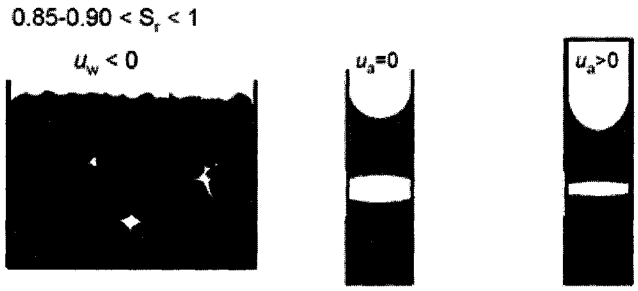

Figure 2.14: Conceptual limitation of the axis translation technique

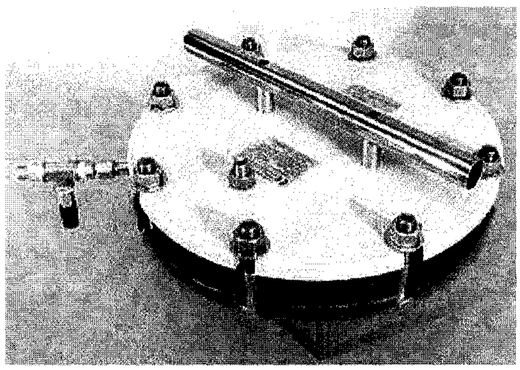

Figure 2.15: Pressure membrane extractor (Soilmoisture, 1999)

- **Pressure membrane**: Pressure membrane apparatus works on the same principle as the pressure plate, except that this apparatus is equipped with a rubber diaphragm that can be inflated to hold the specimen to the membrane as the soil dries (Richards, 1965) (Fig. 2.15).

  Most cohesive soils shrink when they dry. Shrinkage can cause the soil to pull away from the plate, increasing contact resistance and delaying or stopping outflow. The effect of soil shrinkage is to increase equilibrium time, with the net effect of having samples appear wetter than if they were properly equilibrated. Townsend *et al.* (2001) suggested to apply an overburden load but gave no guidance as to what weight should be applied to the specimens to replicate the overburden load and to keep the specimen in intimate contact with the plate. A flexible device such as pressure membranes can maintain plate contact during drying. Nevertheless, its range is limited by the air-entry value of the membrane.

- **Suction plate**: Suction plate consists of a saturated porous ceramic filter disc that separates the soil specimen from a reservoir of water and a mercury manometer. When suction is applied, the soil specimen will imbibe water from the porous disc, causing a drop in the water pressure in the reservoir, which is typically measured using a manometer. When the pore water pressure and the tension in the water of the reservoir are in equilibrium, the flow of water will stop. The range in suction plate is limited to 500 kPa. These plates are not conventionally equipped with flexible membranes, for this reason the plate contact due to shrinkage can be a problem in such apparatus. To deal with this problem, Klute (1986) recommended that a nominal load (i.e., 700 g) be placed on top of each specimen. In contrast, Topp *et al.* (1993) recommended that soil specimens be embedded in a thin layer of kaolinite clay to ensure that contact be maintained during drying. It is not clear which, if either, of these methods is more useful in reducing the impact of soil shrinkage. To the best of the knowledge of the author and his supervisors, there have been no independent comparative studies reported on the matric suction values measured on specimens using both of these methods.

2.4.2 Indirect Measurement Techniques

Indirect methods include primary, secondary and tertiary methods. Thermocouple psychrometers, transistor psychrometers and chilled mirror pyschrometers fall in the primary group of methods whereas filter paper is an example of secondary method. In tertiary methods, thermal conductivity sensors and heat dissipation sensors are used. The primary methods are used for measuring the total suction whereas the secondary method can be used for either total suction or matric suction measurement. The tertiary methods are only utilized in the measurement of matric suction. These methods use measurements or indicators of water content or a physical property that is sensitive to a change in water content (e.g., relative humidity, electrical resistance and rate of heat dissipation).

Thermocouple Psychrometers

Thermocouple psychrometers operate based on the temperature difference between a nonevaporating surface or reference junction, and an evaporating surface or measurement junction (Spanner, 1951). Figure 2.16 shows a schematic diagram of a Peltier-type thermocouple psychrometer commonly used for measuring relative humidity in unsaturated soil testing applications. The working component of the psychrometer is an electrical circuit formed by thin wires of dissimilar metal housed within a shield of porous ceramic or stainless steel mesh.

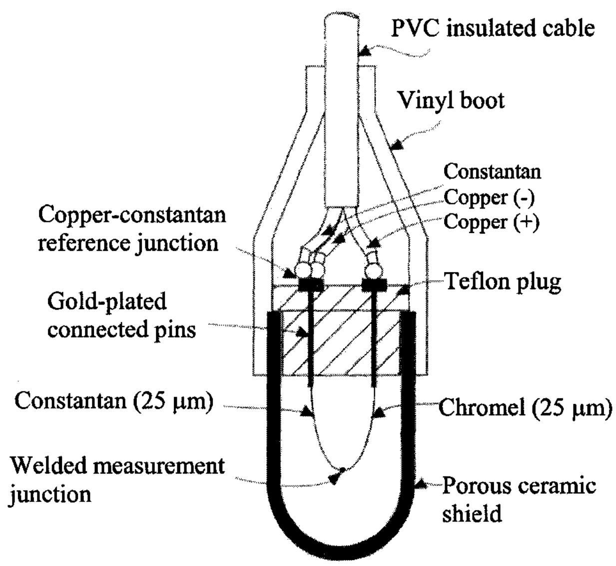

Figure 2.16: A typical thermocouple psychrometer (Wescor, 1998)

The water potential of a porous material is directly related to the vapour pressure of the air surrounding the porous medium (Campbell & Gardner, 1971). This means that the soil water potential can be determined by measuring the relative humidity, RH, of a chamber inside a porous cup equilibrated with the soil solution. From a thermodynamic standpoint, the relationship between pore-water potential and its vapor pressure is expressed by Kelvin's equation in terms of total suction as:

$$\psi_t = -\frac{RT}{v_{w0}\omega_v} In\left(\frac{u_v}{u_{v0}}\right) \tag{2.8}$$

where ψ_t is the total suction (kPa), R is the universal gas constant (8.314 $J/molK$), T is the absolute temperature (K), v_{w0} is the specific volume of water (m^3/kg), ω_v is the molecular mass of water vapor (18.016 $kg/kmol$), u_v is the partial pressure of the pore water vapor (kPa), and u_{v0} is the saturated vapor pressure of free water at the same temperature (kPa). The term, u_v/u_{v0} is also referred to as relative humidity, RH.

The Peltier and Seebeck effects are used to create and measure, respectively, a temperature difference between the measurement junction and the reference junction for relative humidity measurements. A simple electrical circuit demonstrating the Seebeck

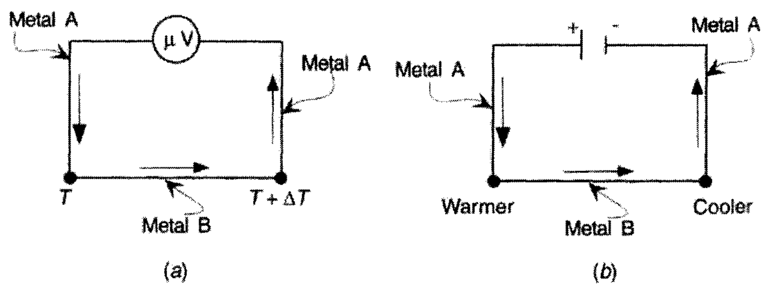

Figure 2.17: Electrical circuits comprised of dissimilar metals for illustrating *(a)* Seebeck effect and *(b)* Peltier effect (Lu & Likos, 2004)

effect for dissimilar metals A and B is shown in Fig. 2.17. The temperature difference between the measurement and reference junction, ΔT, produces a proportional electrical current that is generated in the circuit. The resulting output can then be measured using a voltmeter which is connected in series. The water condenses on the junction at a temperature that is a function of the ambient relative humidity if the temperature of the cooling junction is depressed beyond the dew-point temperature of the ambient environment. Cooling at the measurement junction is proportional to the product of the evaporation rate and the latent heat of vaporization. Although the evaporation rate is primarily a function of the relative humidity of the chamber, it also varies with the diffusivity of water in air, which decreases with atmospheric pressure. The latent heat of vaporization, thermal conductivity, and water vapor diffusivity of air all increase with increasing temperature. Pressure and temperature effects on the psychrometric measurement may be summarized using the conventional psychrometer equation in terms of relative humidity as given below (Campbell, 1979):

$$\mathbf{u}_v/\mathbf{u}_{v0} = 1 - \left[\frac{(s+\gamma^*)}{u_{v0}}\right]\Delta T \tag{2.9}$$

where; s: the slope of the saturation vapor pressure curve γ^*: the apparent psychrometer constant (product of the thermodynamic psychrometer constant and the ratio of vapor transfer to heat transfer resistance) ΔT: wet-bulb temperature depression

The psychrometer sensitivity is dependent on the term $\left[\frac{(s+\gamma^*)}{u_{v0}}\right]$. The temperature dependence of this technique mainly due to the temperature dependence of the terms s and u_{v0}, and pressure dependence of this technique is mainly due to the effect of pressure on γ^*; for example, if the pressure doubles, also γ^* doubles (Rawlins & Campbell, 1986). Figure 2.18 show a schematic drawing and photograph of typical laboratory setup for

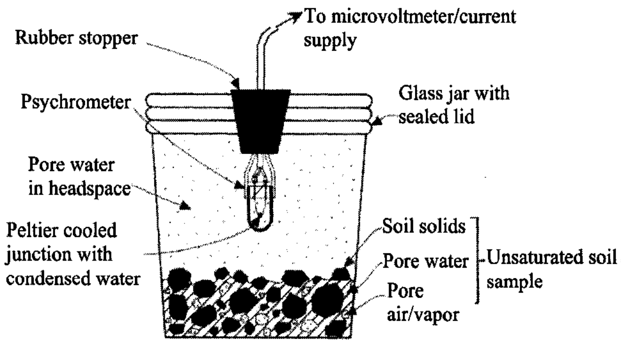

Figure 2.18: Schematic drawing and photograph of typical laboratory setup for measuring total suction using thermocouple psychrometer (Lu & Likos, 2004)

measuring suction using a thermocouple psychrometer. Prior to measurement, a soil specimen is sealed in the sensing chamber and allowed to come to temperature equilibrium with the psychrometer in the headspace above the specimen. The amount of time required for equilibrium is primarily dependent on the volume and initial relative humidity of the chamber, the soil suction, and the type of thermocouple protective housing (i.e., porous ceramic or stainless steel mesh). Equilibrium time typically varies from several hours to several days (Brown, 1970; Campbell *et al.* , 1973). The sensing chamber used for keeping the specimen should be placed in a controlled-temperature water bath or insulated cooler to minimize the effect of temperature fluctutations on the measurement. A controlled temperature environment of $\pm 0.001^0 C$ is required in order to measure total suction to an accuracy of 10 kPa (Edil & Motan, 1987). Two modes of operation may be used to determine relative humidity using thermocouple psychrometers: the "psychrometric" mode and the "dew-point" mode. The physics of each mode is essentially the same differing primarily in terms whether or not temperature is actively controlled at the measurement junction. It is important to note that psychrometers must be calibrated prior to testing by developing a relationship between sensor output at the dew point temperature and known values of RH. The thermocouple output at the dew-point temperature is a function of the ambient RH of the sensor/soil system. Correct calibration of sensors for psychrometric and hygrometric determination of water potential for laboratory and in situ conditions is extremely important because the accuracy of all subsequent measurements and interpretations will be based on this data. Salt solutions of known concentration are generally used for calibration. Figure 2.19 shows portions of soil-water retention curves obtained using this psychrometer for several mass controlled

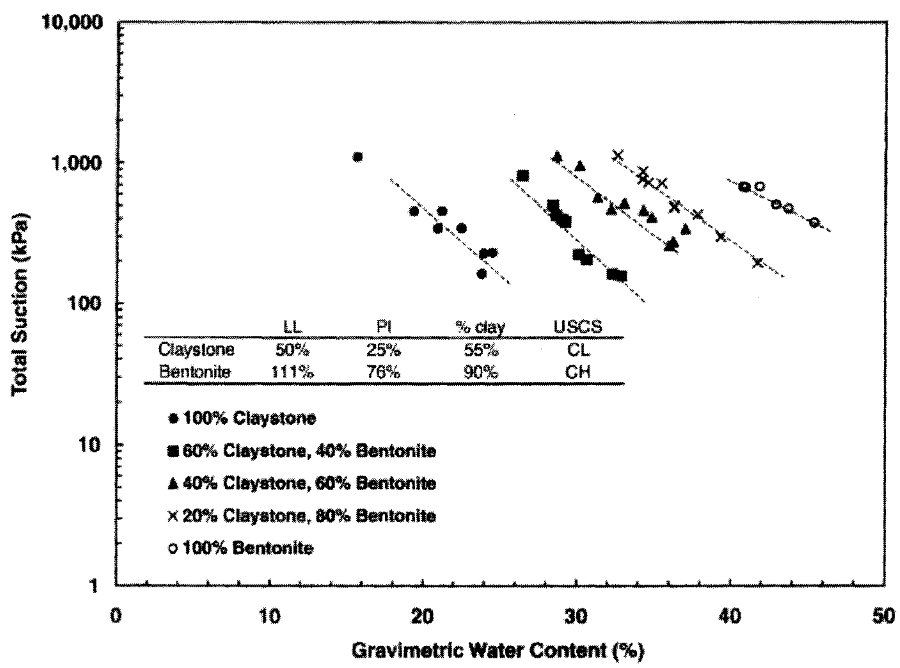

Figure 2.19: Relationships between total suction and water content measured using thermocouple psychrometers for remolded mixtures of natural expansive soils from Denver, Colorado (Lu & Likos, 2004)

mixtures of two expansive soils.

The upper and lower limits of thermocouple psychrometry measurements are strongly dependent on sensor design and measurement protocol (Wiebe *et al.* , 1971). The maximum temperature depression that can be maintained at the measurement junction for Peltier-cooled psychrometer is limited by a resistive heating effect that increases with the square of the applied current. In practice, the lowest possible humidity measurement is about 94%, corresponding to an upper limit in total suction equal to approximately 8000 kPa. As the suction approaches this upper limit, the scatter in the measurement tends to increase. Similarly, at suctions below 100 kPa, where the RH approaches close to 100%, even slight temperature fluctuations can result in uncontrolled condensation on the measurement junction. For this reason, psychrometer measurements below 100 kPa using conventional procedures are generally unreliable (Campbell, 1979).

Transistor Psychrometers

The working principle of transistor pyschrometer is similar to the Peltier psychrometer. The two main differences for a transistor psychrometer are associated with the application of water and the technique used in the measurement of current, the water drop is manually applied and the current is measured using a transistor (Fig 2.20).

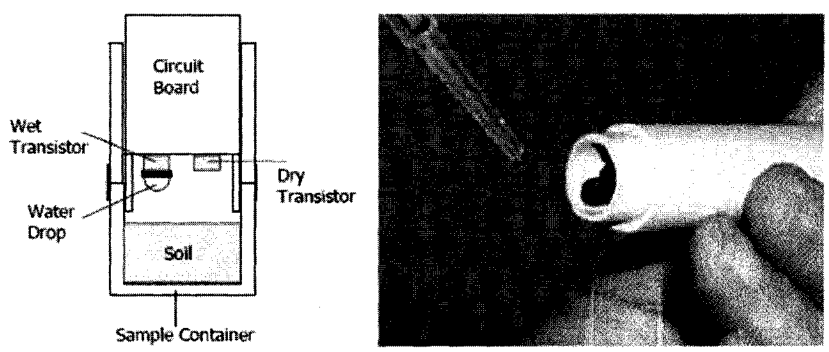

Figure 2.20: A typical transistor psychrometer and its probe

Typical measurement of suction range for transistor psychrometer is 100 - 10000 kPa. The equilibrium time is approximately in the order of 1 hour.

Chilled Mirror Psychrometers

Chilled mirror sensing technology has been used since 1950s for determining of dew-point temperature in a closed, humid environment. Gee et al. (1992) describe the use of chilled-mirror sensing system for soil suction testing equipments. Figure 2.21 illustrates basic operating principle. First, the metallic mirror is chilled thermoelectrically to a temperature at which condensation from ambient water vapor in the closed chamber forms on the mirror surface. A beam of light, typically from a light-emitting diode (LED), is directed to the mirror and reflected back to a photodetector.

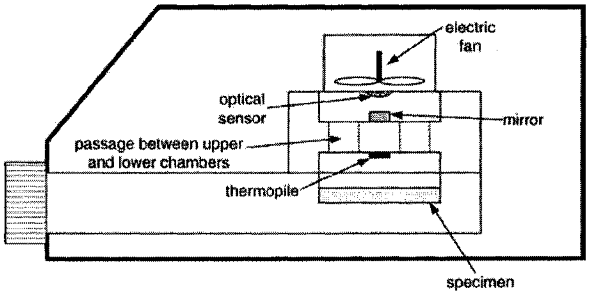

Figure 2.21: Schematic diagram of chilled-mirror sensing technology (Wang & Benson, 2003)

When condensation occurs as the mirror is cooled to the dew-point temperature, the light reflected from the mirror is scattered and the intensity detected by the photodetector is consequently reduced. The dew-point temperature is maintained constant by a microcircuit and measured by a resistance thermometer embedded in the mirror. The dew-point temperature may then be related to the ambient RH and corresponding total suction using Kelvin's law.

Accuracy of the order of ± 0.2 % RH is typically reported for most commercially available chilled-mirror sensing systems (Gee *et al.* , 1992). The practical measurements range is relatively wide, varying from about 3% RH ($\approx$450 000 kPa) to about 99.9% RH ($\approx$100 kPa). Scatter has been shown to increase significantly in the measurements of suction when RH greater than 99% ($\approx$1000 kPa). The primary advantages of chilled mirror sensing technology for soil suction measurement applications are its simplicity and speed. The time required for one measurement of suction can be as low as 5 minutes.

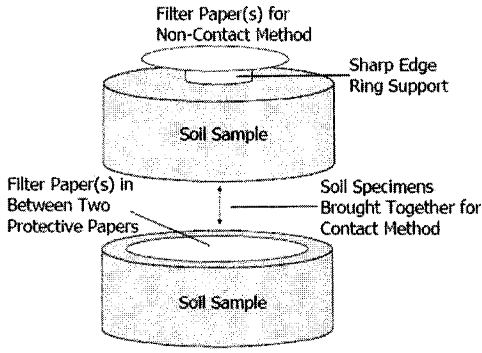

Figure 2.22: General testing configuration for filter paper testing (Likos & Lu, 2002)

Filter Paper Method

Filter paper methods were first developed for agricultural and soil science applications. Gardner (1937) has been credited with introducing filter-paper technique. The technique has been used as a conventional method of measuring soil suction for engineering purposes. Filter paper method is relatively simple, low-cost, and reasonably acurate alternative to many of the other indirect testing techniques used commonly for measuring suction. The American Society for Testing and Materials (ASTM) Standard D5298 describes calibration and test procedures for the measurement of either matric suction using the "contact" filter paper technique or total suction using the "non-contact" filter paper technique. In the contact technique, the filter-paper is placed in direct contact with the soil specimen, by either placing the filter-paper on top of the soil sample (Bulut *et al.* , 2001), or burying them within the sample (Houston *et al.* , 1994). Both the contact and non-contact filter paper techniques estimate soil suction indirectly by measuring the amount of moisture transferred from an soil specimen to an initially dry filter paper (Fig. 2.22). The filter-paper is considered to be the standard material by convention (see ASTM standard D5298-03); however, any absorbent material may be suitable for measurement of soil suction (Sibley & Williams, 1990b). The moisture content of the filter paper at equilibrium is measured gravimetrically and related to soil suciton through a predetermined calibration curve for the particular type of paper used. Commonly used types of paper includes Whatman #42, Schleicher and Schuell #589 White Ribbon, and Fisher 9-790A. Figure 2.23 shows the calibration curves for two of the above mentioned filter papers. Although non-contact filter paper testing is in theory applicable over the entire range of total suction, the method tends to be impractical for

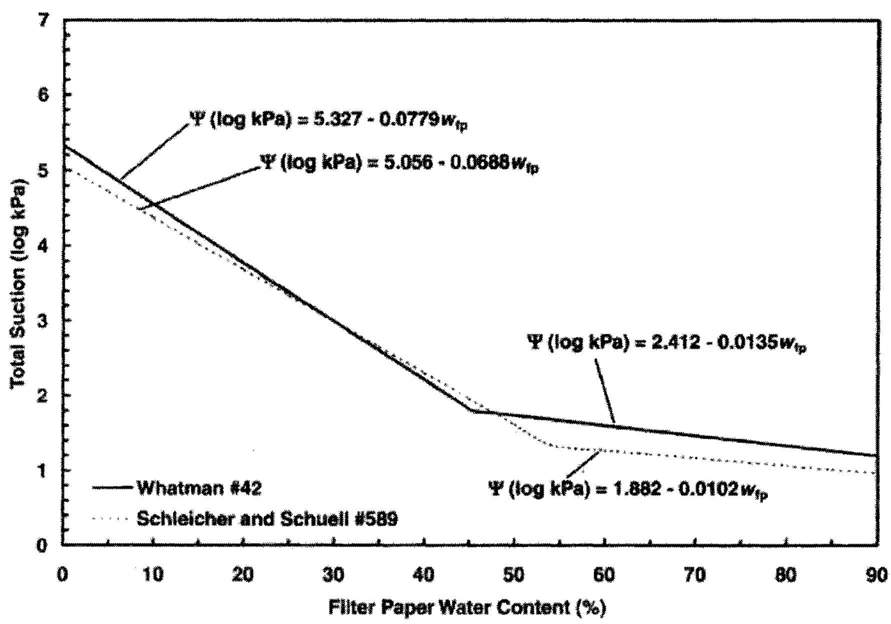

Figure 2.23: Calibration curves for Whatman #42 and Scheicher and Schuell #589 filter papers (ASTM D5298, ASTM 2000)

both extremely high and extremely low values of suction. Reilable measurements tend to be limited to a range spanning about 1000 kPa and 500,000 kPa because the relationship between total suction and RH becomes extremely steep at suction values less than approximately 1000 kPa (Sibley *et al.* , 1990). Total suction in this range is highly sensitive to RH and, thus, to measurements of filter paper water content. Slight temperature fluctuations may also result in significant changes in RH in this suction range. At extremely high values of suction, the filter paper adsorbs relatively small amounts of water vapor and the quality of the measurement becomes exceedingly dependent on the environment conditions, operational procedure, and the precision of the equipment used to determine filter paper water content. It has been shown that filter paper calibration curves can significantly vary among the same type of paper from one researcher to another or among the same type of paper from one "batch" or "lot" to another (Sibley *et al.* , 1990; Leong & Rahardjo, 2002; Likos & Lu, 2002). Between the two extreme cases (lot 77743 and lot 812130), measured values of filter paper water content differ as much as 11% at relatively low values of total suction. At relatively high values of suction, the difference in measured water content is as much as 4% (Lu & Likos, 2004).

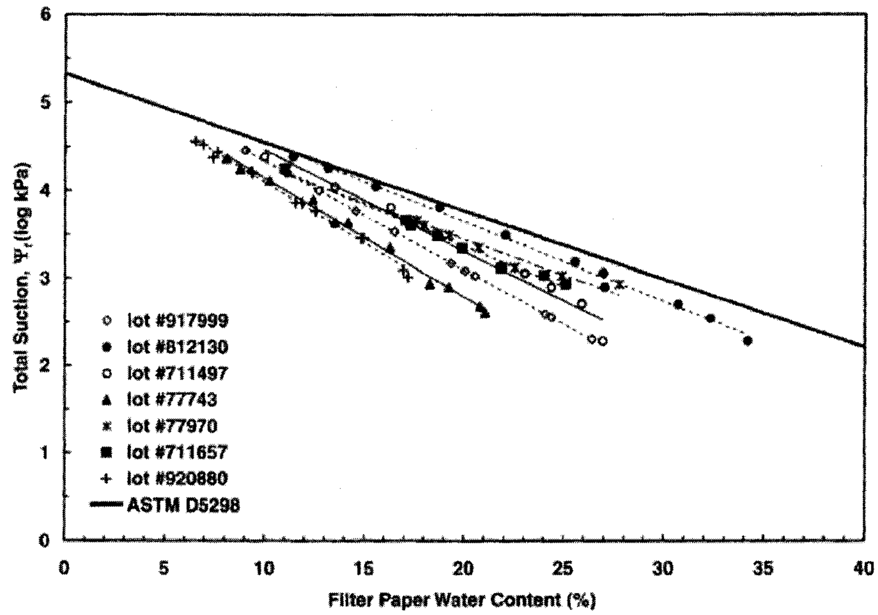

Figure 2.24: Calibration curves for seven batch of Whatman #42 filter paper (Likos & Lu, 2002)

In terms of toal suction, these discrepancies result in 92% error and 57% error, respectively. The main hurdle associated with this method is the development of a proper calibration curve which relates the filter-paper's water content to the soil suction. For this reason several researchers recommend to develop their own calibration curve before applying this technique (Sibley & Williams, 1990b; Power, 2005). Gardner (1937) stated that "if the tedious task of calibrating the filter-paper can be avoided, the method is a simple investigation tool to measure the entire range of soil suction".

Thermal Conductivity Sensors

The temperature change is related to the thermal conductivity of the porous medium and the moisture content using a thermal conductivity sensors. The system consists of ceramic-tipped sensors, a suction sensor controller (datalogger), and a power supply. The sensor tip has a miniature heating element and a temperature sensor embedded in the center (Fig. 2.25). The heating curve of the sensor is obtained by sending a controlled current to the heating element. The temperature rise (ΔT) in the sensor after heating depends on the water content of the sensor, which in turn is a function of the surrounding

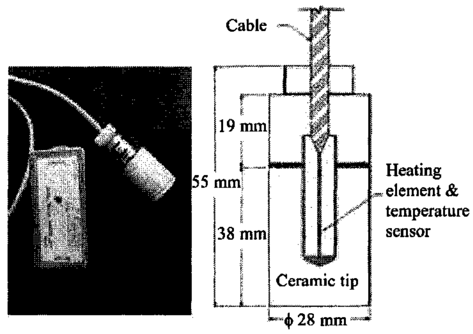

Figure 2.25: A typical thermal conductivity sensor

soil suction. Calibration curves developed in the laboratory are provided to obtain the suction corresponding to field measured ΔT.

The range of the suction that can be measured using this equipment varies 1-1500 kPa with an accuracy of $\pm5\%$. The equilibration time may vary from hours to days. Shuai & Fredlund (2000) show full equalisation time can be about 2 weeks for a wet sensor although a dry sensor may take 4 days. There are both laboratory and field applications of thermal conductivity sensors. Ng *et al.*(2003) showed general agreement between thermal conductivity sensors and tensiometers (suction around 20 kPa) although one sensor showed a significantly higher value (i.e., 250 kPa). According to his study, the thermal conductivity sensors showed a slower response (i.e., 2 days lag) in comparison to tensiometer in which the response is much faster (i.e., couple of hours).

Electrical Conductivity Sensors

There are two main types of electrical conductivity sensors which are commonly used, gypsum blocks and granular matrix sensors. A pair of electrodes inserted into a porous matrix comprises an electrical resistance soil moisture sensor. For the soil moisture measurement, the matrix in these sensors consists of a highly soluble calcium sulfate salt that serves to boost conductivity and insulate the sensor from the fluctuations in the salinity of the external environment (McCann *et al.* , 1992). These sensors are inexpensive compared to its alternatives and suitable for trend measurement rather than accuracy. Skinner *et al.* (1997) suggest a life of 5 years for these sensors in alkaline or neutral soils but they usually need to be replaced every 2-3 years in soils with acidity. Johnston (2000) reports that suction values recorded with gypsum blocks at 2 field sites compared favourably with filter paper estimates for suction, provided blocks are individually cali-

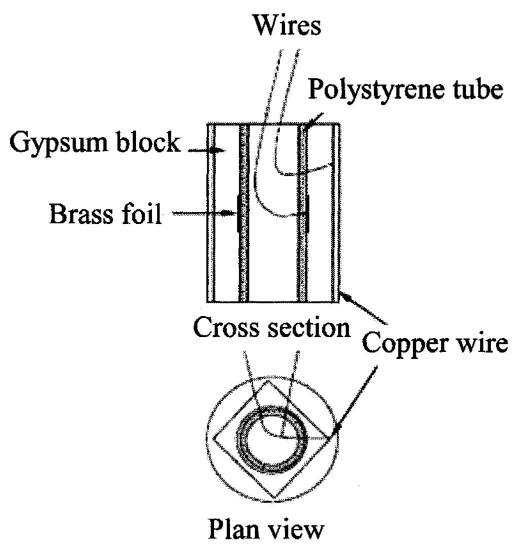

Figure 2.26: Schematic of a typical electrical conductivity sensor

brated (range 20-2100 kPa). Figure 2.27 shows the suction ranges that can be measured using different conventional techniques. It is interesting to note from these results that no single measurement technique spans the full range of matric suction.

2.5 Soil-water Retention Curve

The SWRC can be defined as the variation of water storage capacity within the macro and micro pores of a soil with respect to suction. Buckingham (1907), should have been one of the earliest investigators who systematically measured the SWRC. This relationship has been referred to in the literature using several terms; the widely used terms in geotechnical and geo-environmental engineering fields are the soil-water characteristic curve (SWCC), the soil-water retention curve (SWRC), soil moisture curve (SMC), water-suction relationship, soil-moisture retention curve (SMRC), and numerous other terms. The lack of a consistent terminology associated with SWRC is primarily a result of having numerous disciplines involved with measuring and using the data (Fredlund, 2004).

Several terms have been used to quantify the amount of water in the soil. The main terms are as follows:

- gravimetric water content, w,

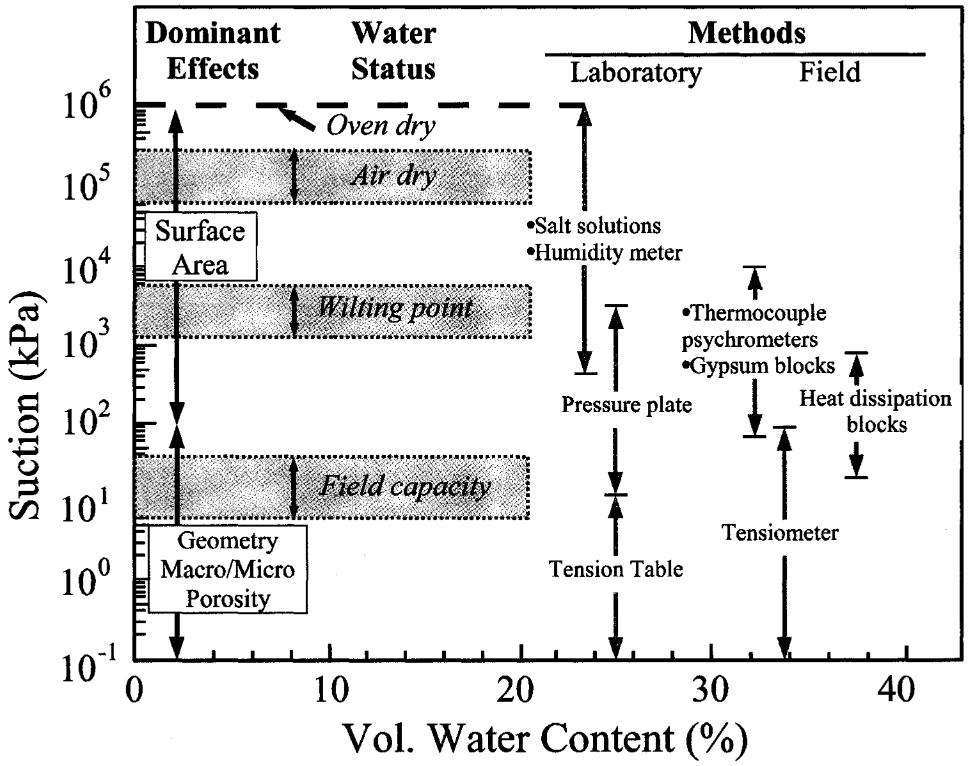

Figure 2.27: Conventional methods for measuring suction (modified after Gee & Ward, 1999)

- volumetric water content, θ,
- degreee of saturation, S,
- volume of water, V_w, referenced to the original volume of the specimen, V_o, or $\frac{V_w}{V_o}$

Gravimetric water content has been most commonly used in geotechnical engineering and is defined as follows:

$$w = \frac{m_w}{m_s} \tag{2.10}$$

where; w: gravimetric water content, m_w: mass of water and m_s: mass of soil solids. Volumetric water content has most commonly been used in agriculture related disciplines and relates the amount of water in the soil to the instantaneous total volume of the soil specimen (Fredlund & Rahardjo, 1993):

$$\theta = \frac{V_w}{(V_s + V_v)} \tag{2.11}$$

where; θ: volumetric water content, V_w: volume of water, V_s: volume of voids, V_s: volume of solids.

The degree of saturation references the volume of the water to the instantaneous volume of voids and for this reason requires a knowledge of the instantaneous total volume of the specimen, when defined (Fredlund & Rahardjo, 1993):

$$S = \frac{V_w}{V_v} \tag{2.12}$$

where; S: degree of saturation.

All the three variables mentioned above provide similar information if the initial volume of the specimen remains constant with an increase in the suction. In other words, if the volume of the specimen is constant, each of the variables is referenced to a constant value. However, if the soil structure is deformable, only the gravimetric water content is referenced to a constant. Several other dimensionless and normalized forms that have been proposed for the representation of water in the soil (see Fredlund & Rahardjo, 1993).

A typical SWRC is illustrated in 2.28. The parameters used to describe the SWRC

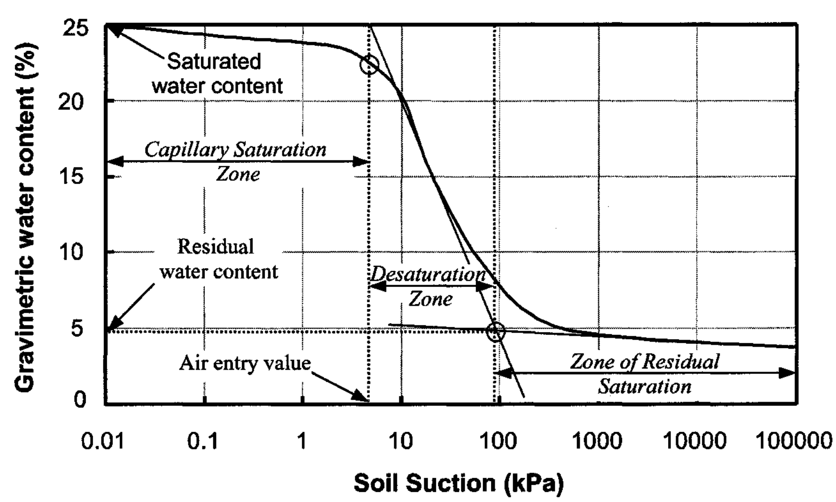

Figure 2.28: A typical SWRC and its essential features

include; the air-entry value, $(u_a - u_w)_b$, the rate of desorption and residual water content,

w_r. The air-entry value, $(u_a - u_w)_b$ is the matric suction value that must be exceeded before air recedes into the macro pores of the soil. This limit is also referred as the "bubbling pressure" in ceramics engineering or the "displacement pressure" in petroleum engineering. The rate of desorption is closely related to the pore-size distribution. The residual water content is the water content at which an increase in suction does not produce a significant change in water content.

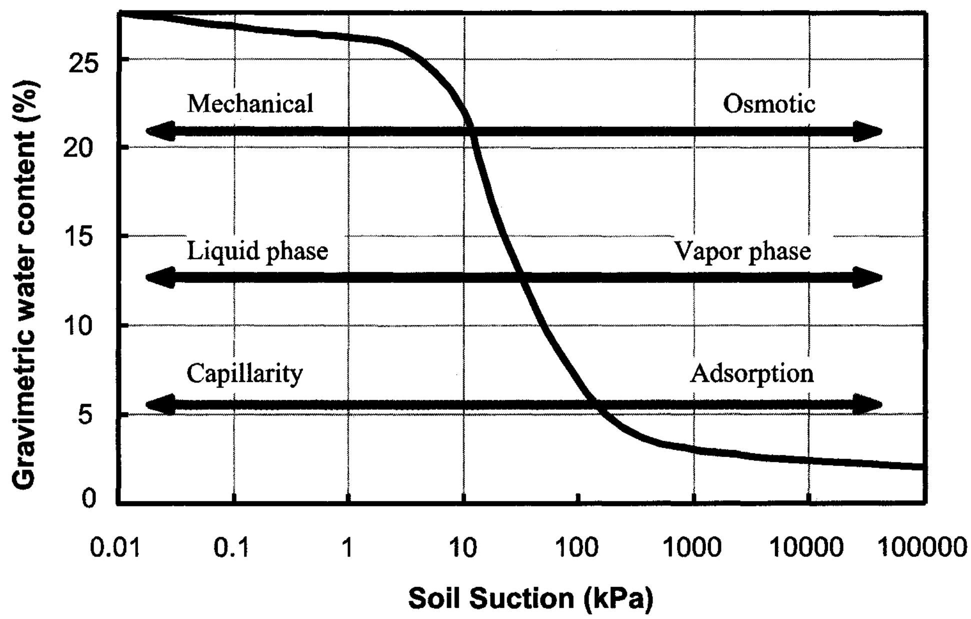

Figure 2.29: Illustration of the influence of the components of soil suction in different ranges of suction (modified after (Barbour, 1998))

Figure 2.29 shows different zones in which each component of soil suction is predominant. The total potential controls the water flow and the suction components influence the mechanical behavior of soils. However, not all the components have the same effect; the mechanical behavior is mainy affected by the matric suction (Krahn & Fredlund, 1972; Fredlund & Rahardjo, 1993). Capillary effects dominate when there is still a significant amount of liquid water in the soil. Therefore, matric suction can be used to describe the mechanical behavior of an unsaturated soil. As soil dries, liquid flow starts to cease and vapor flow begins to dominate. For this reason, the osmotic suction related to the adsorbed salts begin to dominate the soil behavior. The influence of osmotic suction are more pronounced in clay-rich materials.

The shape of the SWRC depends on the pore-size distribution and volume change of the soil. These two characteristics of porous materials are affected by the initial water content, soil structure, mineralogy, and the stress history (Vanapalli *et al.* , 1999; Simms & Yanful, 2005). Moreover, volume change itself cannot be just related to one single stress state variable but must be described by independent functions of net normal stress and suction (Matyas & Radhakrishna, 1968). For a rigid porous material of single pore size (i.e., uniform pore size distribution), whether it is a soil or not, the SWRC should be similar to curve (a) shown in Fig. 2.30. But even in a porous material with uniform pore size distribution, some water would still be present in the material due to surface phenomena. The SWRC shape for a material of single pore size could be more appropriately represented by curve (b) in Fig. 2.30. The curve (c) in Fig. 2.30 represents an example of material with two pore sizes (i.e., bimodal pore structure). A material with larger numbers of pore sizes should present a more gradual reduction in water content with an increase in suction, as shown in curve (d) in Fig. 2.30. Clay soils typically

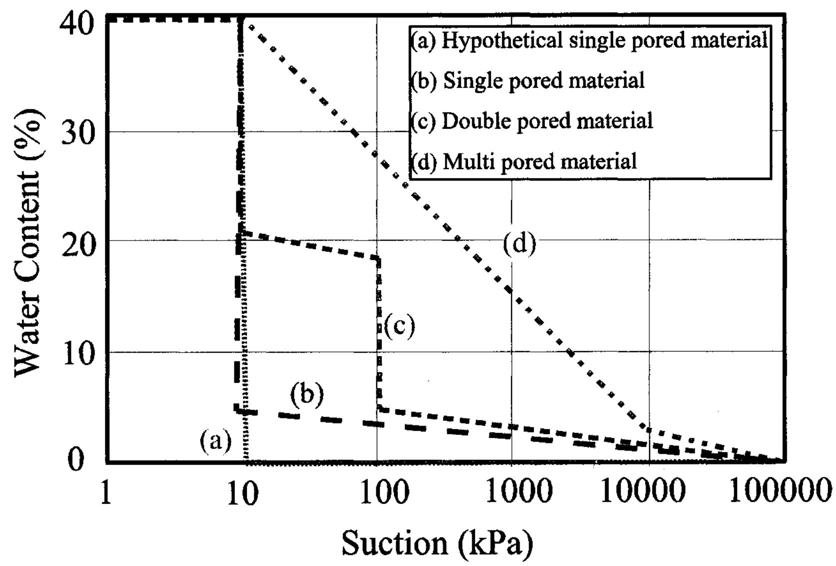

Figure 2.30: General shape of SWRC according to pore-size distribution (Marinho, 2005)

have non-uniform grain size and pore size distributions (Delage & Lefebvre, 1983). As a consequence, SWRCs of clays are wiht slopes that exhibit relatively flatter slopes in comparison to coarse-grained soils.

2.5.1 Estimation of Engineering Properties Using SWRC

The SWRC has repeatedly been identified as the key soil information required for the analysis of seepage, shear strength and volume change problems (Barbour, 1998; Fredlund, 2000). The water storage function and the hydraulic conductivity function for an unsaturated soil can be estimated using the SWRC. The indirect determination of these parameters may be justified not only by the difficulties involved in such tests but also by the costs associated with determinations of these parameters. The general technique follows that the unsaturated soil property functions can be based on the saturated soil properties and the SWRC along with one additional soil parameter (Fredlund, 2004):

$$\textbf{Unsaturated Soil Property} = [Saturated\ Soil\ Property]\, f(SWRC)^{(soil\ parameter)} \tag{2.13}$$

For example, Figure 2.31 shows plots of a typical SWRC and the predicted properties associated with moisture flow. The equations available for the prediction of hydraulic conductivity, k_w are based on empirical observations or on statistical and mechanistic approaches. Features of the property functions, such as the location and steepness of the hydraulic conductivity, k_w and coefficient of vapour diffusion D^{v*} function are illustrated in Fig. 2.31. These features depend on the air-entry value and on the steepness of the SWRC. A detailed explanation is available in Gitirana (2005).

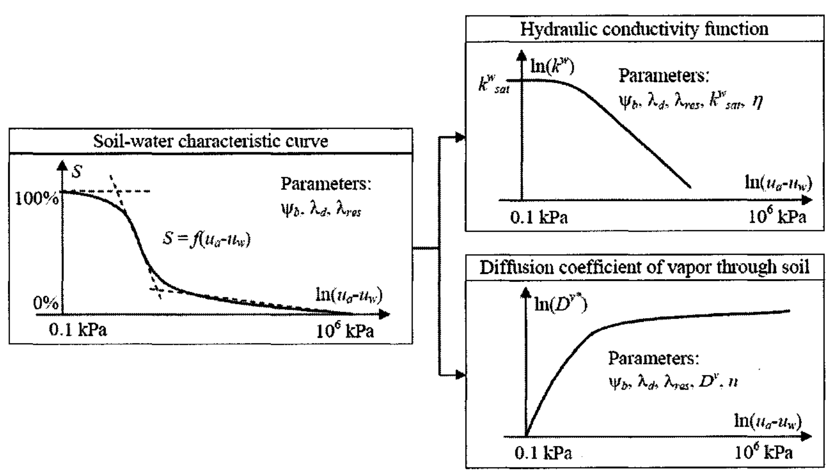

Figure 2.31: Prediction of moisture flow properties based on the soil-water retention curve(Gitirana, 2005)

2.5.2 Review of Soil-Water Retention Curve Fitting Equations

The SWRC data obtained from a laboratory test are a series of disconnected points. A mathematical equation can be used to fit the data points and extrapolate and interpolate the data where no experimental data is available. A number of empirical, analytical and statistical models are postulated in the literature for the mathematical representation of SWRCs (Brooks & Corey, 1964; Brutsaert, 1966; van Genuchten, 1980; Fredlund & Xing, 1994; Leong & Rahardjo, 1997). A comprehensive summary of these models is available in Sillers *et al.* (2001). The evolution and comprehension of the SWRC along with the measurement techniques is summarized in the Nineteenth Canadian Geotechnical Colloquium by Barbour (1998). Commonly used soil-water retention curve-fitting equations are presented in the Table 2.2. Among these SWRC models; van Genuchten (1980) and Fredlund & Xing (1994) equations are found to be more commonly used (Leong & Rahardjo, 1997; Stormont & Anderson, 1999; Gersovich & Sayao, 2002; Vanapalli *et al.* , 2004). Therefore, in this research, the above two equations were used. In addition; a simple equation proposed by Brutsaert (1966) with two fitting parameters is also tested and used for the proposed technique in Chapter 5. Depending on the model, at least two (Brutsaert, 1966) or three experimental data (van Genuchten, 1980; Fredlund & Xing, 1994) are required in order to fit the SWRC. The accuracy of fitting the SWRC increases with an increase in the use of experimental data points for all the SWRC models.

There are several types of SWRC models. One branch of these models is based on statistical relationships between the structural and textural soil properties and water content versus suction values (Gupta & Larson, 1979; Vereecken *et al.* , 1992). Another branch is linking the SWRC equations to the physical characteristics of the porous media based on certain assumptions (Arya & Paris, 1981; Haverkamp & Parlange, 1986; Tyler & Wheatcraft, 1990; Aubertin *et al.* , 2003).

In many situations, it is valuable to have an estimate of the SWRC during early stages of a project, when there is not enough information readily available. The SWRC estimation models, based on easy to obtain properties (i.e., grain size distribution, void ratio, Atterberg limits, and dry density) may be utilized to guide the geotechnical engineers throughout the preliminary analyses and design procedures (Fredlund, 2000; Côté & Konrad, 2002; Vanapalli & Catana, 2005).

Table 2.2: Soil-water retention curve equations used for fitting experimental data

Reference	**Equation**	**Parameters**
Brooks & Corey (1964)	$\theta_w = \theta_r + (\theta_s - \theta_r)\left[\frac{a_b}{\psi}\right]^{b_b}$	a_b: Bubbling pressure b_b: Pore size index
Brutsaert (1966)	$\theta_w = \theta_r + \frac{(\theta_s-\theta_r)}{\left[1+\left[\frac{\psi}{a_b}\right]^{n_b}\right]}$	a_b: The first fitting parameter n_b: The second fitting parameter
van Genuchten (1980)	$\theta_w = \theta_r + \frac{(\theta_s-\theta_r)}{\left[\left[1+\left[\frac{\psi}{a_{vg}}\right]^{n_{vg}}\right]\right]^{m_{vg}}}$	a_{vg}: The first fitting parameter n_{vg}: The second fitting parameter m_{vg}: The third fitting parameter
Mckee and Bumb (1987)	$\theta_w = \theta_r + \frac{(\theta_s-\theta_r)}{1+e^{\left[\frac{(h-a)}{b}\right]}}$	a: The first fitting parameter b: The second fitting parameter
Fredlund & Xing (1994)	$\theta_w = \theta_r + \frac{(\theta_s-\theta_r)}{\left[In\left[e+\left[\frac{\psi}{a_f}\right]^{n_f}\right]\right]^{m_f}}$	a_f: The first fitting parameter n_f: The second fitting parameter m_f: The third fitting parameter h_r: A soil parameter related to the suction at which residual water content occurs

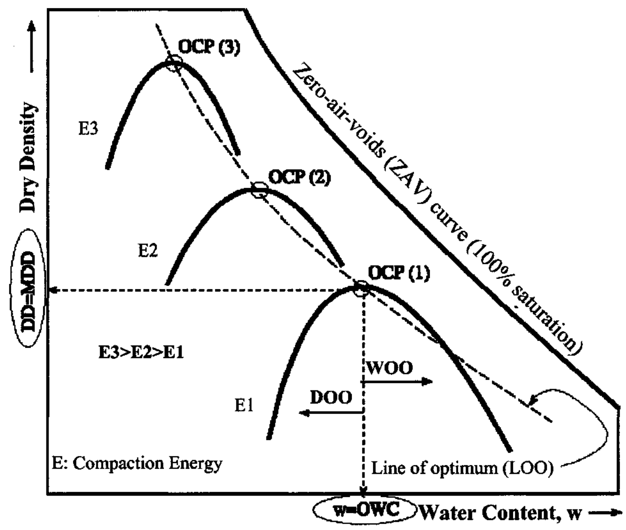

Figure 2.32: Schematic of compaction curves (moisture density relationships) for a hypothetical soil compacted at three energy levels. Also shown are the optimum water content (OWC),maximum dry density (MDD), and the line-of-optimum (LOO)and zero-air-voids (ZAV) lines (Basheer, 2000)

2.6 Compacted Soils

Unlike several other construction materials (i.e., concrete), the properties of soils can not be preset and therefore they may not exhibit the properties desired in the construction of the earth structures. Sometime, soil properties at the site have to be improved to achieve better performance.

There are several remediation techniques which can be carried out by employing a variety of mechanical and chemical stabilization techniques based on the project requirements. In chemical stabilization, chemical agents such as cement, lime or asphalt is blended with soil. On the contrary, mechanical improvement methods include compaction consolidation and soil reinforcement (Bell, 1977). The soil type, cost-related factors and the project requirements play an imporant role in the selection of a specific technique (Basheer, 2000). Compaction is frequently used in the construction of soil structures such as roads, railroad embankments, earth dams, landfill clay liners (Delage *et al.* , 1997; Romero *et al.* , 1999).

Proctor (1933a) demonstrated the influence of compaction energy and moisture content on the dry unit weight of soil. He introduced the use of a 2.5 *kg* hammer falling from a height of 305 *mm* compacting soil into 3 equal layers at 25 strokes per layer. The soil was compacted in a cylinder, 114 *mm* in diameter and 178 *mm* in height. A penetrating needle was additionally used to test penetration resistance after a soil was compacted. His efforts on 200 different soil types showed that an increase in compaction energy results in an increase in maximum dry unit weight and decrease in the optimum moisture content.

A large number of factors, which are either not measured or difficult to control, influence the engineering behavior of compacted soils (Fleureau *et al.* , 2002). In most cases, compaction increases the soil density, enhances its strength, and reduces its compressibility and hydraulic conductivity. In addition, compaction can result in a significant reduction in potential settlement, an increase in slope stability, an increase in bearing capacity, a reduction of the detrimental effects that may cause due to the volume change (i.e., frost heave, swelling and shrinkage) and control of water flow (i.e., seepage, subsurface contaminant transport) (Basheer, 2000). However, since compacted soils are typically in a state of unsaturated condition, the mechanics of unsaturated should be used in understanding the engineering behavior of these soils.

2.6.1 Influence of the Soil Structure

Many studies are reported in the literature that discuss the influence of soil structure or fabric on the engineering properties of compacted soils (Alonso *et al.* , 1987; Cui & Delage, 1996; Romero *et al.* , 1999; Simms & Yanful, 2005). The parameters that influence the engineering behavior of unsaturated soils also influence the SWRC behavior. In recent years, several studies are reported in the literature to understand the influence of various parameters that influence the SWRC behavior (Vanapalli *et al.* , 1999; Ng & Pang, 2000; Leong & Rahardjo, 2002; Vanapalli *et al.* , 2004). Some of these factors include initial compaction water content used for compaction, soil structure, void ratio, type of soil, texture, stress history, mineralogy and method of compaction. Of the factors stated above, the soil structure and stress history have the most influence on the SWRC behavior of fine-grained soils (Vanapalli *et al.* , 1999).

The specimens with an initial compaction water content representing the dry of optimum conditions have relatively large pore spaces which are located between the clods of soil compared to the pore spaces within the clods. The relatively low suction values associated with removing water from the large pores are significantly different from the large suction values required to remove water from the microscopic pore spaces between soil particles within the clods of clay (Vanapalli *et al.* , 2004). Therefore, the macro-structure controls the initial desaturation of compacted clayey specimens with initial water contents, which are dry of optimum.

On the contrary, the pore spaces in a clayey soil compacted at an initial water content on the wet of optimum side are not generally interconnected, in other words, they are in an occluded state. These soils are relatively more homogeneous than the specimens compacted at dry of optimum and consequently, have a higher storage capacity due to their different structure. They have no visible interclod pores and offer more resistance to desaturation under an applied suction in comparison to those specimens compacted dry of optimum (Cui & Delage, 1996; Vanapalli *et al.* , 2004). In contrast to the specimens compacted dry of optimum, the micro-structure in the specimens compacted wet of optimum controls and resists the desaturation (drying) characteristics of the soil. As a result, the slope of the SWRC is relatively flatter for the wet of optimum specimen compared to the dry of optimum initial water content specimen in the lower suction range, where the desaturation was attained mainly by the liquid-phase drainage (i.e., 0 to 1,500 kPa). The boundary between occluded pore space and the open pore conditions occurs at water contents approximately equal to the optimum water content (Marshall, 1979; Tarantino & Tombolato, 2005), and therefore, the specimen prepared at optimum water content condition lies between these two.

Vanapalli *et al.* (1999) studies show for all initial conditions of water content (i.e., dry of optimum, optimum and wet of optimum) and stresss history, the SWRC behaviour appears to be similar at higher suctions (i.e., 20,000 to 300,000 kPa). In other words, the inter-aggregate structure appears to be the same for the specimens at these higher suctions. Presumably, the water films at these suctions are so thin that all the water is within the range of influence of the osmotic and adsorptive fields. SWRCs of a glacial till compacted with different initial water contents and densities are shown in Fig. 2.33. The SWRCs of the same soil can vary significantly in the suction range of 0 to 1,500 kPa when the soil is compacted at different initial water contents representing dry of optimum, optimum and wet of optimum conditions (Vanapalli *et al.* , 1999). Benson & Tinjum (1997) worked on four different compacted clays used as a barrier in waste management structures. They conducted experiments to determine SWRCs for different initial compaction water contents and different compaction efforts. They concluded high air-entry values are obtained with more plastic soils when compacted on wet of optimum or when higher compaction effort is applied (Fig. 2.34).

Fine-grained soils typically have two levels of structure: a macro-level structure and

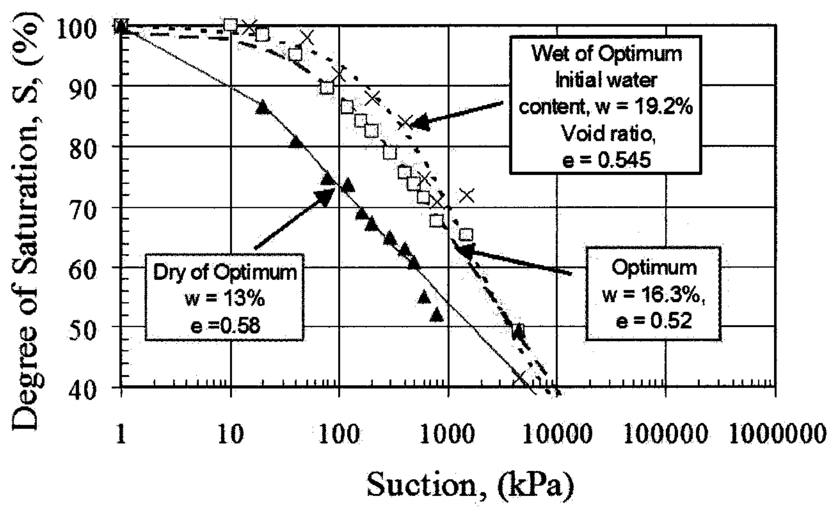

Figure 2.33: SWRCs of Indian Head till for dry, optimum and wet of optimum (Vanapalli, 1999)

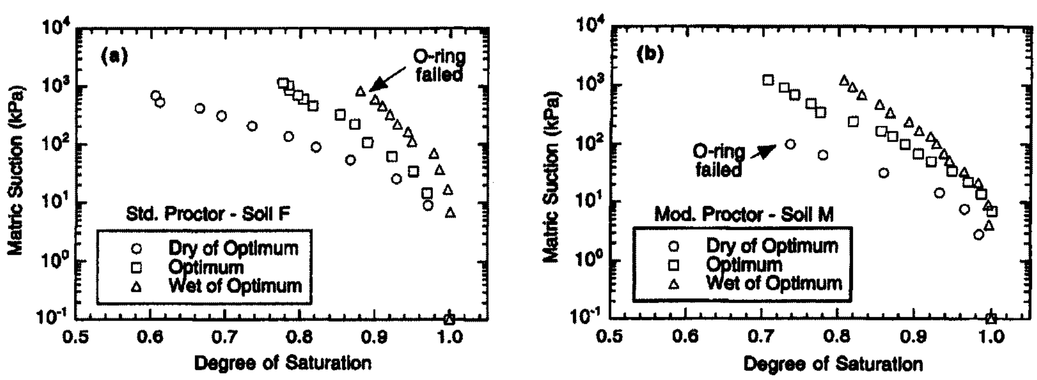

Figure 2.34: SWRCs of compacted clay barrier soils for dry, optimum and wet of optimum (Benson & Tinjum, 1997)

micro-level structure. The soil microstructure is described as the elementary particle associations within the soil, whereas the ar-rangement of the soil aggregates is referred to as macrostructure (Mitchell, 1993). Typically, both the macro and micro-levels of structure are present in natural and compacted clayey soils. The resulting macrostructure of specimens prepared at different initial water contents is different in spite of their identical mineralogy, texture and method of preparation.

2.6.2 Influence of Fine Fraction

Côté & Konrad (2002) present a comprehensive experimental study to provide a simple relationship between the air entry value, ψ_b, and the overall porosity of the soil (Fig. 2.35). The study suggests the maximum pore size (i.e., which is related to matric suction) is controlled by the percentage of fines rather than the coarse fraction of the material.

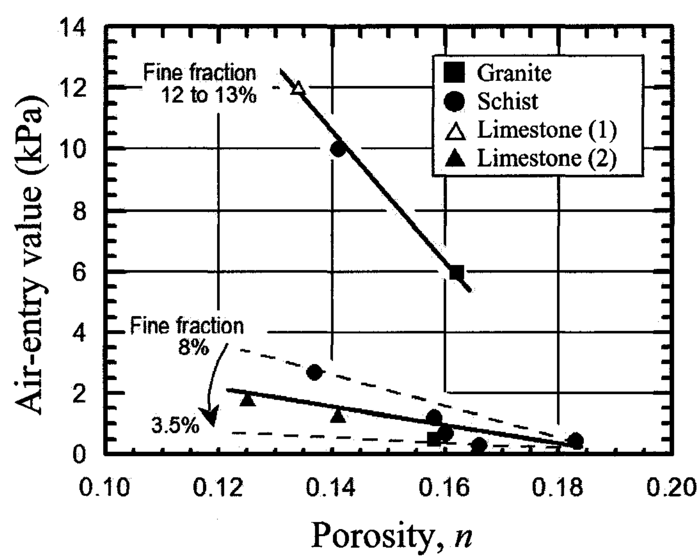

Figure 2.35: Influence of the overall porosity, n, and fine content on the air-entry value, ψ_b (Côté & Konrad, 2002)

2.6.3 Influence of Compaction Effort

The mechanical behavior of unsaturated soils is significantly influenced by compaction effort. Several investigators including Olson (1965), Sridharan (1968), and Bell (1977) worked on the engineering behavior of compacted soils. For example, Bell (1977) compacted specimens of sandy silty clays (CL-ML), with kneading, static, and impact methods at various moisture contents. The studies show that the static method was three to ten times more efficient in reaching 100% standard Proctor (18.8 kN/m^3 at 13.8% optimum) than kneading and impact methods at a given moisture content. The greater efficiency was determined by observing that at dry of optimum (10.6%) static compaction required 187 kJ/m^3 of energy to achieve maximum dry unit weight while kneading and impact required 435 and 626 kJ/m^3, respectively. Wet of optimum (15.7%), static compaction needed only 52 kJ/m^3 of energy with kneading and impact requiring 609 and 370 kJ/m^3 of energy. Figure 2.36 shows the efficiency of each compactive method obtaining maximum dry unit weight in the spectrum of moisture contents.

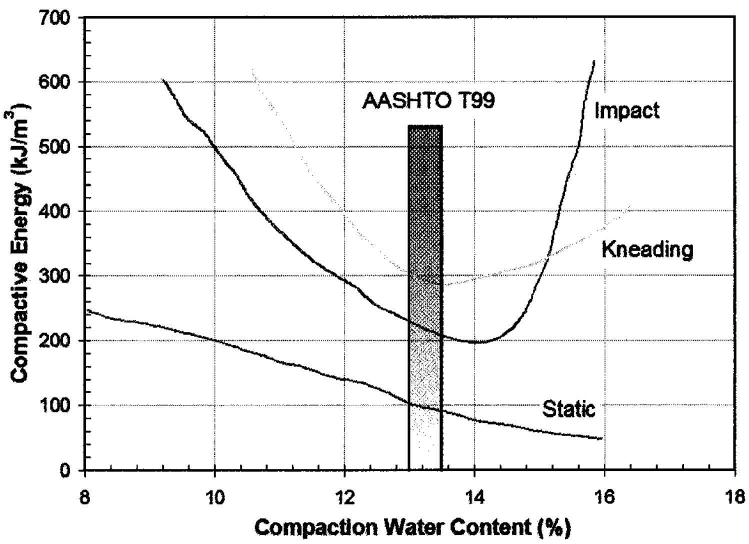

Figure 2.36: Compactive effort required to obtain maximum standard Proctor dry unit weight for three compaction methods after (Bell, 1977)

Leong & Rahardjo (2002) studied the influence of compaction effort on the SWRC of a mudstone residual soil. Three different energies were applied to the soil specimens as shown in Fig. 2.37: Standard Proctor effort (i.e., 598 kJ/m^3), Modified Proctor effort (i.e., 2693 kJ/m^3) and a variation of Modified Proctor, termed as Enhanced Proctor effort (i.e., 1619 kJ/m^3) (Fig. 2.38). Typically, the soil pore size decreases with an increase in the compaction effort for fine-grained soils. Due to this reason, it is likely there will be some differences in the storage characteristics (i.e., SWRC) of the

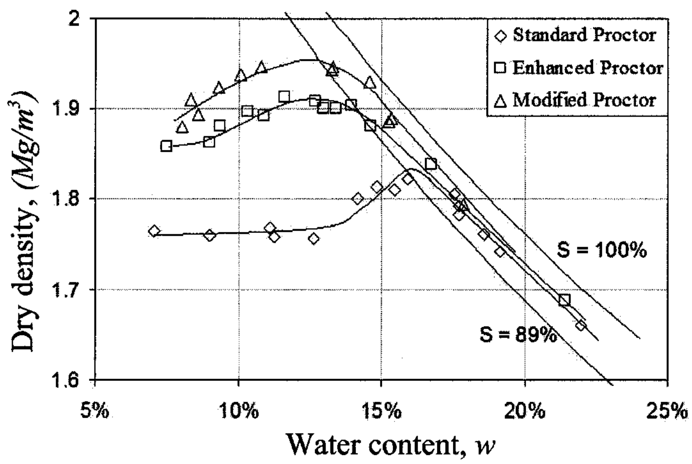

Figure 2.37: Compaction curves of Jurong formation mudstone residual soil (Leong & Rahardjo, 2002)

same soil when it is compacted with different energies. The SWRC of the compacted mudstone residual soil specimens at different compacted efforts are shown in Fig. 2.38 (Leong & Rahardjo, 2002). Several observations can be made from this study. First, the difference between the SWRC of compacted soils at the same compaction effort is not very distinct. Second, as the compaction effort increases, there is a general increase in the air-entry value. Third, the band of the SWRC tends to narrow as compaction effort increases.

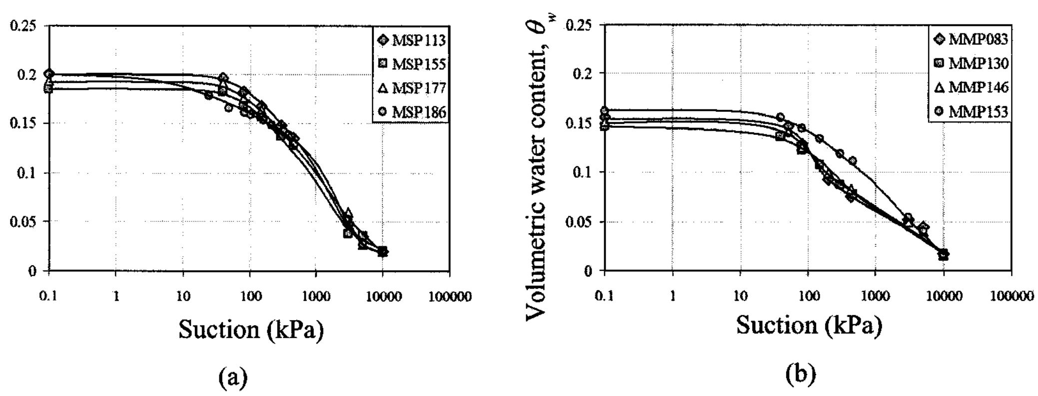

Figure 2.38: Soil-water characteristic curves of soil specimens compacted at different compaction efforts: (a) Standard Proctor, (b) Modified Proctor (Leong & Rahardjo, 2002)

In a different study, Sugii *et al.* (2003) presented the influence of compaction effort on the SWRC behavior of a sandy soil. Figure 2.39 shows the SWRC is unique for the different compaction energies beyond the transition stage for the tested sandy soil (i.e., 2 kPa suction value in Fig. 2.39).

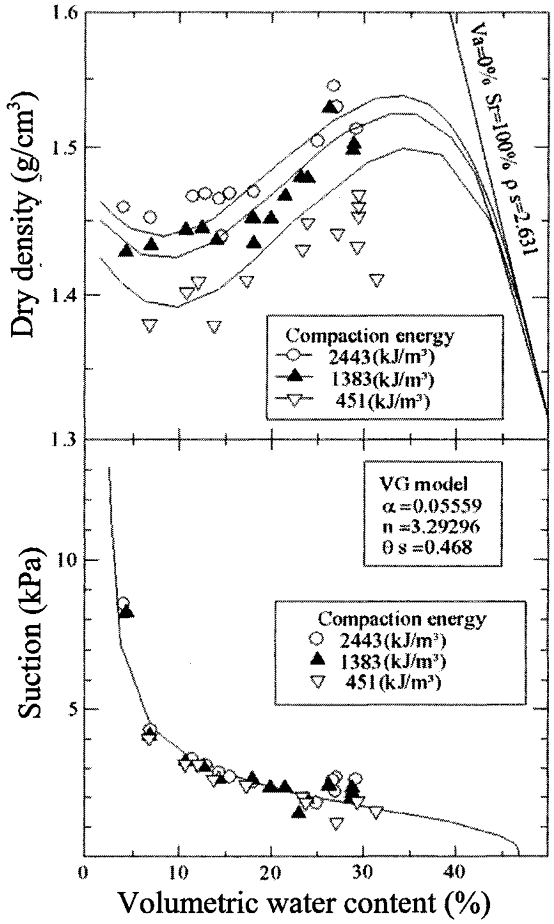

Figure 2.39: Compaction and SWRCs (Sugii *et al.* , 2003)

The results presented by Leong & Rahardjo (2002) and Sugii *et al.* (2003) are interesting and valuable. It should be noted that the resulting pore-size distribution in a fine-grained soil is significantly influenced by the compaction energy and the initial water content used for compacted fine-grained soils. The SWRC behavior of fine-grained soils is sensitive to those parameters and others such as the stress history and clay mineralogy. However, the pore-size distribution in a coarse-grained soil is not predominantly influ-

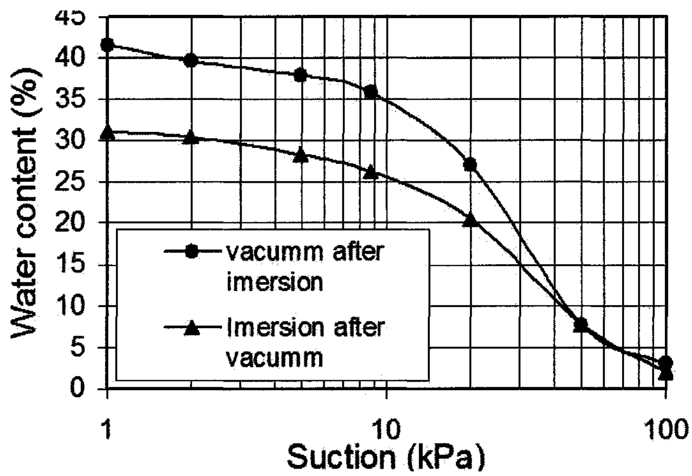

Figure 2.40: Effect of saturation technique on SWRC of a compacted soil (Barbosa *et al.* , 2002)

enced by all the above parameters. Due to this reason, it is likely coarse-grained soils exhibit a relatively "unique" SWRC. Several investigators have used this characteristic behavior of coarse-grained soils and were succesful on predicting or estimating the SWRC using the grain-size analysis data (Arya & Paris, 1981; Haverkamp & Parlange, 1986; Fredlund *et al.* , 1997; Vanapalli & Catana, 2005).

2.6.4 Influence of the Specimen Height and Saturation Technique

Barbosa *et al.* (2002) studied the influence of soil specimen height and saturation techniques on the SWRC behavior of a Brazilian soil. The two different techniques used for saturating the compacted soil specimen were: (i) vacuum application followed by submersion and (ii) submersion followed by vacuum application. The water content of specimens was higher in specimens which were saturated by vacuum application after immersion (Fig. 2.40). Also, these specimens desaturated at a faster rate in the low suction range in comparison to specimens that were submerged followed by vacuum application. Similar desaturation characteristics were observed at higher suction range (greater than 50 kPa) irrespective of saturation technique. However, similar soil-water characteristics were observed for specimens of different heights (20 to 40 mm).

2.6.5 Hydraulic Conductivity

Attom (1997) studied the changes in saturated hydraulic conductivity values at compacted impact energies of 355, 987, 1637, and 2693 kJ/m^3 for expansive clay (CH) specimens.

Table 2.3: Compaction energy applied to the clay specimens (after Attom, 1997)

Sample ID	**Hammer mass(kg)**	**Height of drop(cm)**	**Number of blows**	**Number of layers**	**Volume of cylinder(cm^3)**	**Energy applied(kJ/m^3)**
E1	2.5	30.5	15	3	934.5	355.6
E2	2.5	30.5	20	3	934.5	474.2
E3	2.5	30.5	25	3	934.5	592.7
E4	2.5	30.5	30	3	934.5	711.3
E5	2.5	30.5	20	5	934.5	790.3
E6	2.5	30.5	25	5	934.5	987.8
E7	2.5	30.5	30	5	934.5	1185.4
E8	4.5	45.7	15	5	934.5	1637.8
E9	4.5	45.7	20	5	934.5	2155.1
E10	4.5	45.7	25	5	934.5	2693.8

At optimum moisture content, the saturated hydraulic conductivity decreased from 5.9 x 10^{-9} cm/sec at 355 kJ/m^3 to 1.8 x 10^{-11} cm/sec at 2693 kJ/m^3. For the specimens compacted at dry of optimum, the saturated hydraulic conductivity ranged from 9 x 10^{-9} to 5.37 x 10^{-7} cm/sec at 355 kJ/m^3 (Fig. 2.41). At higher compactive efforts (987 to 2693 kJ/m^3) hydraulic conductivity decreased, ranging from 1 x 10^{-11} to 2.8 x 10^{-9} cm/sec. As compaction energy increases, the voids decrease, reducing hydraulic conductivity. Plotted against moisture content, hydraulic conductivity, at every energy level, decreased from dry to optimum moisture contents and then increased beyond optimum. Similar conclusions were also reported by work previously performed on compacted clays (Lambe, 1958; Elsbury *et al.* , 1990).

2.6.6 Swelling

Attom (1997) have also demonstrated that swell pressure in an expansive clay (CH) increases at dry and optimum moisture content with an increase compaction energy levels. Specimens were prepared at impact compaction energies of 355, 592, 987, 1637,

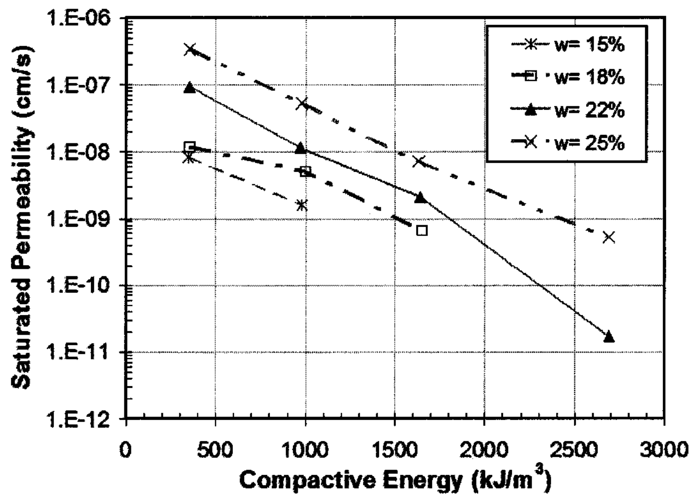

Figure 2.41: Compactive energy versus hydraulic conductivity for clays dry of optimum (after (Attom, 1997))

and 2693 kJ/m^3 (Table 2.3), seated in a 12 consolidation cell with an initial load of 6.9 kPa, and saturated. The procedure was termed a zero swell test where swell pressure was defined as the amount of pressure that discontinued soil expansion. Figure 2.42 shows that dry of optimum, average swell pressure ranged from 1.3 kg/cm^2 (355 kJ/m^3) to 3.4 kg/cm^2 (987 to 2693 kJ/m^3). Swell pressure at optimum moisture increased from 1.6 kg/cm^2 (355 kJ/m^3) to 4.5 kg/cm^2 (2693 kJ/m^3). An Increase in swell pressure with an increase in compaction energy was attributed to lower air voids in the soil with increasing energies. For the specimens compacted at wet of optimum, the compactive effort had little effect on swell pressure of the specimens because of high initial moisture contents.

2.7 Summary

A detailed review of the effective stress equations proposed for unsaturated soils and the role of suction in unsaturated soil mechanics is presented in this chapter. A summary of the suction measurement techniques is detailed highlighting the advantages and disadvantages of each of these techniques.

A brief review of soil-water retention curves was also presented. Several models used

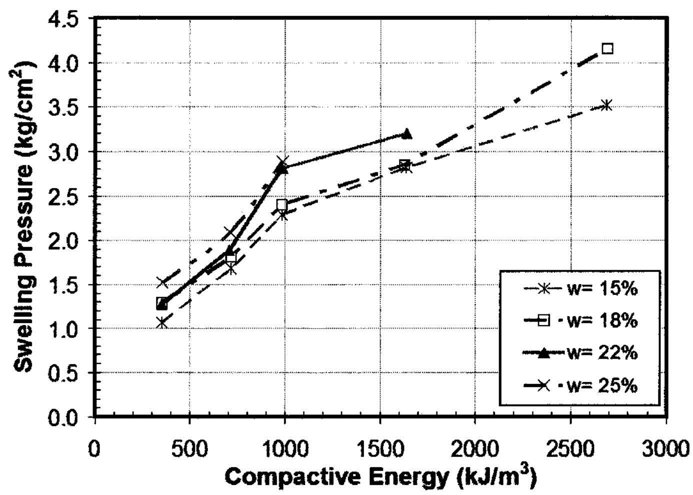

Figure 2.42: Swelling pressure versus compactive energy (after Attom, 1997)

to obtain a closed form SWRC were reviewed. The main factors that effect the engineering behavior of compacted soils were addressed. It was found that the soil structure of the soil governs the engineering behavior of compacted plastic soils. Different type of soil structures can be attained depending on the compaction type, initial compaction water and the activity of clay minerals present in the compacted soil. This literature also shows that the engineering properties of the compacted soils will be significantly influenced by the volume change behavior. For this reason, the volume change behavior with respect to suction should be taken account of while measuring the SWRC of compacted fine-grained soils.

Chapter 3

Equipment Details

3.1 Introduction

The laboratory testing program involved the determination of the water retention characteristics of Champlain sea clay taking account of volume change with respect to suction. Several compacted specimens of Champlain sea clay were prepared using both static and dynamic compaction energies at different initial water contents using three different energy levels. The suction in the compacted specimens were determined using axis-translation technique and thermocouple psychrometer. The volume change of the specimens were also measured at each suction increment while measuring SWRC.

Several equipments including compaction tools, null-pressure plate apparatus, psychrometer and triaxial cell were used in the experimental program. The following sections also provide a brief description of the equipment used in the laboratory testing program.

3.2 Compaction

The Champlain sea clay specimens were prepared using with two different compaction methods namely; static and dynamic compaction. The statically compacted specimens were prepared at varying water contents and densities using the brass compaction equipment shown in Figure 3.1. Care was taken to ensure that the specimen rings would not deform during the compaction process. The bottom of the compactor mold was designed to hold the specimen rings to achieve this objective. The specimen rings were securely fastened to the compactor base by four screws to allow for easier handling. The base of the ram is made of tapered Teflon to reduce friction between ram and the walls of the

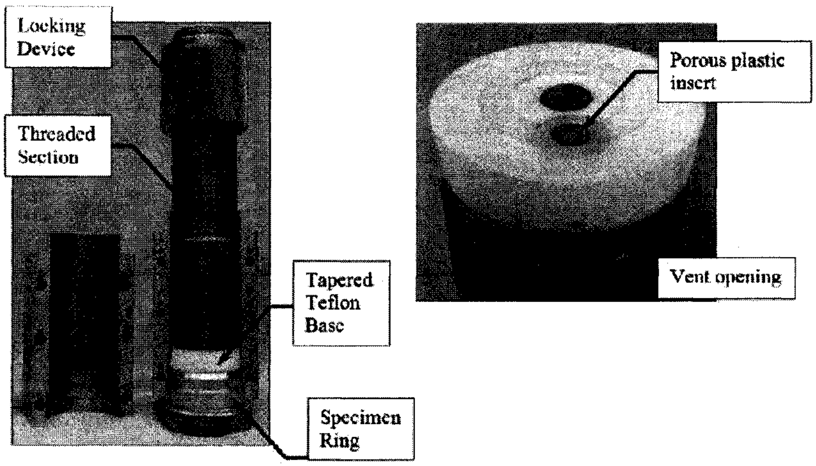

Figure 3.1: Specimen compactor mold and ram

mold thereby maximizing the compaction energy imparted to the soil. The Teflon base also formed a tight seal with the mold to prevent the soil particles from jamming the ram. A 25 *mm* circular piece of porous plastic was inserted into the Teflon base leading to an air vent to eliminate the possibility of vacuum developing inside the mold during compaction. The vent would allow any trapped air to escape out of the mold (Figure 3.1). For this research project, the specimens were compacted in one layer within the specimen ring. The diameter of ring used in this study was 50 *mm*. The initial height of the specimens were equal to 18 *mm*.

Three different stress levels were chosen for the static compaction tests; 1000, 2000 and 4000 *kPa*. A minimum of 10 specimens with different initial water content were compacted for every stress level. During static compaction, load cells and linear potentiometers were used to determine the compaction effort imparted to the specimen (Figure 3.2). ASTM D-698 standards were followed for preparing the specimen using dynamic compaction. All specimens were compacted at an energy level of 593 kJ/m^3 for Proctor tests. This energy level of 593 kJ/m^3 was attained by compacting the soil in three layers with a 2.5 *kg* hammer at 25 blows per layer.

3.3 Measurement of Soil Specimen Suction

Several devices that were conventionally used for the measurement of suction are detailed. Techniques and limitations associated with each device are summarized. Most of these

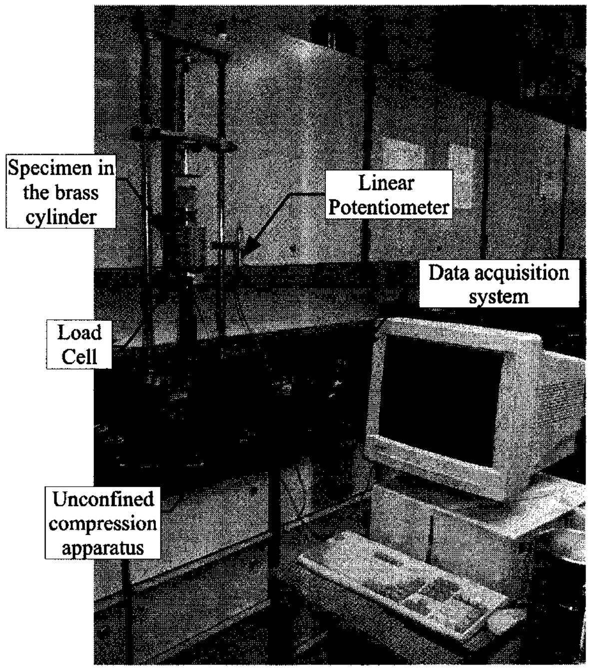

Figure 3.2: Statically compacting specimens with a constant strain rate

equipments were used in this research program.

3.3.1 Direct Measurement Techniques

The direct measurement of matric suction (i.e., negative pore water pressure with respect to the atmospheric pressure) using a tensiometer have generally been limited to a suction range of about 0-90 kPa. High capacity tensiometers or axis translation technique is commonly used for the direct measurement of matric suction values greater than one atmosphere. In this study, axis translation technique is selected for direct measurements for the suction range of 0 to 500 kPa.

Axis-translation Technique

The axis-translation technique works by shifting the reference pressure from the negative pore water pressure of the specimen to the applied positive air pressure within the pressure chamber (Hilf, 1956). This is achieved through use of a high air entry disc. The high air entry disc acts as a semi-impermeable membrane that allows the flow of

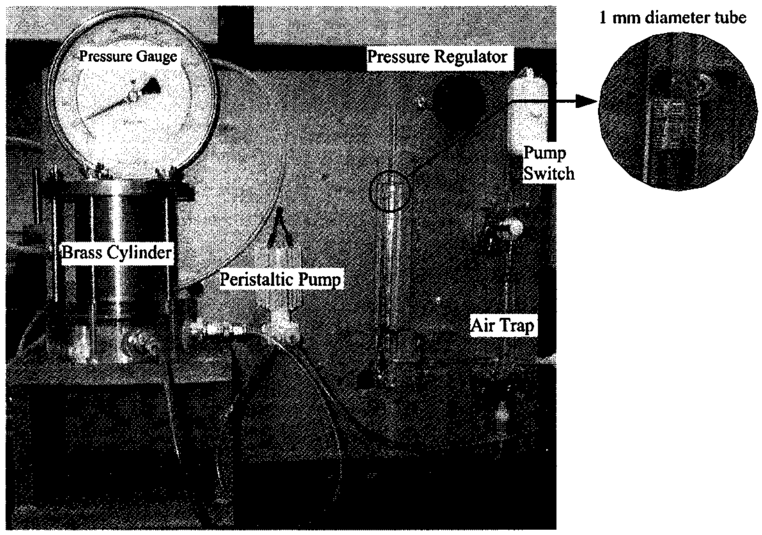

Figure 3.3: Modified axis-translation apparatus

water through its pores but restricts the flow of the applied air flow. In other words, the high air-entry disc acts as a divider between the negative pore water pressure of the soil specimen and the atmospheric pressure conditions.

Figure 3.3 shows the details of a null pressure plate system that was designed and developed to measure the matric suction of compacted unsaturated soil specimens following the axis translation technique (Hilf, 1956). The four main components of the null pressure plate system are: the pressure chamber with a high air-entry stone (air-entry value equals to 500 kPa), pressure gauge or transducer for measuring and recording of the matric suction measurements, and the flushing system.

The two pressure chambers used in the null pressure plate system were designed and developed at the University of Ottawa's in-house machine shop (see Figure 3.3) (Power, 2005). The apparatus has a brass cylinder, cap, and an acrylic base. Matric suction is measured by increasing or decreasing the applied air pressure of the chamber. The pressure within the chamber is measured by a pressure gauge which has a maximum limit of 700 kPa. Figure 3.4 shows the details of the acrylic base of the pressure chamber.

The base was made from acrylic instead of brass to facilitate the viewing of the air bubbles developing during the test, if any, with the naked eye. The spiral groove pattern in the bottom of the base is to aid in the removal of air bubbles that may develop during testing. The grooves are small enough but facilitate the water pumping of through it using the peristaltic pump to remove the air bubbles trapped within the grooves and force them to flow out into the air-trap burette of the flushing system. Because the base was made from acrylic, "O-seal straight threaded" fittings were used for the inlet and outlet connections between the base and the flushing system. Care has taken when tightening the regular National Pipe Thread (NPT) pipe fittings located on the base such that it would not crack the base and allow both air and water leak into the system.

An O-ring located in a separate circular groove on the bottom of the base was the original method of sealing the connection between the high air entry disc and the pressure chamber base (Figure 3.5). It was discovered that the O-ring would compress as the air pressure within the chamber is increased producing erroneous matric suction measurements during preliminary testing. The new design called for a separate circular O-ring groove to be placed around the outside of the base (Figure 3.5). The new O-ring groove would allow the stone to sit flush with the bottom of the acrylic base and be sealed around the outside diameter of the metal ring. The five, 150 *mm* screws that pass through the base are bolted to the cap of the pressure chamber to securely seal the specimen inside.

Figure 3.6 shows the ceramic discs used in the null pressure plate apparatus. The disc sits flush with the bottom of the acrylic base and is sealed into place using a 3 *mm* diameter O-ring.

It is essential to remove any air bubbles that form under the saturated ceramic discs in order to apply the axis-translation technique in reliably determining the matric suction of a specimen. Although distilled, de-aired water was used in the null pressure plate system, over time, more dissolved air can come out of solution producing erroneous

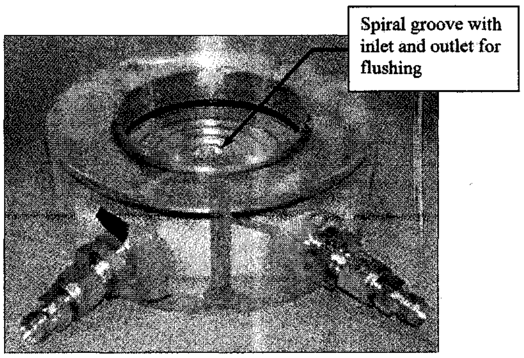

Figure 3.4: Pressure cell base with O-ring seal straight threaded fittings

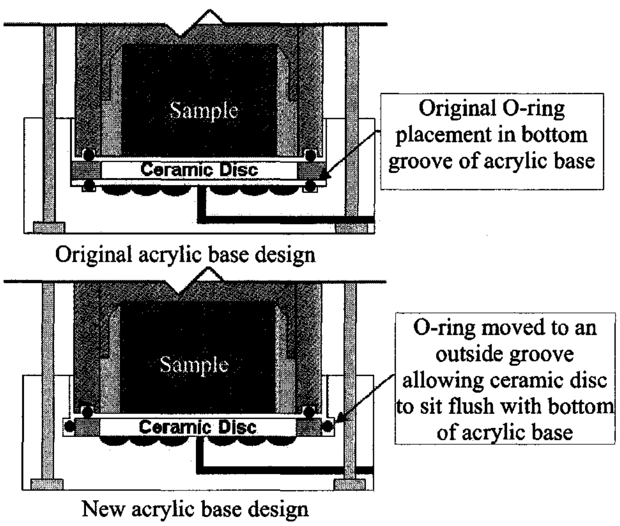

Figure 3.5: O-ring details for sealing ceramic discs in acrylic base

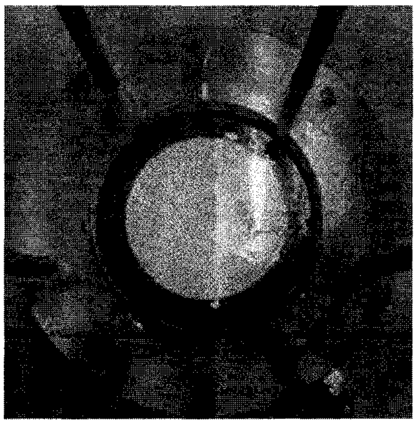

Figure 3.6: A 500 kPa high air entry disc saturated and sealed in the pressure cell base

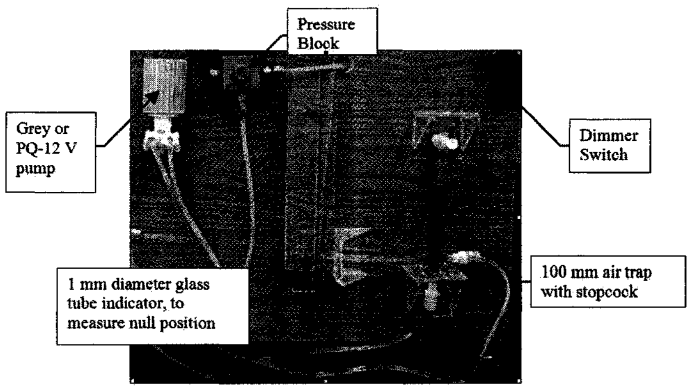

Figure 3.7: Flushing system for null pressure plate system

suction measurements. Garga & Zhang (1997) studied the rate at which de-aired water would re-oxygenate when left in a container open to the atmosphere. Through this study it was shown that diffusion of air into the container was substantial even after short period of time. It is therefore important to incorporate a flushing system to periodically remove any dissolved air that can appear within the null pressure plate system during testing (Bishop & Donald, 1961). The important features of the flushing system are: the pump and dimmer switch, the air trap with stopcock, and the glass tube to indicate the null position during testing (Figure 3.7). The applied air pressure in the pressure chamber is increased or decreased depending on the movement of water from the original null position in the glass tube. A decrease in water volume in the glass tube means that the water is being absorbed by the specimen. This means that the matric suction of the specimen is greater than the air pressure in the chamber. Flow of water into the system is stopped by increasing air pressure within the chamber. A 1 mm diameter tube was used to indicate a change in the null position which makes it possible to determine a change of 0.785 mm^3 of water with a change o f 1 mm change in the tube.

Pressure Plate Apparatus

The pressure plate apparatus essentially works on the same principle as null pressure plate apparatus but has a larger diameter high air-entry disc (Figure 3.8). This apparatus is useful to test several specimen at a time. A flushing system is necessary for the pressure plate apparatus as well for reliable determination of the SWRC. However, the same flushing system similar to the null-pressure plate apparatus was not applicable in that case since the chamber was not equipped with grooves underneath the ceramic disc.

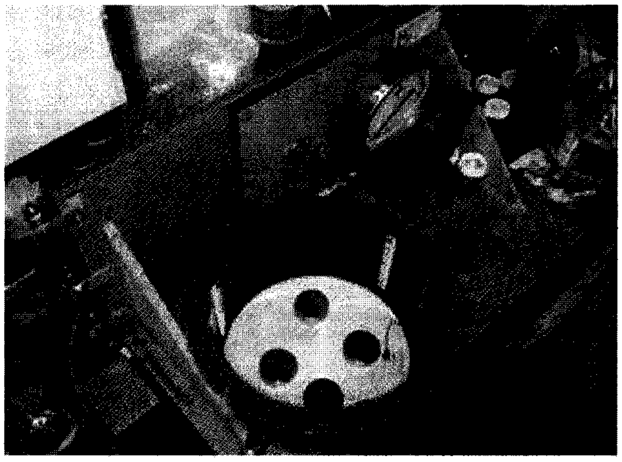

Figure 3.8: Testing using pressure plate apparatus

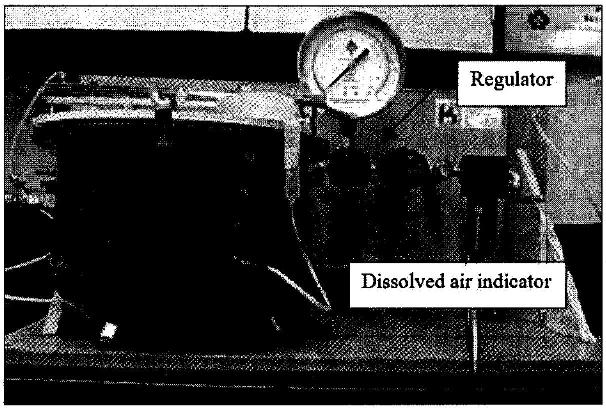

Figure 3.9: The flushing system used for the pressure plate

Therefore, flushing was accomplished by first reducing the pressure in the tank, through the use of a syringe attached to an aspirator and turning the water on to apply the suction to remove the air bubbles that had formed under the ceramic disc (Figure 3.9).

3.3.2 Indirect Measurement Techniques

Psychrometer

Wescor HR-33T Microvoltmeter, referred to as psychrometer through the remainder of the text, was used for the indirect determination of water potential (Figure 3.10). This psychrometer allows measurements to be made with either the hygrometric (dew point depression) or the psychrometric (wet bulb depression) method. The details of the working principle of psychrometers are summarized in Chapter 2. The physics of each mode is essentially the same, differing primarily in terms whether or not temperature is actively controlled at the measurement junction. In other words, both methods of measurement after proper calibration would provide a value of the same water potential. However, the sensitivity coefficient of the hygrometric method is approximately twice that of the psychrometric mode. Therefore, the hygrometric method is often prefered.

The hygrometric measurement technique was first introduced by Neumann & Thurtell (1972) and modified by Campbell et al. (1973). The basic working principle of this technique can be explained as; if held at the dew point temperature, a wet thermocouple junction will neither lose water through evaporation nor gain water through condensa-

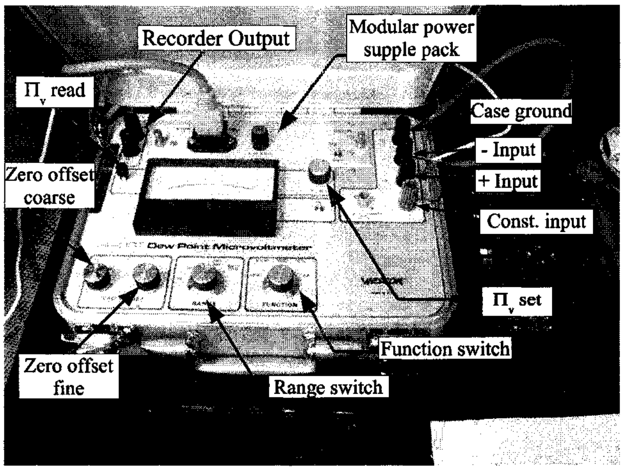

Figure 3.10: HR-33T Microvoltmeter

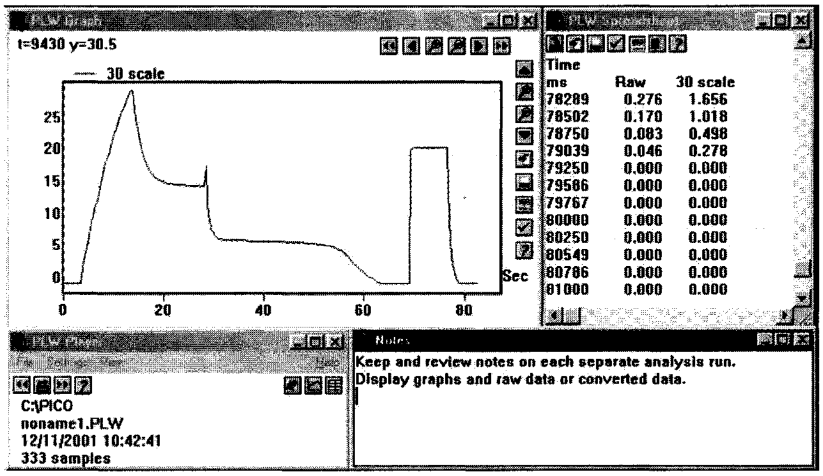

Figure 3.11: A typical result obtained using the psychrometer

tion. Vapor pressure is regulated by controlling the applied Peltier cooling current to maintain the temperature of the water on the sensing junction at the dew point. Thus, the heat flow to the sensing junction from the surrounding air is offset by adjustment in the applied cooling current. Due to this reason no water evaporates or condenses and measurements can be made without disturbing the vapor equilibrium in the chamber. This technique eliminates most of the temperature-dependent parameters that influence the psychrometric measurement. The pressure dependence of the measurement is also eliminated as no water-vapor diffusion occurs. The fact that dew point temperature depression is greater than wet bulb temperature depression increases the sensitivity of the hygrometric technique over that of the pscyhrometric technique. Theoretical considerations show sensitivity to be 7.5 $\mu V\ MPa^{-1}$ at 25^0C; this value is about 1.7 times greater than psychrometric sensitivity (Campbell *et al.* , 1973).

Figure 3.11 shows a typical result obtained from the psychrometer using hygrometric method.

Sample chamber sensors are typically used for laboratory measurements of soil water potential. Various chamber-wall materials and chamber -thermocouple-sample geometries have been used since original chambers of Spanner (1951) and Richards & Ogata (1958). Experiments showed that the time required for samples to reach equilibrium with chamber air varied due to the influence of these factors. Chambers made of brass and stainless steel adsorbed less water and equilibrated more rapidly than chambers with materials such as polyethylene and Teflon. Eventually, stainless steel was selected for use in the chamber because it is much more resistant than brass towards oxidation or corrosion and is easy to clean for maintenance purposes (Millar, 1971).

The sample chamber made of stainless steel (available from Wescor, Inc.) is used in this study (Fig. 3.12). This chamber allows single samples contained in metal sample holders to be inserted into the position for measurement without disassembling the apparatus. When the sample is in place, the metal thermocouple mount is pressed against the sample holder and the measurement chamber is sealed with an O-ring by turning the cap screw. This unit does not permit the sensing junction to protrude into a cavity within the soil, but rather the sensing junction is placed just above the sample. The metal-to-metal contact and thermal shielding provided by the aliminum housing give adequate thermal stability for measurement to be made in the laboratory without a controlled temperature water bath. This sample chamber uses a Peltier sensor that can be used either with the pscyhrometric or hygrometric mode depending on the type of equipment used. The measurement range is from about -0.05 MPa to -8 MPa nominally, but with a capability to -300 MPa using special pscyhrometric techniques (Wiebe, 1981; Wescor, 1998).

The thermocouple transducer was calibrated using NaCl solutions with molalities of 0.053, 0.157 and 0.55 corresponding to 250, 725 and 2500 kPa suction values respectively. Figure 3.13 shows the calibration curve for the transducer used in this study.

3.4 Triaxial Cell

The saturated hydraulic conductivity values, k_{sat} of compacted specimens were measured using a triaxial cell assembly unit. Several accesories of the cell are shown in Fig. 3.14.

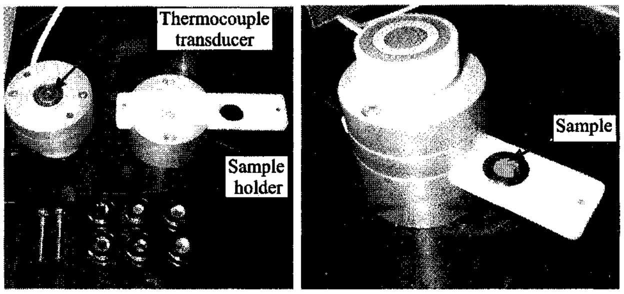

Figure 3.12: The sample chamber

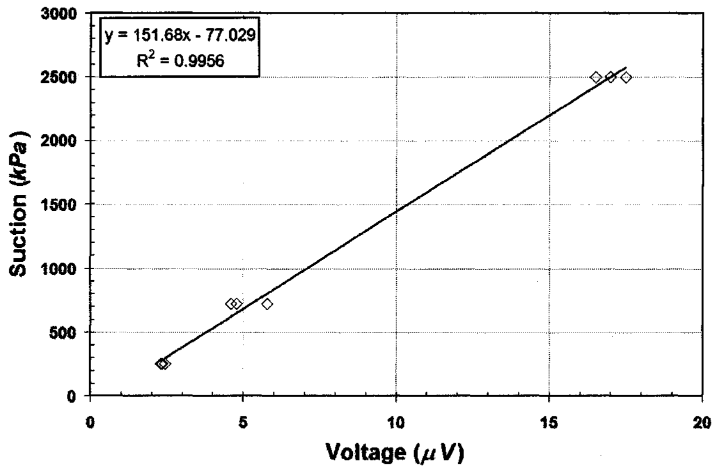

Figure 3.13: The calibration curve for the psychrometer

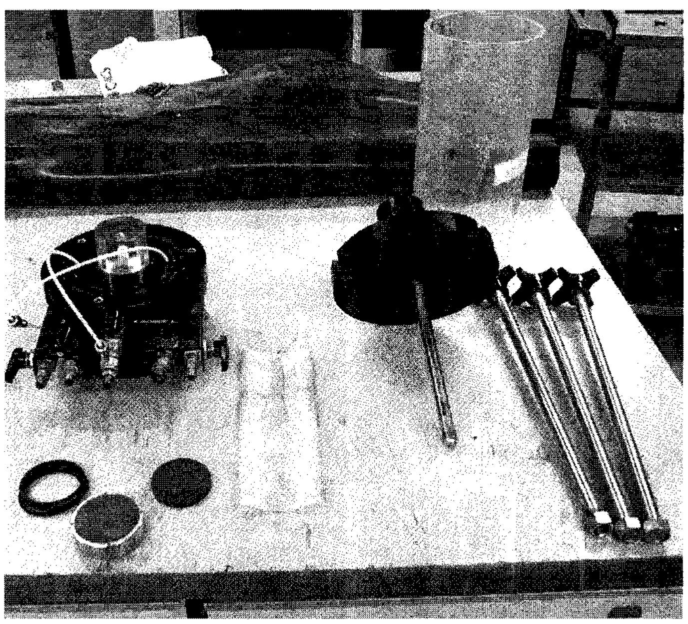

Figure 3.14: The triaxial cell and accessories

3.5 Additional Tools

X-ray Diffractometer

The X-ray diffraction method was used to determine the minerals present in the Champlain sea clay tested in this research program. This experiment was undertaken in University of Ottawa, Earth Sciences Department Laboratory.

X-rays are electromagnetic radiation of wavelength about 1 $\AA$, which is about the same size as an atom. As an X-ray beam travels through any substance, its intensity decreases with the distance that the X-ray travels through the substance (Warren, 1969). Bragg's law should be satisfied in order to diffraction occur. (Figure 3.15).

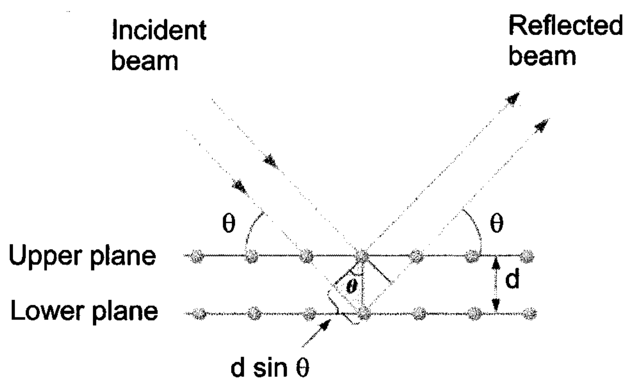

Figure 3.15: Bragg's law application

To achieve diffraction, either a range of X-ray wavelengths are used or the crystal is rotated or a powder or polycrystalline specimen is used. X-ray diffraction has been in use in two main areas, for the fingerprint characterization of crystalline materials and the determination of their structure. Each crystalline solid has its unique characteristic X-ray powder pattern which may be used as a fingerprint for its identification. Once the material has been identified, X-ray crystallography may be used to determine its structure, (i.e. how the atoms pack together in the crystalline state and what the interatomic distance and angle)

X-ray diffraction is one of the most important characterization tools used in solid state chemistry amd materials science (Warren, 1969). However, this process is tedious and cumbersome because every soil mineral has several different crystalline states. For example, montmorillonite has 50 different crystalline states.

Transducers

A linear vertical displacement transducer (LVDT) was used to measure the vertical deformation of the specimen as shown in Fig. 3.2. The LVDT was calibrated using a micrometer(Figure 3.16).

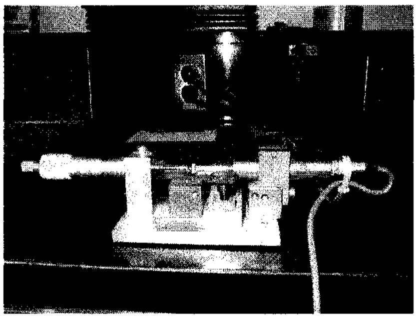

Figure 3.16: LVDT calibration method

Figure 3.17 shows the calibration curve developed and used for the experimental analysis.

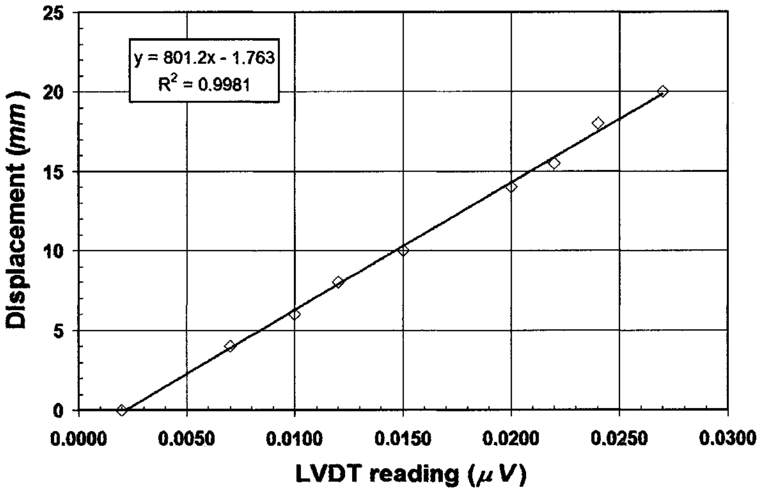

Figure 3.17: Calibration curve for the LVDT

A load cell with a maximum capacity of 4500 *kg* (i.e., 10000 *lb*) was used to measure the load that is applied to the specimen. The calibration technique and resulting calibration curve are shown in Figs. 3.18 and 3.19, respectively. These transducers are

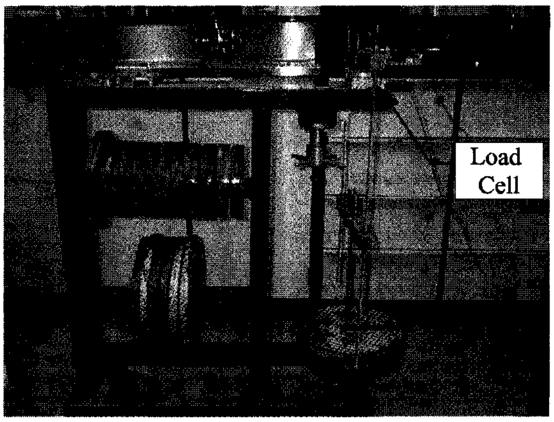

Figure 3.18: Load cell calibration method

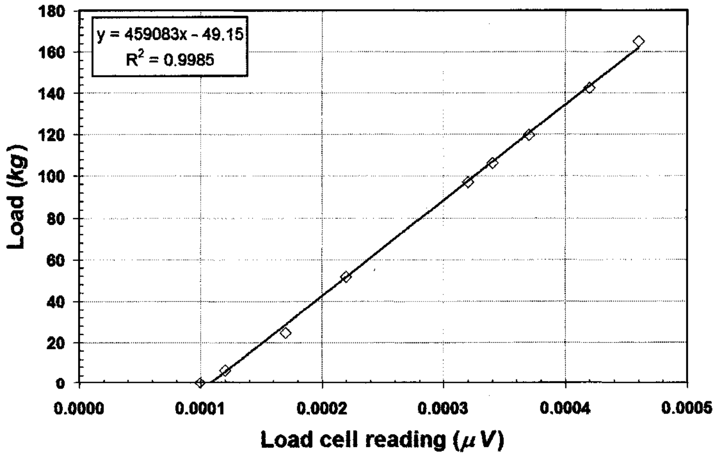

Figure 3.19: Calibration curve for the load cell

connected to a PC-based data acquisition system, thus allowing the specimens state to be continuously monitored.

Figure 3.20 shows the specimen extractor from the compacted specimens. The equipment was made of stainless steel and the shaft has a clear diameter of 20 *mm*. Specimens with a volume of 3000 to 4000 mm^3 were extracted from the compacted specimens using this extractor, .

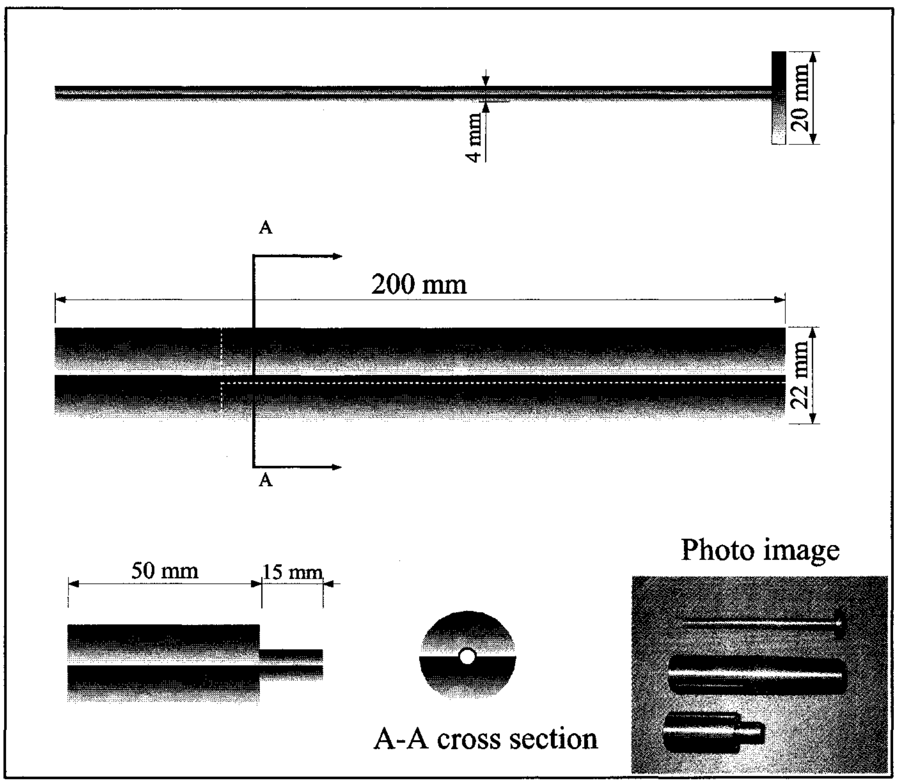

Figure 3.20: Specimen extruder details

3.6 Summary

This chapter summarizes details of the equipment employed in determining both the water retention behavior and the suction values of the Champlain sea clay specimens used in this research project. Pressure plate apparatus and triaxial cell was used to measure SWRC and K_{sat} values respectively. To measure suction, two different methods were used namely; the axis-translation technique, and the psychrometer. To determine the matric suction using the first method, a null pressure plate system was specially designed to perform the axis-translation technique. Details of additional tools (i.e., specimen extractor, LVDTs, load cells) were also presented.

Chapter 4

Experimental Results and Discussions

4.1 Introduction

This chapter begins with the details on the soil and specimen preparation used for the compaction and water retention tests. Experimental procedures and results are then presented. First, the compaction results are detailed along with the post-compaction suction values. Second, the water retention results are discussed; the SWRCs are plotted using different variables such as gravimetric water content and degree of saturation to show the effect of volume change (i.e., shrinkage). The saturated hydraulic conductivity values which are determined using triaxial cell are also presented. Finally, the unsaturated hydraulic conductivity functions which are determined using the saturated hydraulic conductivity and the SWRC information are discussed.

4.2 Testing Program

Figure 4.1 presents the experimental program in the form of a flow chart that was followed in this study.

4.2.1 Soil

The soil used in this research project was Champlain sea clay obtained from Ottawa, Ontario. This soil was chosen because it is abundantly found in Ontario and Quebec

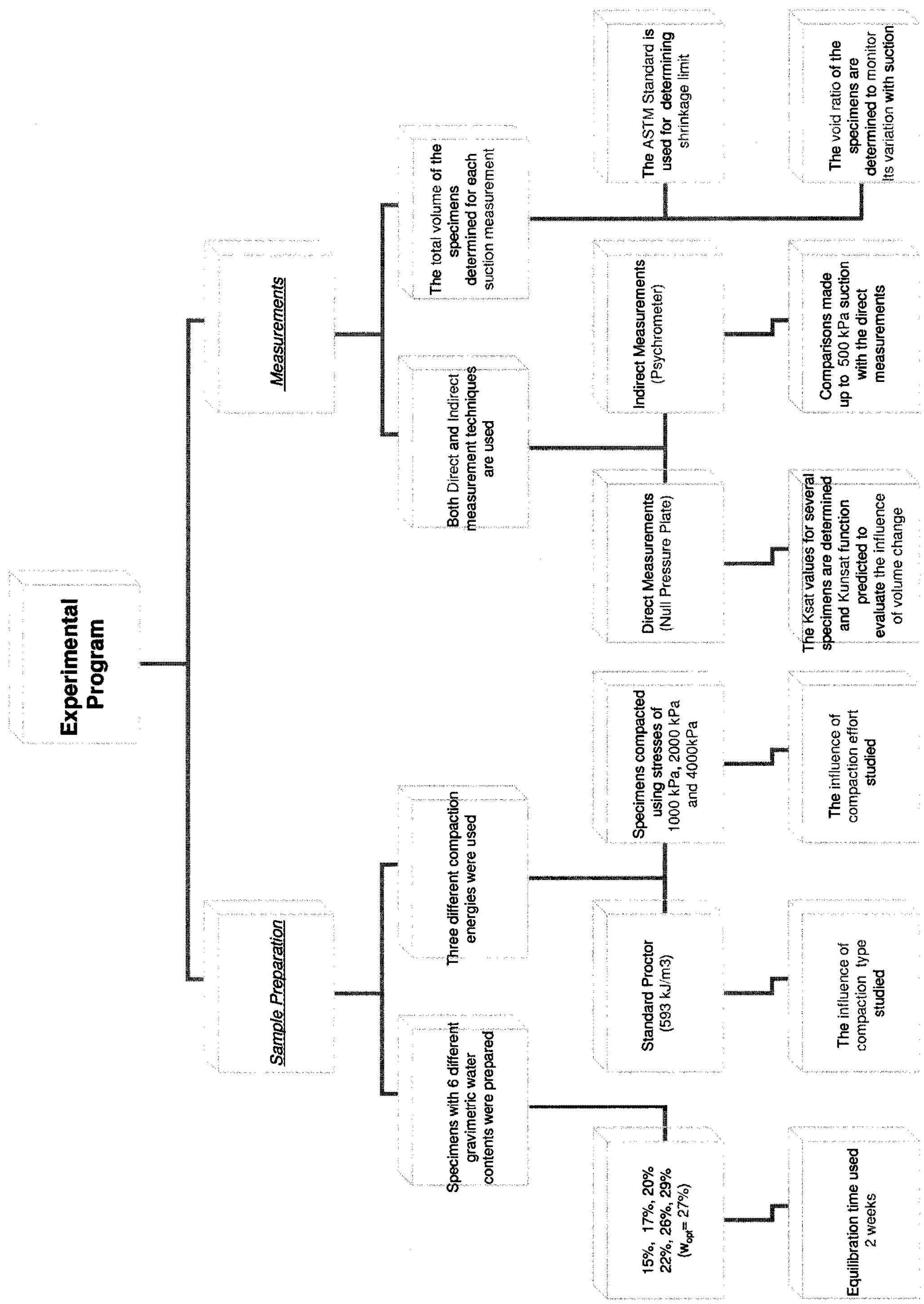

Figure 4.1: Flow chart for the testing program

region and used in several projects related to geotechnical engineering (Bozozuk, 1962; Tavenas *et al.* , 1974; Chiasson, 2005). In addition, extensive research studies have been undertaken using Champlain sea clay over the last couple decades and valuable information is available in the published literature (Bentley, 1979; Quigley, 1980; Torrance, 1999).

The following laboratory tests were performed on the soil in general accordance with ASTM standards:

- Grain-size analysis: mechanical and hydrometer method (ASTM D-422)
- Atterberg limits tests (ASTM D-4318)
- Shrinkage limit test (ASTM D-427)
- Specific Gravity (ASTM D-854)

Figure 4.2 shows the grain size distribution of the clay obtained from wet sieving and hydrometer tests and Table 4.1 shows the basic properties of the the soil.

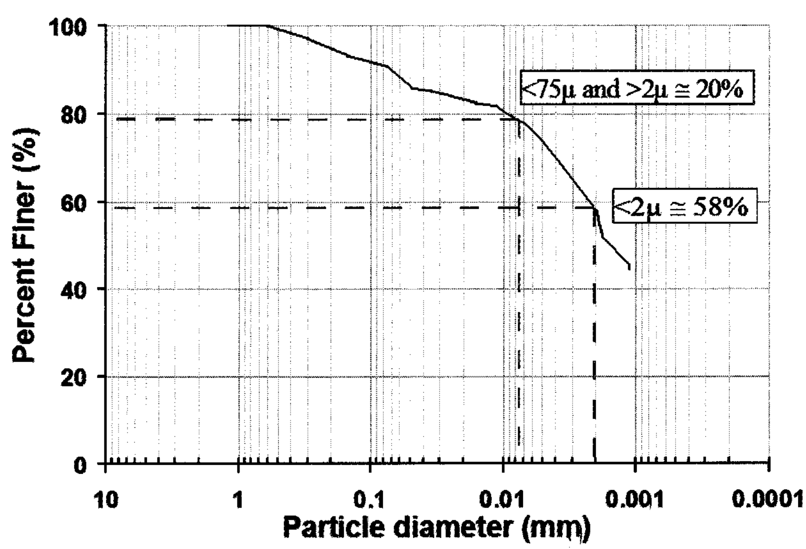

Figure 4.2: Grain-size distribution for the Champlain sea clay

4.2.2 Compaction Considerations

Two different compaction procedures were used in this study; static and dynamic compaction. The specimens were compacted to three different energy levels using static

Table 4.1: Basic properties of the clay used in this study

Soil Property	**Value**
Natural water content	40 %
Plastic limit, w_p	26 %
Liquid limit, w_L	63 %
Plasticity index, I_p	37 %
Shrinkage limit, w_s	19.5 %
Specific gravity, G_s	2.75
USCS Classification	CH

compaction procedure (i.e. 1000, 2000, 4000 kPa). The force applied to the specimen and the displacement of the specimen were continuously monitored while the specimens were being statically compacted. This information is used to compute the energy imparted to the specimen.

In the dynamic compaction, standard proctor tests were performed on the specimen to obtain the compaction energy that could be imparted to the soil by following ASTM D-698 Standard. The specimens were compacted in 3 lifts. For each lift, the water content and suction values were determined. These values were then plotted as a profile to discuss the heterogeneity of the dynamically compacted specimens.

These two methods; static and dynamic compaction are also compared in the light of experimental results. Comparisons were also presented with respect to the energy that is imparted to the soil and the post-compaction suction values of the specimens.

4.2.3 Soil Preparation

The Champlain sea clay used in this testing program was collected from a site in Ottawa by digging an open pit. A large quantity of dug up soil in a disturbed state was collected from a depth of 2 m and stored in barrels. The in-situ water content was approximately 40%, and the X-ray diffraction tests show that the mineralogy is dominated by quartz, feldspars, pargasite, and kaolinite (See Appendix A). The results were consistent with the data of Torrance (1999).

All non-soil particles (i.e. grass and bark) and the larger sized pebbles and rocks were manually removed. The soil collected from the site was relatively wet with respect to natural water content. The wet soil was first air-dried, and subsequently grinded and sieved. The soil particles passing through the U.S. Standard # 10 sieve (i.e., 2 mm opening) was used in the testing program.

The soil was thoroughly mixed with a predetermined amount of water according to the planned testing schedule before preparation of specimens for compaction and water retentions test. The prepared sample was then stored in double plastic bags, and left for moisture equilibrium for at least 2 weeks. Several researchers used similar procedures for equilibration for the moisture equilibrium for fine-grained soils (Marinho & Chandler, 1993; Cui & Delage, 1996; Vanapalli *et al.* , 1999; Tarantino & Tombolato, 2005). The water content of the specimens were determined by taking a couple of specimens from different parts of the bags after 3 weeks. The specimens were then placed into the compaction mold and either statically or dynamically compacted according to the planned testing schedule.

The specimens were again left for moisture equilibrium for a period of one week after preparing the compacted specimens to be used for the determination of SWRC measurements. The specimens were then placed into pressure plate apparatus after saturating the high air-entry ceramic disc. The ceramic disc was simply saturated by applying a water pressure of 50 kPa from the bottom of the disc for a period of 2 days. The specimens were then saturated using a pressure of 20-30 kPa in the pressure plate apparatus. Several trial studies showed typically a time period of 1 day was sufficient to fully saturate the specimens. After the specimens were saturated in the pressure plate, they were subjected to 25 kPa suction value, to drain the free water on the surface of both the specimen and the ring. An applied air pressure of 25 kPa had little or no influence on was not effecting the water within the soil pores since the air-entry pressure for fine-grained soils is typically well over several hundreds of kPa.

The specimen volume and mass properties were determined after saturation. The specimens were then subjected to air pressure values of 100, 200, 400 kPa for a time period of 3 days (Fig. 4.3). The height and mass measurements were again determined using a displacement gauge after equilibrating each applied suction value. Next, small specimens, with a volume of approximately 3000-4000 mm^3 were extracted from these specimens to continue the SWRC (Figs. 4.4 and 4.5). Fleureau *et al.* (2002) followed similar procedures in their reseach for determining the SWRCs of Jossigny silt and FoCa clay.

There are three main reasons of extracting small size specimens from the prepared compacted specimens in 50 mm diameter ring;

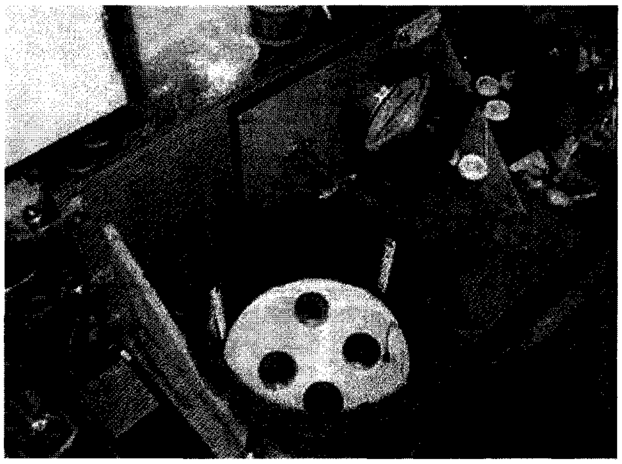

Figure 4.3: Compacted specimens placed in pressure plate apparatus

- In the preliminary tests, it was noticed that the specimens tend to crack during drying (i.e., after 500 kPa suction) due to the size of the specimen being relatively large. As a result, it was difficult to reliably determine the total volume of the specimens. Using small specimens reduces cracking due to the shrinkage problem.
- The maximum air pressure that can be applied using pressure plate is 500 kPa, (i.e., air-entry value of the ceramic disc). At this suction value, the specimens are still close to saturated conditions. For this reason, there was a need to use other

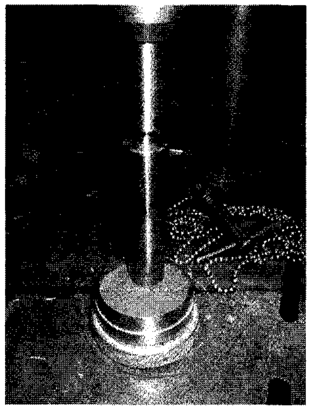

Figure 4.4: Procedure and tools for extracting the specimens

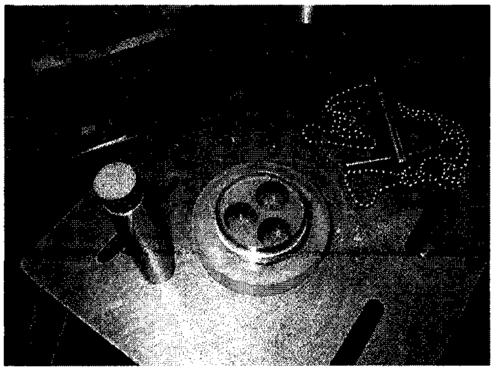

Figure 4.5: Extracted specimen

techniques for the measurement of suction values in specimens above 500 kPa

- The testing period reduces significantly using small specimens. Also several small specimens can be prepared from each specimen.

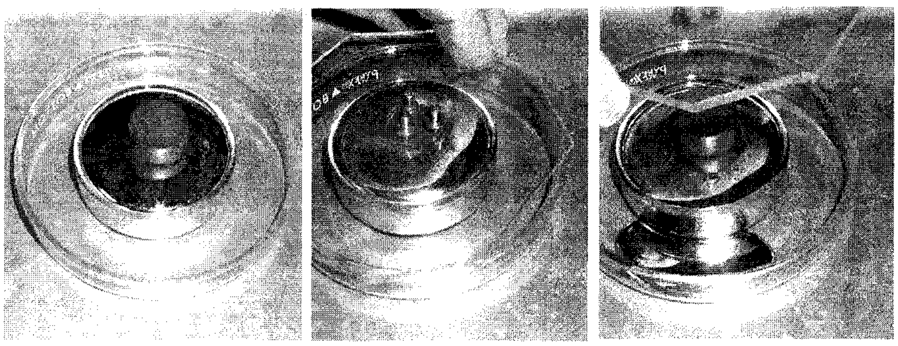

(a) (b) (c)

Figure 4.6: Volume measurements using mercury

The prepared small specimens were then air-dried in a humidity controlled environment while the mass of the specimens were continuously monitored. The specimens were put into sealed bags and left for moisture equilibrium for a period of 3-4 days after achieving the desired mass that was calcualted. The specimen volume and suction measurements were then determined (Fig. 4.6).

The change in degree of saturation was determined as follows:

$$\mathbf{\Delta S} = \frac{V_{v_f}V_{w_i} - V_{v_i}V_{w_f}}{V_{v_i}V_{v_f}} \tag{4.1}$$

where;
ΔS : change in degree of saturation
V_{v_i} : initial volume of voids
V_{v_f} : final volume of voids
V_{w_i} : initial volume of water
V_{w_f} : final volume of water

The volume of voids in the above equation can be determined using the total volume and volume of solids. Then, the change in degree of saturation, ΔS was plugged in the following equation for determining the change in void ratio, Δe:

$$\mathbf{\Delta e} = \frac{\Delta w G_s - \Delta S e_i}{S_f} \tag{4.2}$$

where;
Δe : change in void ratio
Δw : change in water content
G_s : specific gravity
e_i : initial void ratio
S_f : final degree of saturation

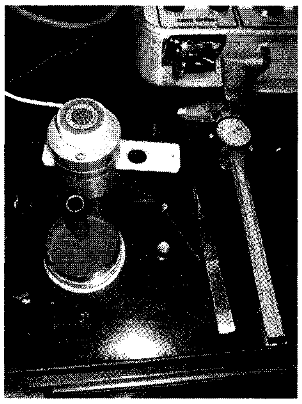

Figure 4.7: The procedure and tools for extracting the specimens for the psychrometer measurements

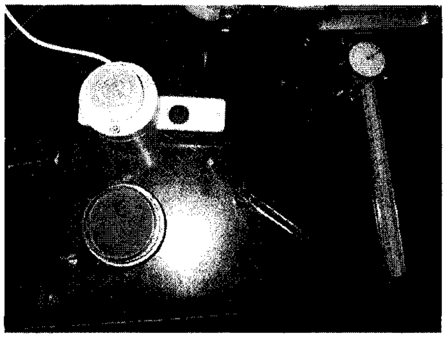

Figure 4.8: Extracted specimen for the psychrometer measurements

The suction values of the specimens were then measured using a psychrometer. Since the specimen holder size was 10 *mm* in diameter and 9 *mm* in height, a small specimen extruder was used to obtain the specimens for suction measurements (Figs. 4.7 and 4.8). Specimens of 50 *mm* in diameter were extracted from the compaction mould as shown in Figs. 4.9 and 4.10 to be used for soil-water retention curve measurements.

4.3 Results and Analysis

The experimental results are reported in two sections. In the first section, the compaction results are summarized. In the second section, the water retention properties are presented and discussed.

Figure 4.9: Extracting the specimen after dynamic compaction

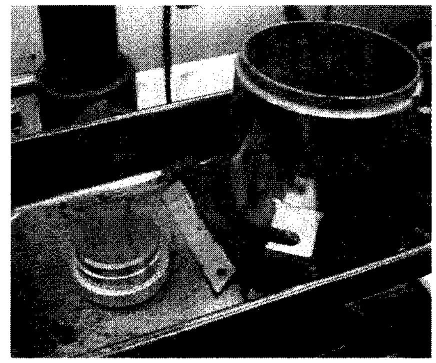

Figure 4.10: Extracted specimen from the compaction mold

4.3.1 Compaction Results

Static Compaction Test

A total of 34 statically compacted specimens were prepared using different levels of compaction stresses, 1000, 2000 and 4000 kPa and water contents ranging from 13% to 29% covering both the dry and wet of optimum water content conditions. The testing program was planned to study a broad range of initial compaction water contents on the water retention and compaction characteristics. The unit weight-water content compaction curves associated with compaction vertical stresses are shown in Fig. 4.11. The contours of equal degrees of saturation are also shown. The maximum dry unit weight for the soil specimens tested was achieved by the 2000, 4000 kPa compaction curve at a degree of saturation of about 92% and 88% respectively. All the data points that belong to the 1000 kPa compaction curve lie on the dry of optimum side for the water content ranging from 13% to 29%. These specimens were compacted with a constant strain rate of 0.8 mm/min as explained in Chapter 3. Figure 4.12 shows the force-displacement curves for each specimen.

It is interesting to note from this graph that the 'close to saturation' and 'close to dry' specimens, with initial compaction water contents of 13.2% and 28% respectively, have almost the same force-displacement relationship. Any further increase of force beyond 300 kg (or 1350 kPa) does not produce a significant displacement. This shows that the trapped air in 'close to dry' specimen, and trapped water in 'close to saturation' specimen prevent the further deformation of the specimens.

The energy that is imparted to the soil by statical compaction was also calculated

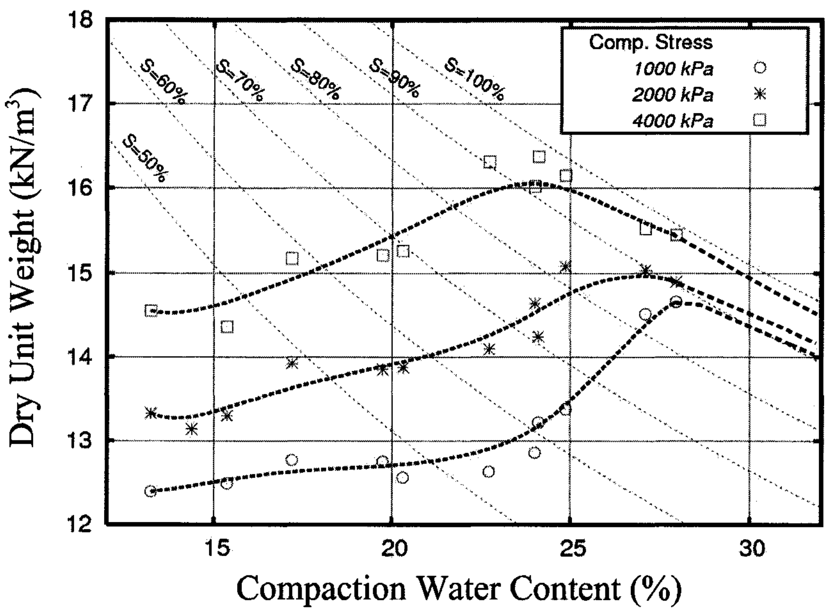

Figure 4.11: Compaction curves for three different stress levels

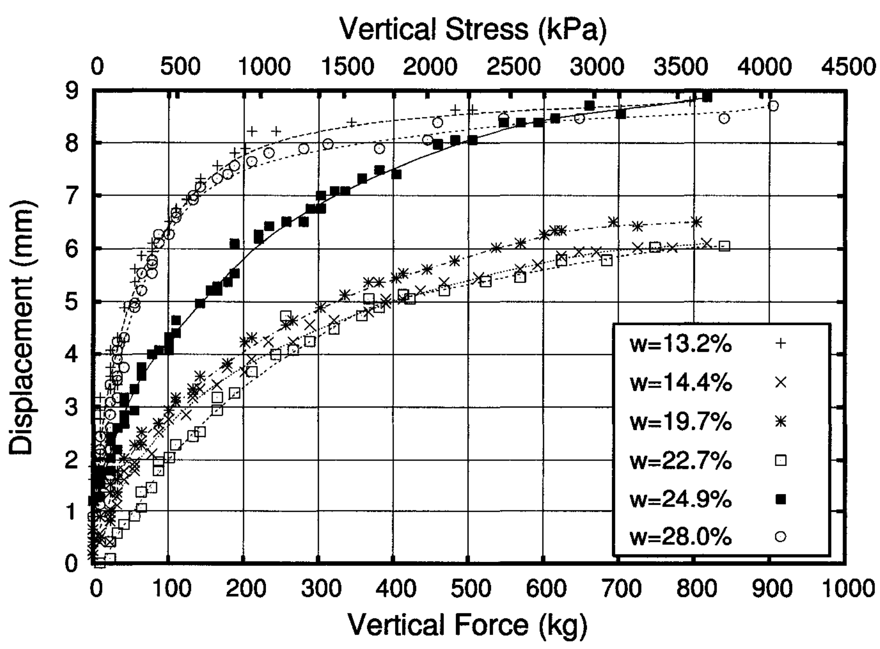

Figure 4.12: Force-stress-vertical displacement data for compaction tests (essentially undrained)

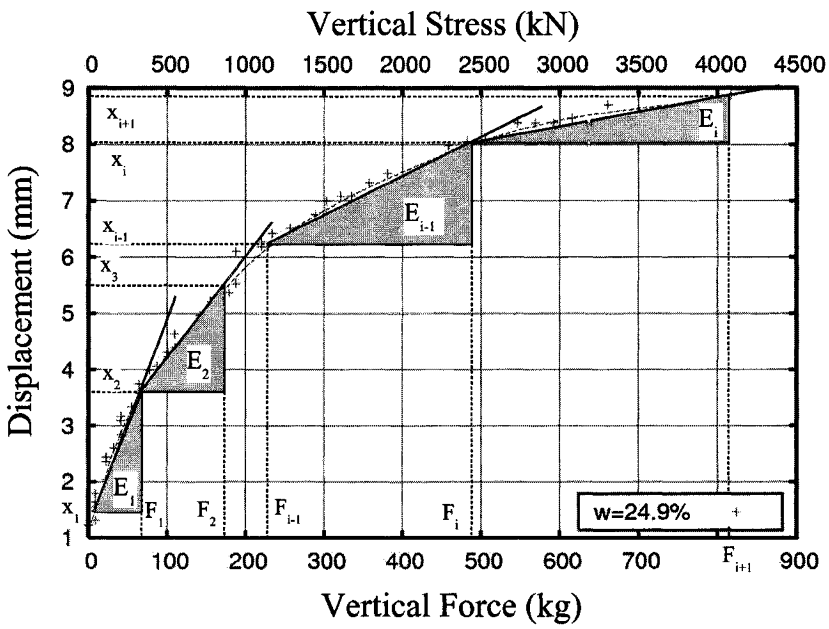

Figure 4.13: Energy Calculations

from the force-displacement curves of the specimens (Fig. 4.13):

$$\sum_{i=1}^{n} E_i = \frac{1}{2}\sum_{i=1}^{n}(F_i - F_{i-1})(x_i - x_{i-1}) \tag{4.3}$$

The highest energy is imparted to the soil specimen compacted at optimum water content with the same stress level(See Fig. 4.14).

The post-compaction suction values of the specimens compacted at the wet of optium were first tried to be measured using axis-translation technique. However, it was found that even the specimens compacted at the wet of optimum have suction values higher than 500 kPa. Therefore all the post-compation suction values were determined using psychrometer. The comparisons for the psychrometer and axis translation technique were conducted on loosely compacted and close to saturated specimens. These results show that psychrometer provides meaningful and comparable results for suction values starting from 400 kPa.

Figure 4.15 shows the post-compaction suction values associated with each specimen. At least two specimens were extruded from each compacted specimen to be used for suction measurements. The suction values were typically ranging from 1700 kPa to 8500 kPa. At least three measurements were taken from a specimen to determine the suction

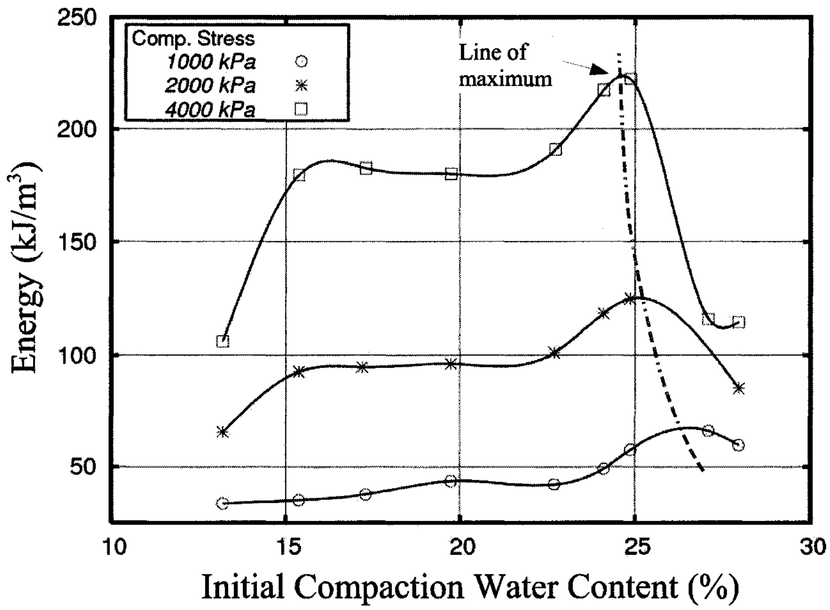

Figure 4.14: Energy - initial compaction water content relationship

of that particular specimen. The variation of these measurements never exceeded ± 260 kPa. This value corresponds to ± 2 μV for the psychrometer (See Fig 3.13 in Chapter 3).

Fig. 4.16 shows the degree of saturation and post-compaction suction of the compacted specimen. These results are grouped for each compaction vertical stress. It is interesting to note that the air-occlusion suction for the specimens compacted at the same vertical stress is close to the post-compaction suction of the specimen at the corresponding optimum water content. This result shows that the transition from dry to wet of optimum states corresponds to the transition from continuous to discontinuous air phase. Similar observations were reported by other researchers (Olson & Langfelder, 1965; Tarantino & Tombolato, 2005).

Fig. 4.16 shows the relationship between the degree of saturation, S, versus suction, ψ. This relationship looks like the suction values are increasing as the dry unit weight decreases and as initial compaction water content increases. In other words, an increase in dry unit weight causes an increase in the degree of saturation when the initial compaction water content kept constant.

It is also possible to get a better representation of the suction trends by plotting post-compaction suction values in 3D plots. Figure 4.17 shows 23 suction points on the

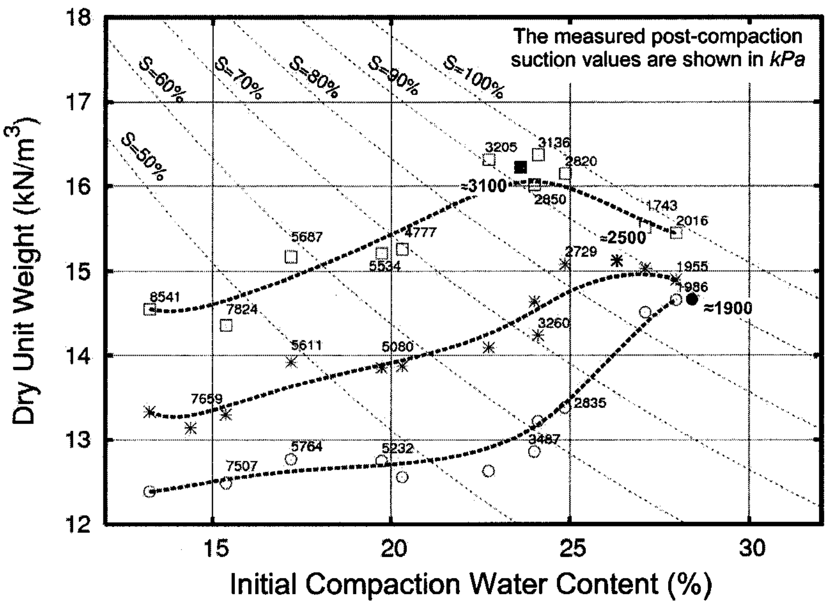

Figure 4.15: The post-compaction suction values (The red points show the suction values associated with optimum water contents, $\psi_{optimum}$)

dry unit weight-initial compaction water content plane. With a simple algorithm that uses an averaging method of $\frac{1}{d^2}$ (where d is the distance between the points) a 3D mesh was obtained and a suction surface was plotted 4.18 (Williams *et al.* , 2004).

These suction values were then projected on the dry unit weight, compaction water content plane, and plotted as contours (Figure 4.19). These results were discussed in a later section.

Dynamic Compaction Tests

The soil specimens with 3 different water contents were compacted using standard proctor energy. The post-compaction suction values of dynamically compacted specimens (with standard proctor energy) were consistently lower than the specimens compacted to the same dry unit weight with the same initial compaction water content. This result suggests that it is the soil structure that governs the engineering behavior of compacted fine-grained soils and not the compaction induced conditions. In other words, having the same void ratio and same initial compaction water content does not necessarily mean

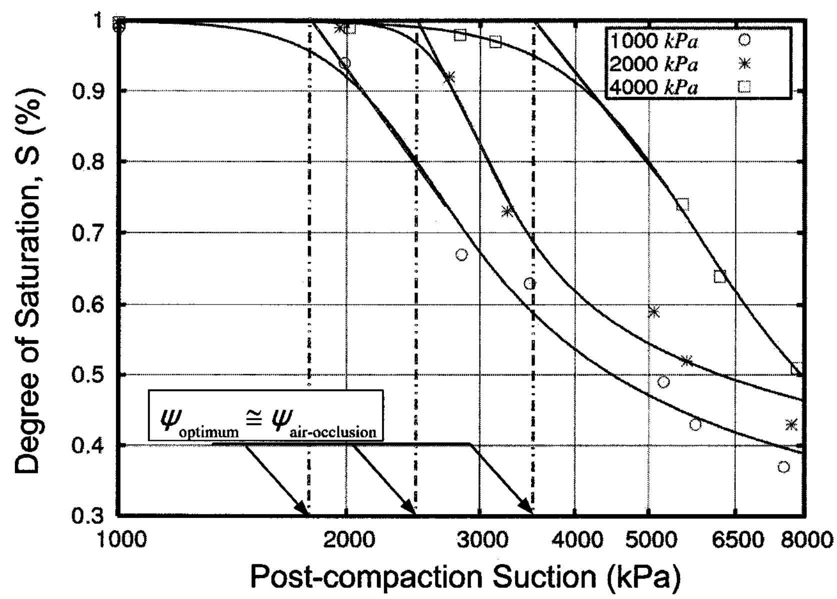

Figure 4.16: The degree of saturation versus post-compaction suction data for individually compacted specimens

that the soil structure will be the same. Several other researchers also highlighted this behavior (Cui & Delage, 1996; Vanapalli *et al.* ,1999; Tarantino & Tombolato, 2005). The specimens were compacted in three layers following ASTM D-698 standard. To check the variation of suction and water content values in the compacted specimens, small specimens were extracted from each lift right before the next lift was placed and compacted. When the compaction is complete, two more specimens are taken from the top and bottom of the dynamically compacted specimens. As a result, from each dynamically compacted specimen, a total of 4 measurements have been determined. The suction and water content profile of these compacted specimens are shown in Fig 4.21. From this graph, a variation of 1.8% was observed in terms of water content, which corresponds to a variation of 18% was determined in terms of suction for the specimens compacted in the Proctor mould. These results support the findings of Bouabdallah (1998). In fact, Fleureau *et al.* (2002) studies also demonstrates that in the case of a dynamic compaction, several additional factors such as the metal of the mould or the material on which it is placed during compaction, will influence the propagation of the shock waves and lead to different results in addition to the factors that influence

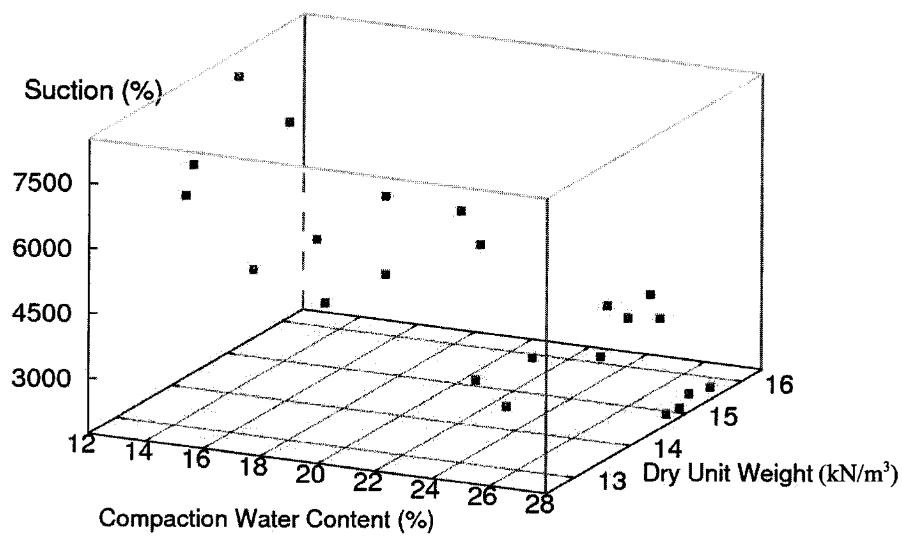

Figure 4.17: The relationship between compaction water content, dry unit weight and post compaction suction

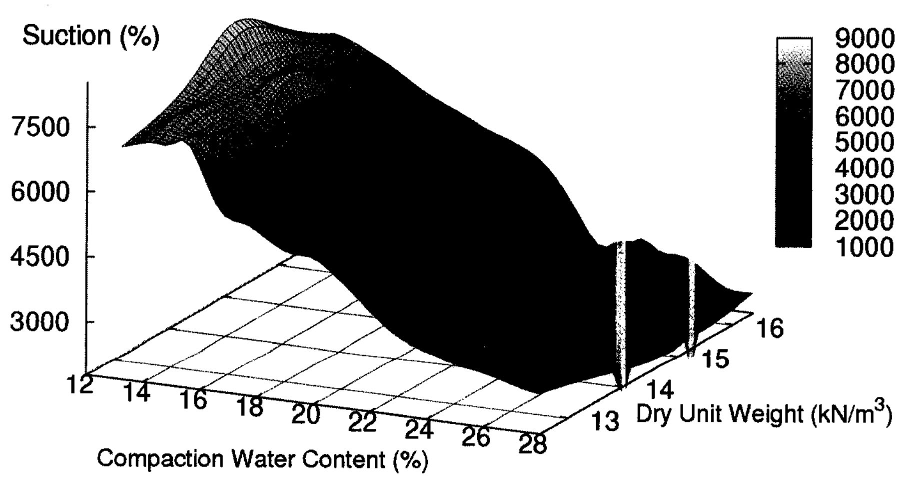

Figure 4.18: Suction contours for compaction curves as a 3D plot

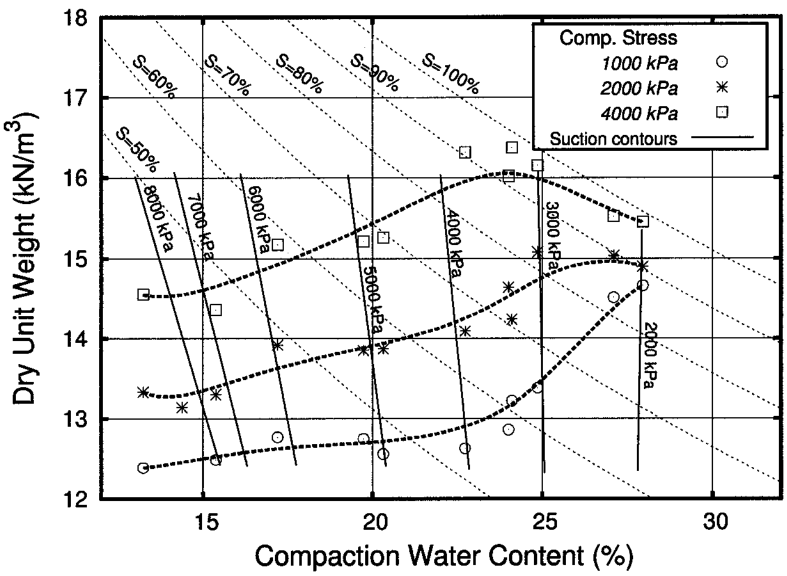

Figure 4.19: Compaction curves with suction contours

the specimens compacted using static compaction procedure (i.e., structure, mineralogy, compaction energy, etc.).

4.3.2 Influence of Void Ratio

Figure 4.19 summarizes the post-compaction suction contours for the statically compacted specimens measured using psychrometer. These suction contours are referred to as positive when the angle of the contour measured in clockwise with respect to the vertical axis is less than 90^0. The contour is said to have a negative slope otherwise. Fig. 4.19 shows that the suction contours have negative slopes for the specimens compacted at dry of optimum water content conditions. In other words, when the water content is constant, an increase in dry unit weight increases the degree of saturation, thereby causing a decrease in suction. However, the slope of the contours increases as the initial compaction water content gets closer to the optimum water content. The suction contour of 2000 kPa has a positive slope.

The positive slope of the contours of post-compaction suction can be explained by considering the dependence of the main wetting water retention curve on void ratio. The compacted soil reaches the highest degrees of saturation and is therefore subjected to main wetting when the it is compacted under constant water content to 1000 kPa.

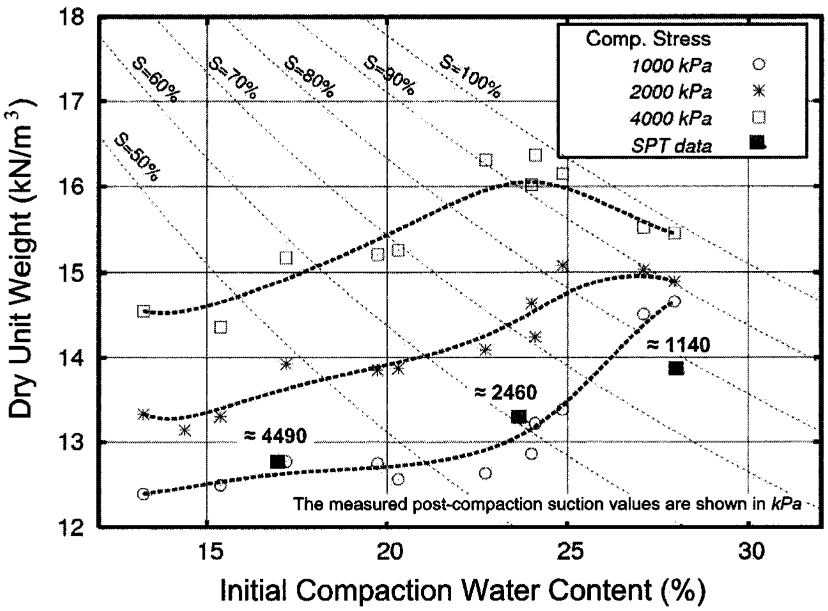

Figure 4.20: Compaction curves with standard Proctor test results

The specimen moves to A_1, situated on the main wetting curve of the specimen associated with the void ratio e_A (Fig. 4.22). Subsequent unloading causes a decrease in degree of saturation, and the resulting path is therefore a scanning drying path to A_2. The specimen again reaches to A_1 along the scanning wetting path following the reloading to a higher vertical stress.

At this point, any subsequent loading would result in an upward movement on the main wetting curve reaching point C_1, if the soil has a constant void ratio. However, for deformable soils plastic compression occurs and the main wetting curve moves upwards towards higher degrees of saturation as the previous vertical stress is exceeded. Since the main wetting curve represents the lower bound of the region of attainable states, it drags the specimen to point B_1, situated on the curve corresponding to the void ratio e_B.

Therefore, for deformable soils, compaction may cause an increase in the degree of saturation of the specimen. However, such a behavior depends on the plasticity characteristics of the soil. It should be noted that when the specimen is unloaded, the final post-compaction suction value may be higher than the initial suction.

Figure 4.23 shows the influence of volume change on the the water content and suction. This figure shows the volume change is more pronounced during dryingfor the

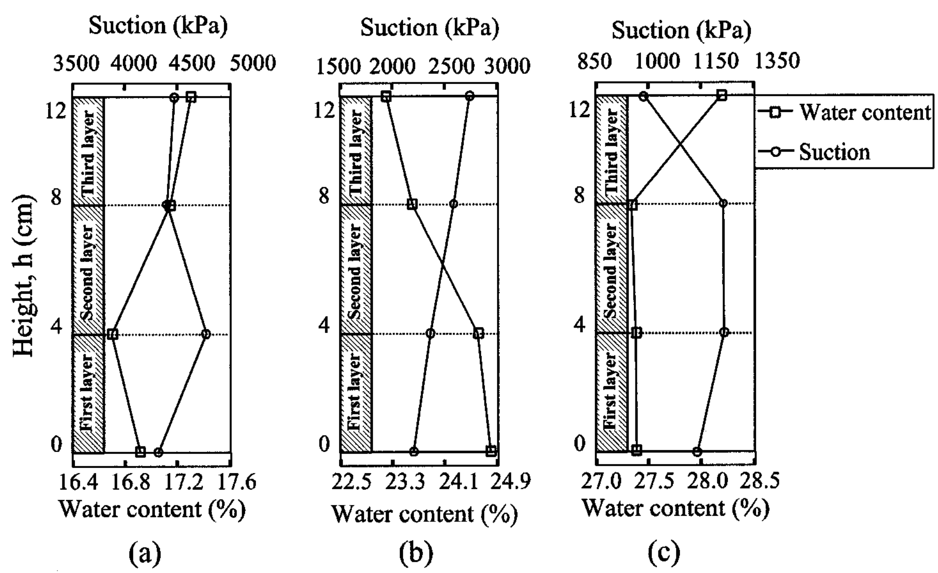

Figure 4.21: The water content and suction profiles of dynamically compacted specimens with initial compaction water content (a) 17% (b) 24% (c) 28%

specimens comacted at wet of optimum in comparison to dry of optimum. This in turn, may produce a significant difference between the degree of saturation versus suction relationship as compared to gravimetric water content versus suction relationship. For example, Figures 4.24 through 4.27 show the degree of saturation-suction-water content relationship of specimens compacted at initial compaction water contents of 17% and 29% which compacted to 2000 and 4000 kPa stress values. This figure shows that for the specimen compacted at the dry of optimum side (i.e., 17%), the degree of saturation versus suction and gravimetric water content versus suction curves are almost parallel. In other words, even though the specimen is shrinking during drying, the air-entry value can still be determined just using water content-suction data. However, for the specimen compacted at the wet of optimum, the degree of saturation versus suction and gravimetric water content versus suction curves are not parallel. Therefore, the void ratio should be determined in order to reliably estimate the air-entry value for these specimens. In other words, any further estimation of air-entry value based on just gravimetric water content versus suction relationship may provide erroneous results.

The above mentioned observation can also be presented using relationship between degree of saturation and suction with and without considering the volume change correction. Figure 4.28 shows the SWRC for the specimen statically compacted to 4000

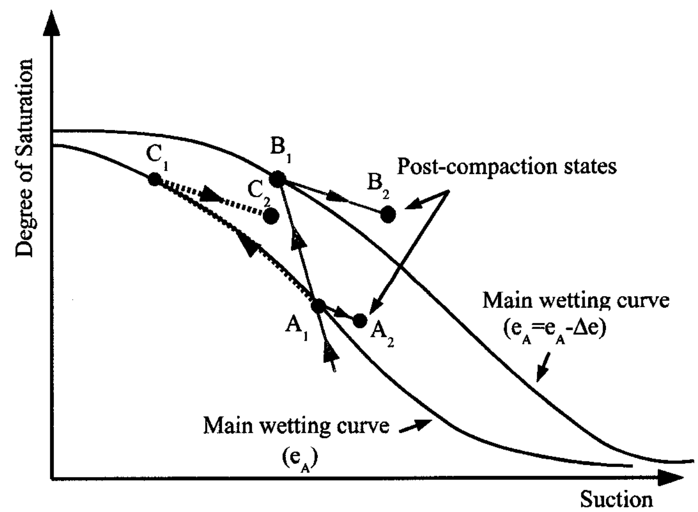

Figure 4.22: Effect of void ratio on SWRC (modified after Tarantino & Tombolato, 2005)

kPa with an initial compaction water content of 29.5% with and without volume change correction.

Figure 4.28 clearly shows the influence of volume change on the water retention behavior or the Champlain sea clay specimen compacted at wet of optimum.

4.3.3 Influence of Initial Compaction Water Content

The influence of the initial compaction water content on the soil structure is well documented in the literature (Cui, 1993; Tinjum *et al.* , 1997; Vanapalli *et al.* , 1999). Much attention has been paid to the understanding of the structure of compacted soils and to the effects of water content changes on the structure (Fig. 4.29). Observations at a microstructural level involving elemental clay platelets and their aggregations are important as they help to better understand influence of structure (Cui & Delage, 1996). Previous studies (Brackley, 1975; Cui & Delage, 1996; Toll, 2000) show the development of an aggregated fabric in soils compacted with dry of optimum moisture content. This type of aggregation was not found to exist in the materials compacted on the wet side of optimum moisture content. Lambe (1958) also stated that for a given compactive effort and dry density, the soil tends to be more flocculated for compaction on the dry side as compared to compaction on the wet side (i.e., the arrangement of particle is more dispersive). In addition, Cui's (1993) study using scanning electron microscope (SEM)

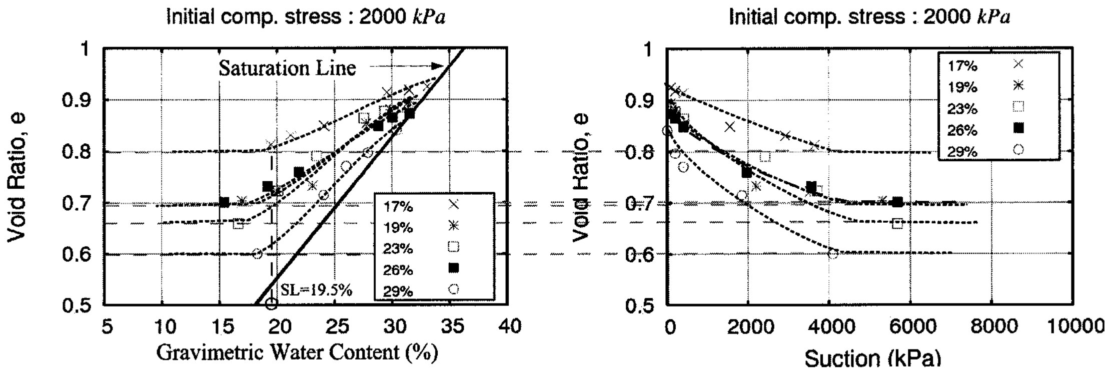

Figure 4.23: The drying paths for the specimens compacted to different initial water contents

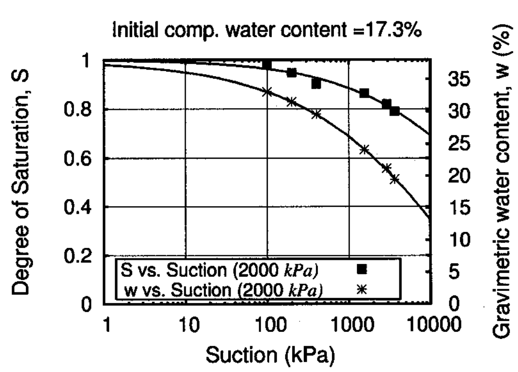

Figure 4.24: SWRCs for specimens compacted to 2000 kPa compaction stress with an initial compaction water content of 17.3%

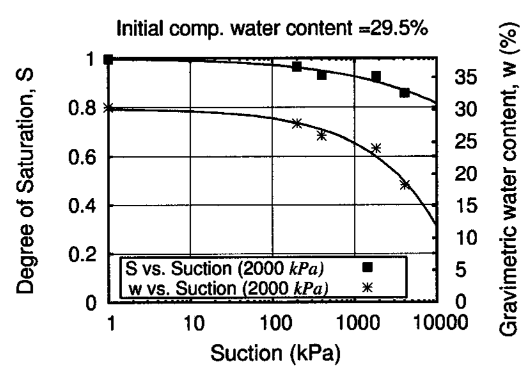

Figure 4.25: SWRCs for specimens compacted to 2000 kPa compaction stress with an initial compaction water content of 29.5%

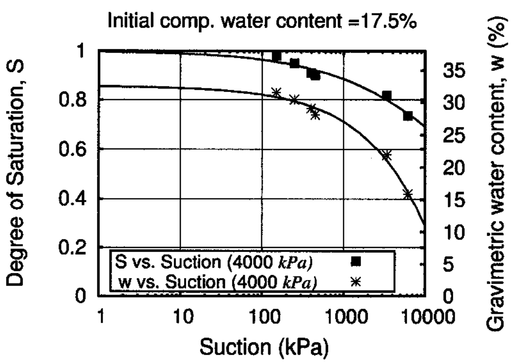

Figure 4.26: SWRCs for specimens compacted to 4000 kPa compaction stress with an initial compaction water content of 17.5%

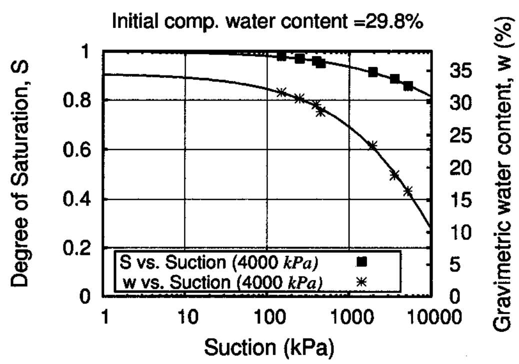

Figure 4.27: SWRCs for specimens compacted to 4000 kPa compaction stress with an initial compaction water content of 29.8%

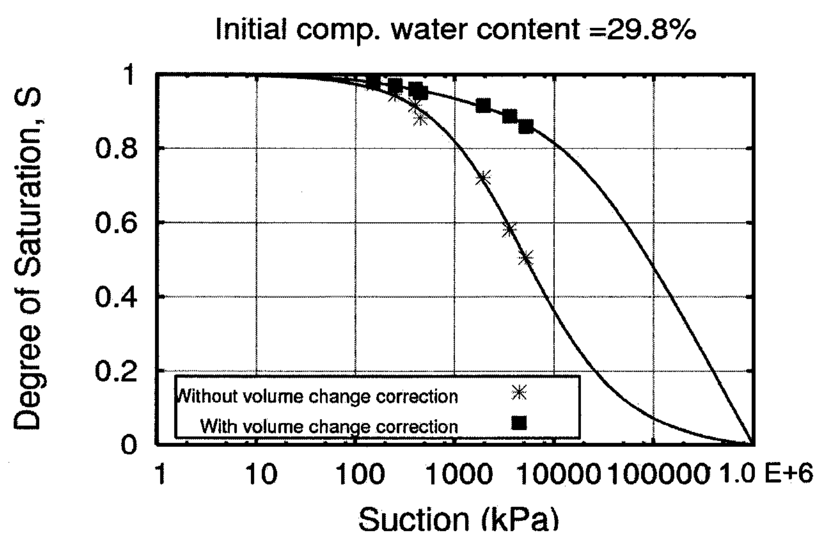

Figure 4.28: The SWRCs for the compacted specimen with an initial water content of 29.5%

showed that the macrostructure was predominant in soils compacted at dry of optimum, while the microstructure was more important in soils compacted at optimum or at a water content higher than optimum.

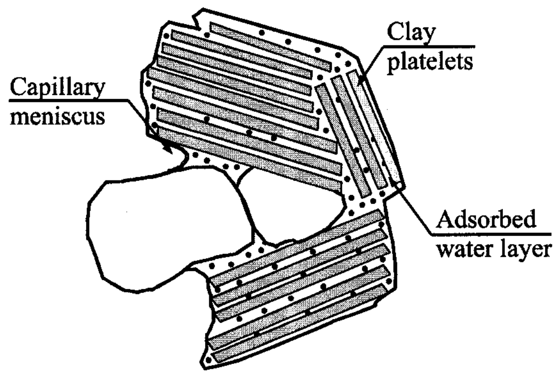

Figure 4.29: Adsorbed water in clay structure

In clays, the water content controls the ease with which particles and particle groups can be rearranged under the compactive effort (Mitchell, 1993). Increasing the moisture content tends to increase the interparticle repulsions, thereby permitting a more orderly arrangement of the soil particles to be obtained with a given amount of effort. In general, an element of flocculated soil has a higher strength than the same element of soil at the same void ratio but in a dispersed state (Lambe, 1958).

In the light of these explanations, SWRCs obtained from the experimental testing program were analyzed. Figures 4.30 and 4.31 show the SWRCs for specimens with initial compaction water contents corresponding to dry of optimum, close to optimum and wet of optimum conditions (19.4%, 23.8%, 29.5%) for two different compaction efforts; 1000 and 2000 kPa. In addition the SWRCs of specimens compacted to an initial compaction stress of 4000 kPa is shown in Fig. 4.32 for water contents 17.5%, 23.9%, 29.8%. The specimen compacted at wet of optimum can hold more water at relatively high suctions. This can be attributed to the clay volume being much larger, thus forming a clay paste surrounding the quartz grains as a result of hydration (Delage *et al.* , 1997). Whereas on the dry of optimum, due to high suctions, compaction may not entirely break the structure down, causing large interaggregate pores resulting less water retention capacity at high suctions (Cui & Delage, 1996; Vanapalli *et al.* , 1999).

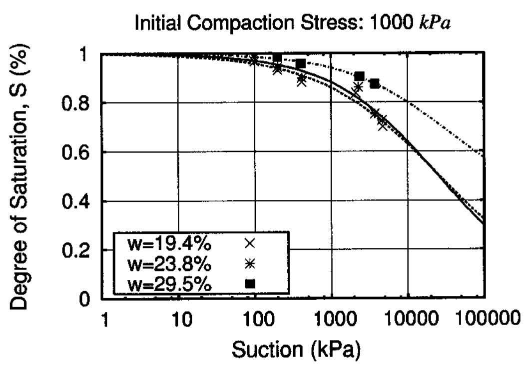

Figure 4.30: SWRCs of specimens compacted to 1000 kPa initial compaction stress

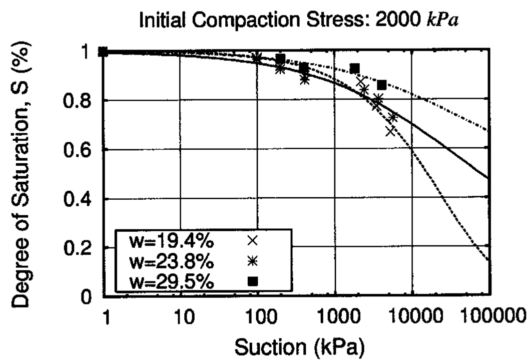

Figure 4.31: SWRCs of specimens compacted to 2000 kPa initial compaction stress

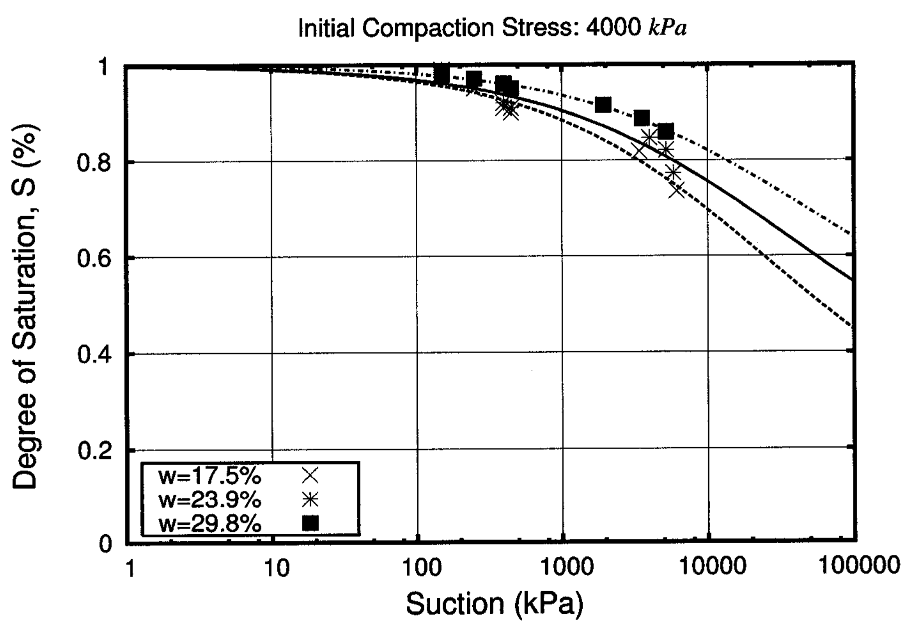

Figure 4.32: SWRCs of specimens compacted to 4000 kPa initial compaction stress

4.3.4 Influence of Compaction Type and Effort

Figure 4.33 shows the SWRCs of the specimens compacted with similar initial water content values but different compaction types (static and dynamic). These results shows that the compaction type has an effect on the water retention characteristics of plastic soils.

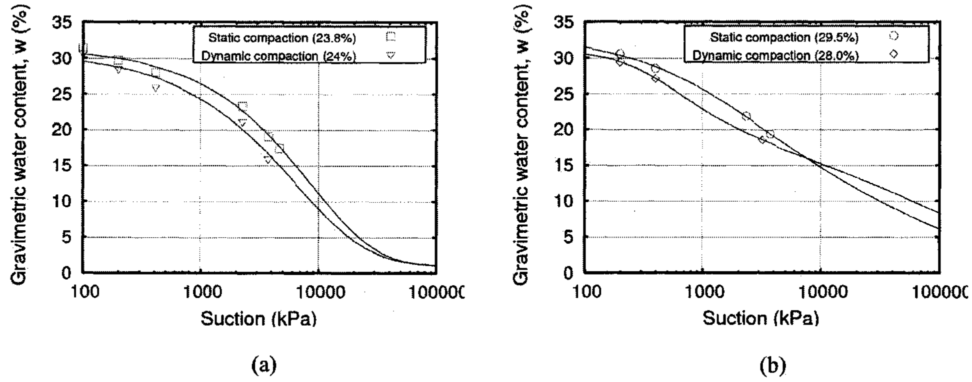

Figure 4.33: The SWRCs of specimens compacted with static and dynamic procedure

In order to investigate the influence of compaction effort, three different energy levels were used in the static compaction tests. In addition, to investigate the influence of compaction effort, 3 specimens were dynamically compacted following ASTM standard for Proctor test. Figures 4.34 through 4.37 show the SWRCs for specimens with initial compaction water contents of 17%, 23%, 26% and 29% respectively for three different compaction efforts; 1000, 2000 and 4000 kPa. From the results presented in these figures, it can be deduced that the compaction effort has an influence on water retention characteristics of the Champlain clay studied. However, this influence is marginal especially upto 10000 kPa suction. Therefore, it is the initial compaction water content not the compaction effort that controls the soil structure (Vanapalli *et al.* , 1999).

4.4 Hydraulic Conductivity

4.4.1 Saturated Hydraulic Conductivity Results

Several techniques are available in the literature for determining the hydraulic conductivity function for unsaturated soils (Childs & Collis-George, 1950; Marshall, 1958; Mualem, 1976; van Genuchten, 1980). All of them requires the SWRC and saturated

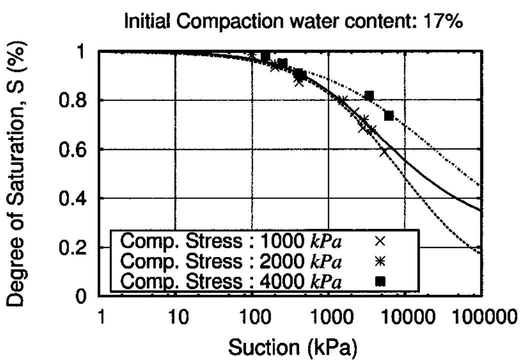

Figure 4.34: SWRCs for specimens with an initial compaction water content of 17%

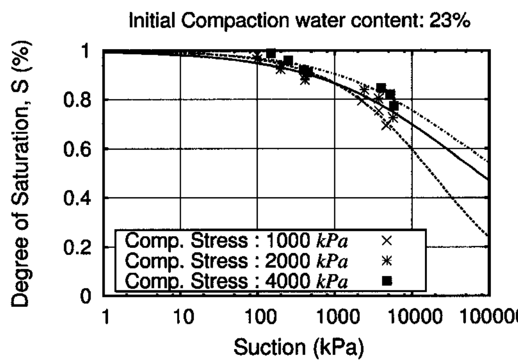

Figure 4.35: SWRCs for specimens with an initial compaction water content of 23%

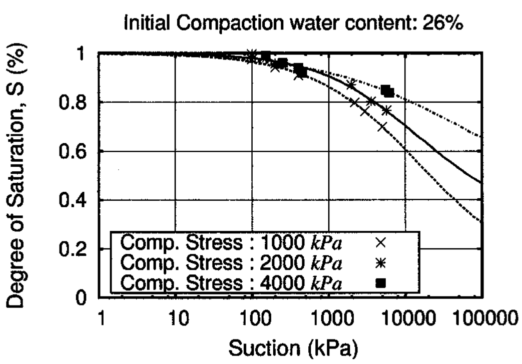

Figure 4.36: SWRCs for specimens with an initial compaction water content of 26%

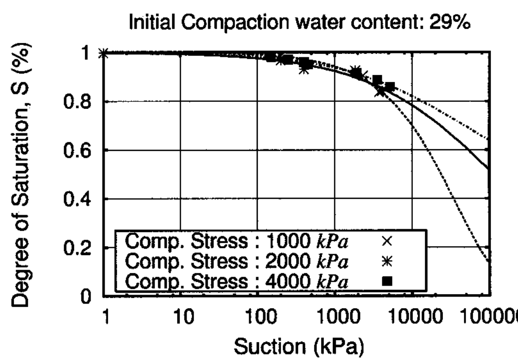

Figure 4.37: SWRCs for specimens with an initial compaction water content of 29%

hydraulic conductivity, K_{sat}, as input parameters. In this section, first, the measured saturated hydraulic conductivity values along with the measurement technique were discussed. Next, the unsaturated hydraulic conductivity functions were estimated using Mualem (1976) technique.

The primary factors affecting K_{sat} in a laboratory environment include the texture (grain-size distribution) and structure (i.e., cracks, worm holes, root channels) of the soil core or column, the temperature of the water, the ionic (salt) speciation and concentrations in the water and the presence of air bubbles in soil pores (Bouma *et al.* , 1971; Klute, 1986; Benson & Gribb, 1997).

The saturated hydraulic conductivity is directly proportional to water viscosity, and water viscosity is inversely proportional to temperature. Consequently, the measured value of K_{sat} is affected by the water temperature. For example, an increase in water temperature from 10 to 25^oC will result in a 45% increase in K_{sat}, all other factors remaining constant. Therefore, the K_{sat} values determined in this study were corrected to a reference temperature of 20^oC using the following equation:

$$\mathbf{k_{20}} = k_T \frac{\eta_T}{\eta_{20}} \tag{4.4}$$

where;
k_{20}: the saturated hydraulic conductivity at temperature 20^0C
T: temperature of the water in the test in degree celcius
k_T: the saturated hydraulic conductivity at temperature T
η_T/η_{20}: the viscosity correction

The ion (dissolved salt) speciation and concentration in the water can also affect K_{sat} through flocuculation or dispersion of clay within the porous medium. Flocculation of clay will cause K_{sat} to increase by increasing the size and/or number of water conducting pores. Whereas dispersion of clay will decrease K_{sat} by plugging pores with clay particles. In fact, extensive clay dispersion can reduce the K_{sat} of a soil to virtually zero . The water used for measuring the K_{sat} of a porous medium should therefore be either "native" water extracted from the porous medium, or a laboratory "approximation" that has the same major ion speciation and concentrations as the native water. Therefore, in this research, local municipal tap water was used for saturating the specimens as well as the K_{sat} laboratory tests (Reynolds, 1993).

There appear to be three main difficulties associated with the measurement and interpretation of saturated hydraulic conductivity (K_{sat}) in saturated swelling clay soils with continuous macropores (Bouma, 1982):

- The K_{sat} value changes continuously with time as a result of soil swelling and shrinkage (Benson & Gribb, 1997).
- The K_{sat} value is a function of specimen size due to the effect of macropore continuity patterns.
- Bubbles of air entrapped within the porous medium physically block pores and can thereby cause the measured K_{sat} to be less than when the material is fully saturated.

The first problem mentioned above, was minimized by taking a specimen which was wetted for at least 3 weeks, thus allowing little additional swelling during the K_{sat} measurement (Bouma, 1982). The third problem was alleviated by slow wetting of the specimen from bottom up under 10-20 kPa of positive water pressure.

In this research the K_{sat} values of three compacted specimens were measured in triaxial cell. The specimen preparation is illustrated in Figs. 4.38 and 4.39. Only the outflow from the bottom of the specimen was measured during the experiments. The height of the specimen used for hydraulic conductivity tests was approximately 10 mm. A cell pressure of 200 kPa was applied during the tests. The top and bottom pressure values were kept at 250 kPa and 245 kPa, respectively.

The measured K_{sat} values with the initial compaction water content and dry unit weight are shown in Fig. 4.40. The procedure suggested by Al-Dhahir (1969) was followed for determining the K_{sat} value from the outflow versus time data.

Figure 4.41 shows the experimental data obtained from the conductivity tests for the specimen statically compacted to 4000 kPa with an initial compaction water content of 26%, which is close to optimum water content.

4.4.2 Prediction of Unsaturated Hydraulic Conductivity Functions

This saturated hydraulic conductivity value, K_{sat}, was then used along with the SWRC to estimate the unsaturated hydraulic conductivity function. The following closed-from equation, which is a combination of the model proposed by Mualem's model (1976) and van Genuchten (1980) water retention equation, was employed:

$$\mathbf{K}_{(\mathbf{S_e})} = K_o {S_e}^L \left[1 - \left[1 - S^{\left(\frac{n}{n-1}\right)}\right]^{\left(1-\frac{1}{n}\right)}\right]^2 \tag{4.5}$$

Figure 4.38: Sample preparation in tri-axial cell (a)

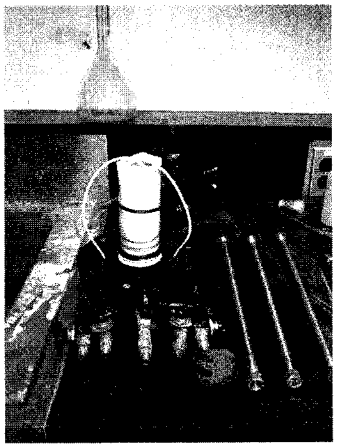

Figure 4.39: Sample preparation in tri-axial cell (b)

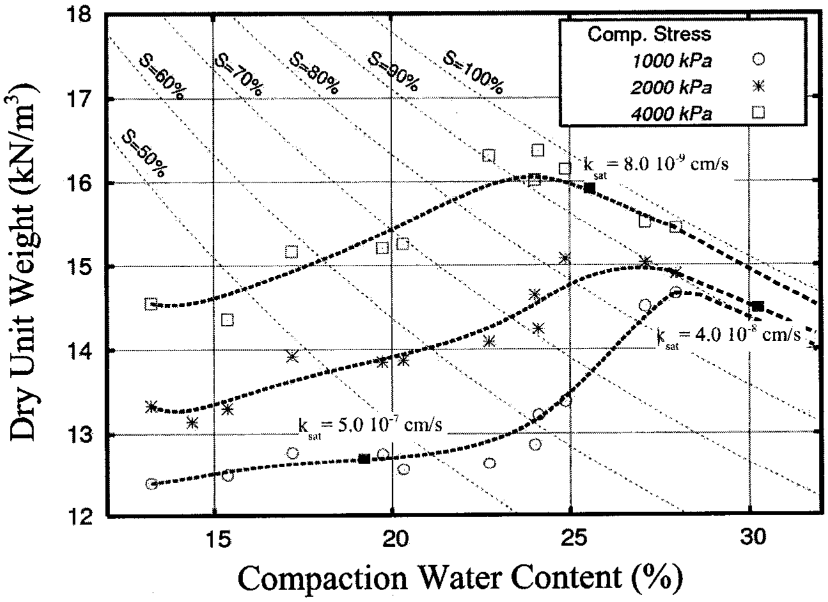

Figure 4.40: K_{sat} values on the compaction curve

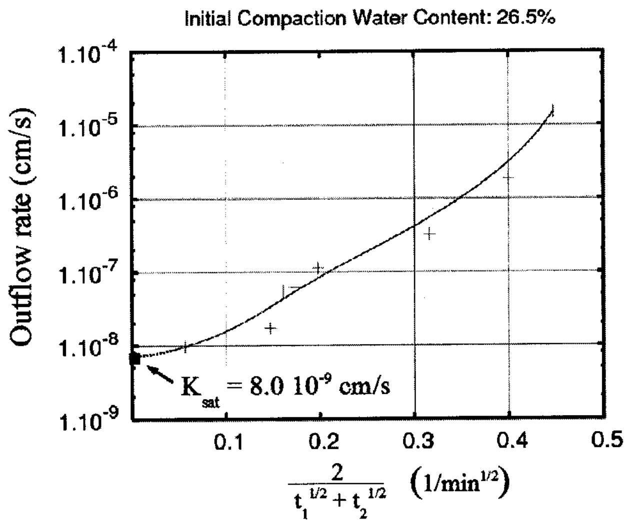

Figure 4.41: Outflow data for the specimen compacted at optimum water content

where K is the unsaturated hydraulic conductivity, S_e is the relative saturation, K_o is a hydraulic conductivity acting as a matching point, and L is a lumped parameter that accounts for the pore tortuosity and pore connectivity.

Generally, the saturated hydraulic conductivity, K_{sat}, is used for K_o since its measurement is relatively simple. However, several investigators argue that K_{sat} may not be suitable matching point since it is sensitive to macropore flow, whereas unsaturated flow occurs in the soil matrix (van Genuchten & Nielsen, 1985; Luckner *et al.* , 1989). They stated that a matching point at slightly unsaturated conditions would yield better results.

Figure 4.42 shows the unsaturated hydraulic conductivity function, k_{unsat} for the specimen specimen statically compacted to 4000 kPa with an initial compaction water content of 26%. In addition k_{unsat} curves for 17% and 30% initial compaction water content values are also presented (Figs. 4.43 and 4.44).

These figures underline the importance of volume corrections on the water retention characteristics of compacted Champlain sea clay specimens. Figure 4.43 shows that the volume change influence is marginal when the specimens are compacted at dry of optimum. However, as the initial compaction water approaches optimum water content, the volume change effect becomes predominant as shown in Figs. 4.43 and 4.44.

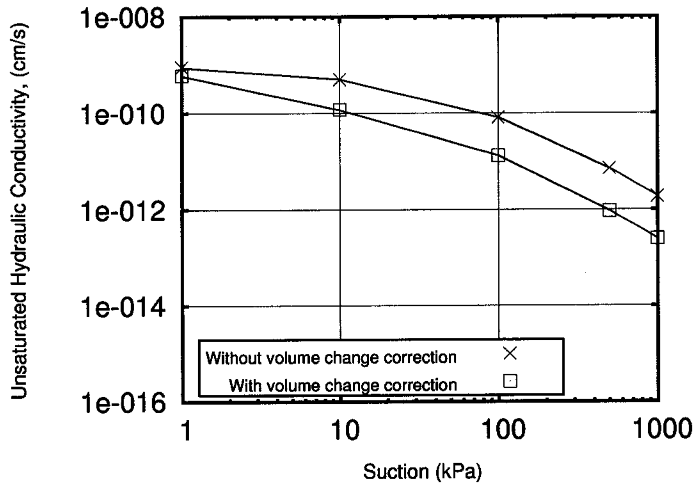

Figure 4.42: K_{unsat} function for the specimen statically compacted to 4000 kPa with an initial compaction water content of 26%

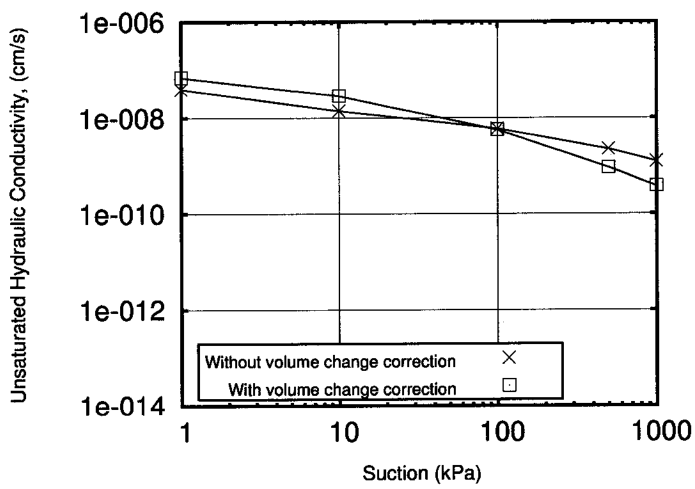

Figure 4.43: K_{unsat} function for the specimen statically compacted to 1000 kPa with an initial compaction water content of 17%

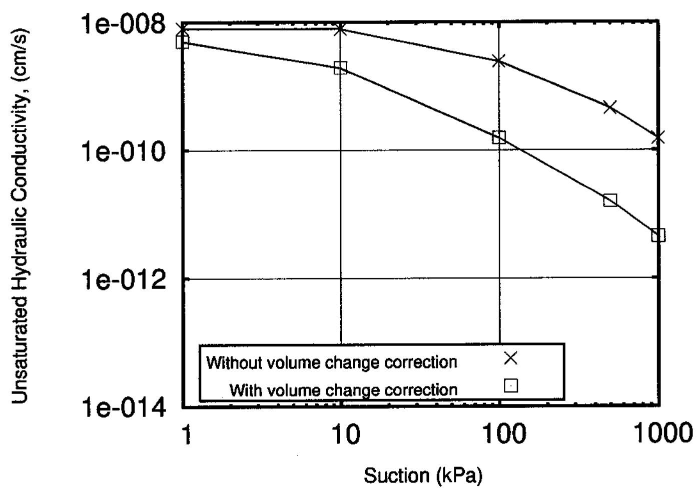

Figure 4.44: K_{unsat} function for the specimen statically compacted to 2000 kPa with an initial compaction water content of 30%

Chapter 5

A Technique for the Estimation of SWRC of Compacted Soils

5.1 Introduction

Several investigations have been devoted towards the development of prediction or estimation techniques to obtain the θ-ψ relationship of soils. One branch of these techniques include functional regression methods using empirical SWRC equations, where the fitting parameters are related to textural parameters (Gupta & Larson, 1979; Vereecken *et al.* , 1992). Another branch of methods estimate the SWRC based on physical characteristics of the media (Arya & Paris, 1981; Haverkamp & Parlange, 1999; Aubertin *et. al.,*2003).These models or techniques have been reviewed in journals, textbooks and monographs (Klute, 1986; Fredlund & Rahardjo, 1993; Sillers *et al.* , 2001). The evolution and understanding of the SWRC and of the corresponding prediction and estimation techniques have been presented by Barbour (1998) in which he provided a historical perspective.

In many situations it is valuable to have estimates of the SWRC during early stages of a project when there is not enough information readily available. The SWRC estimation models, based on easy to obtain properties (i.e., grain size distribution, void ratio, Atterberg limits, and dry density) may be utilized to guide the geotechnical engineers throughout the preliminary analyses and design procedures (Fredlund, 2000; Côté & Konrad, 2002). However, most of the methods mentioned above deal with non-plastic soils or soils with low plasticity. There is limited published research on estimating the SWRC for compacted plastic soils (Simms & Yanful, 2002; Marinho, 2005). In this research an attempt is made to develop a simple technique to predict the SWRC of compacted plastic soils using conventional soil properties such as Atterberg limits and volume-mass properties.

Figure 5.1a and b shows that a roughly bilinear relationship exists between suction and gravimetric water content for plastic compacted soils both on arithmetic and semi-logarithmic scale. A relatively steep gradient at low suction values or relatively high water content values is followed by a smooth transition to a flatter gradient at high suction values (Figure 5.1a). Even at low suction values, relatively large pores (or macro pores) are unable to retain water against the applied suction. The steep portion of the curve reflects the outflow of water from the macro pores. The primary reason responsible for the release of water at low suction values is the liquid phase flow. The pore-water in macro pores are mainly held by capillary tension. Approaching to the flatter portion of the curve, the relatively small pores (or micro pores) are progressively emptied and hydrated water layer covering the clay minerals starts reducing (Delage *et al.* , 1997; Harrison & Blight, 2000). Thus, both the capillary tension effects and adsorption effect the transition curve. Soil water continuity progressively diminishes over this range as air filled channels begin to form within the soil voids. At relatively high suction values, the water retention capacity is considered to be primarily due to the adsorptive forces and the flow takes place predominantly in vapor phase.

In this chapter, data on SWRCs of compacted fine-grained soils along with their conventional soil properties from published literature has been summarized. This database is used to estimate the relationship between the key parameters of the SWRC such as rate of desorption and the conventional soil properties. Finally, a technique is proposed to estimate the SWRC of compacted plastic soils with only one point measurement (i.e., matric suction versus gravimetric water content). There is a good comparison between the measured and the estimated SWRCs of compacted fine-grained soils for the soil studied in this research and the compacted soils presented in the database.

5.2 Background

Several researchers studied the relationship between the indicator tests (i.e., Atterberg limits, shrinkage limit, stress history, compaction effort) and the parameters of SWRC such as air-enrty value, rate of desorption and residual water content (Jucá, 1993; Reddi & Poduri, 1997; Harrison & Blight, 2000; Aubertin *et al.* , 2003; Marinho, 2005). For example, the influence of soil plasticity and soil stiffness on the SWRC is shown schematically in Figs 5.2a and b.

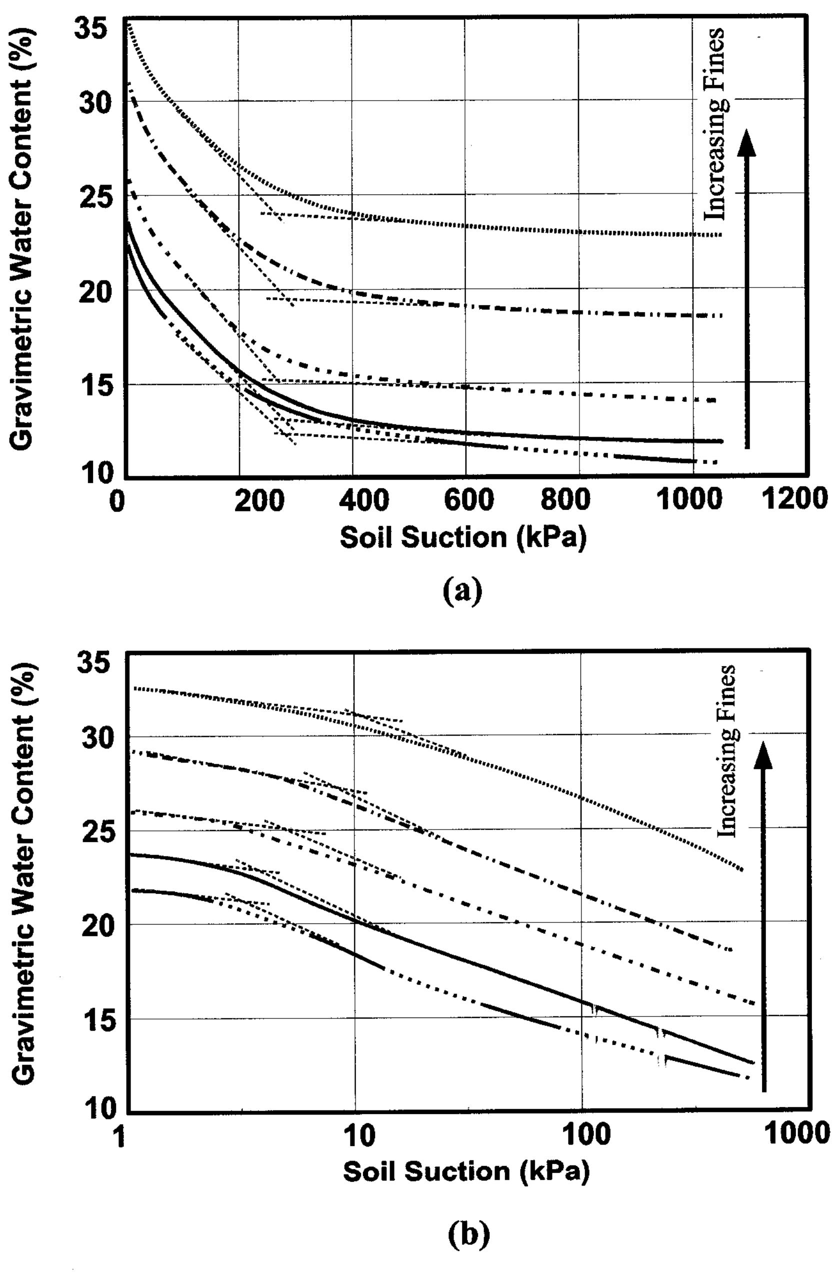

Figure 5.1: The effect of fine content on SWRC in (a) arithmetic scale and (b) semi-logartihmic scale (modified after Harrison, 2000)

Fig. 5.2a shows that the slope of SWRC increases with liquid limit when a log scale is used for representing the suction. Whereas, Fig. 5.2b shows the general behavior of clay specimens with different stress histories or different preparation procedures.

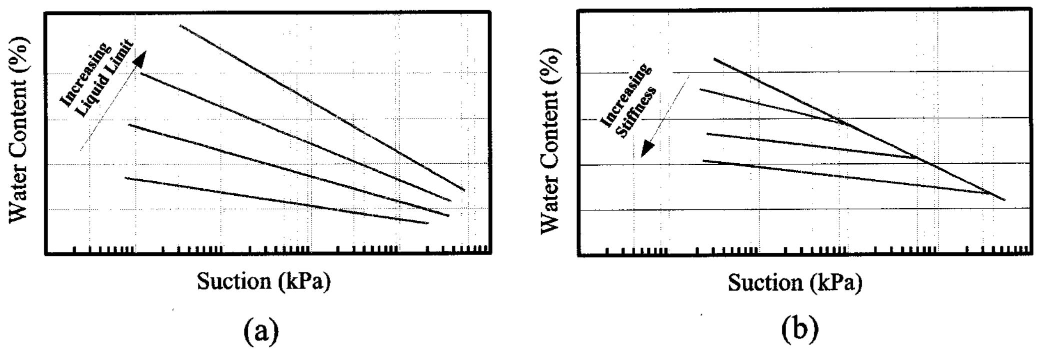

Figure 5.2: Plasticity effect on water retention characteristics (modified after Marinho, 2005)

Compacted plastic soils exhibit shrinkage during drying. Typically, plastic soils with a liquid limit above 25% experience significant shrinkage when dried. This phenomena is illustrated in Fig. 5.3 where the liquid limit, w_L and plastic limit, w_P values for some soils are presented (Marinho, 2005). These results suggest that the shrinkage limit by itself may not be a sufficient parameter for identifying soils behavior.

Sanchez-Leal (2002) studies show that the behavior of compacted soils can be related to clay hydration. Based on test results from 142 specimens, he postulated the correlation between Modified Proctor Maximum Dry Density (MDD) and Optimum Moisture Content (OMC) with a characteristic factor which is defined as follows:

$$\mathbf{F_p} = \frac{(1+w_L)F}{1+G} \tag{5.1}$$

$$\mathbf{F_{np}} = \frac{D_{60}}{D_{10}}F \tag{5.2}$$

where w_L is the liquid limit, F is the clay fraction, G is the gravel fraction, and D_{60}/D_{10} is the uniformity coefficient.

Equations 5.1 and 5.2 are used for plastic soils and non plastic soils respectively. Figures 5.4a and 5.4b show the correlation results for different types of clayey soils, and it appears that there is a good relationship between MDD and OMC and F_p factor,

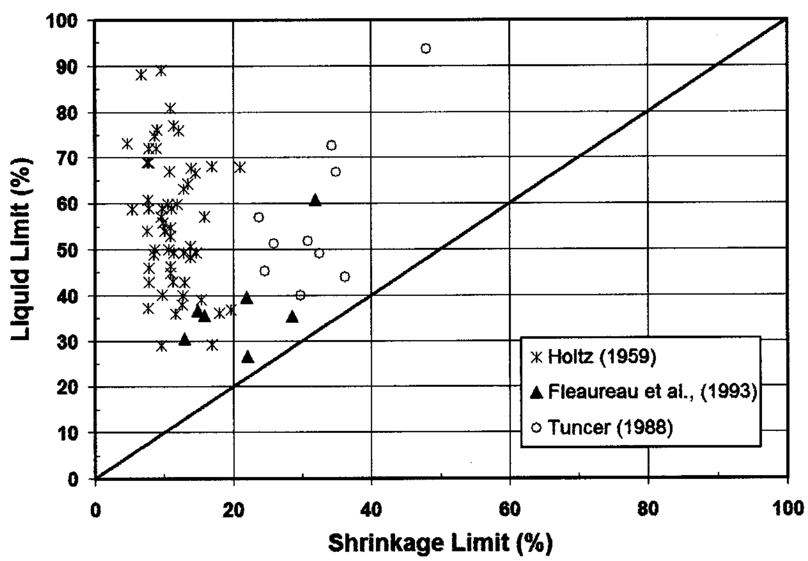

Figure 5.3: Relation between liquid limit and shrinkage limit for some soils

which takes into account the effect of clay quantity, F and clay activity, w_L. However, the correlation results for non plastic soils are not satisfactory(Fig. 5.4b).

The influence of soil plasticity on the SWRC has been demonstrated in the literature (Black, 1962; Mitchell & Avalle, 1984). Black (1962) showed that there is a relationship between the water content and the plasticity index of different British clays and this relationship can be uniquely related to different matric suction values, $(u_a - u_w)$, for different soils (Fig. 5.5). All data analyzed by Black (1962) were above the A line on the plasticity chart and the relationship between the soil suction and water content presented a well defined correlation with the plasticity index, I_P. McQueen & Miller (1974) also postulated that the SWRC plotted water content against suction for most soils with a liquid limit of more than 25% can be assumed to be a straight line between suctions of 100 and 10000 kPa, on a semi-log plot, regardless of the suction method used.

Burland (1990) introduced the concept of intrinsic properties for saturated clays, which was based on the void ratio of samples prepared between the liquid limit, w_L and $1.5w_L$. The relationship between water content and stress during isotropic ocnsolidation can be obtained provided the specific gravity, G_s is known. Reddi & Poduri (1997) presented a study in which the void ratio, e at the liquid limit,w_L was used to obtain the water retention properties of the soil at other states.

Through later studies, Juca (1993), Marinho & Chandler (1993) and Ridley & Romero

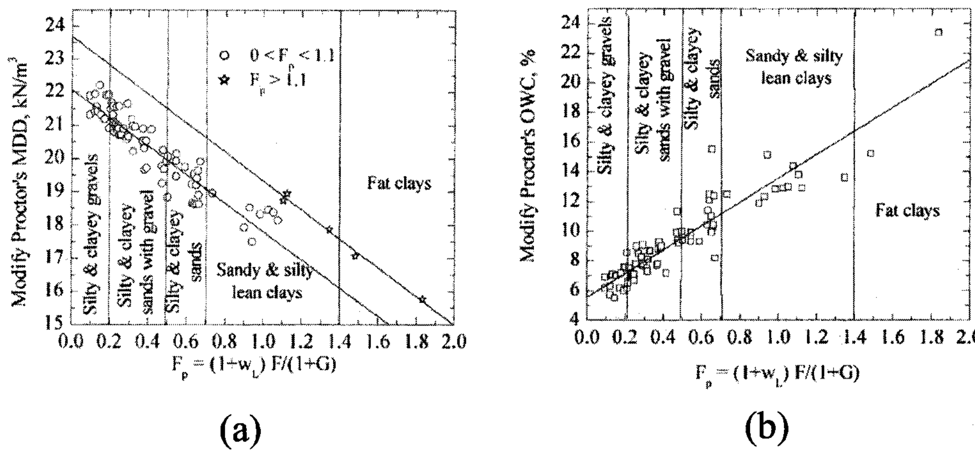

Figure 5.4: MDD and OMC correlations with F_p and F_{np} factors for plastic and non plastic soils

(1998) have presented the SWRCs of reconstituted compacted soils as a semi-logarithmic plot. They found a linear relationship between log suction and water content for the soils studied. The gradient of the curve for suction values greater than 100 kPa was termed the suction capacity, C by Marinho & Chandler (1993). Harrison & Blight (2000) observed that the relationship did not present good correlation for residual soils. Soils such as residual soils are typically influenced by void size that may induce a change in suction capacity.

Marinho (2005) reported that there was a well defined relationship between the slope of the SWRC and the rigidity of the soil in relation to increase in suction. The results of his study shows that there is an upper limit for the suction capacity, C. The upper limit is related to the specimen prepared and tested from slurry. Whereas, the lower limit for the suction capacity was related to the overconsolidated clays.

5.3 Analysis

5.3.1 The compilation of the SWRCs of compacted plastic soils

Along with the compacted Champlain sea clay specimens tested in this research, additional data were obtained from the literature in which the procedure followed was consistent with the approach used in this testing program. The properties of all these

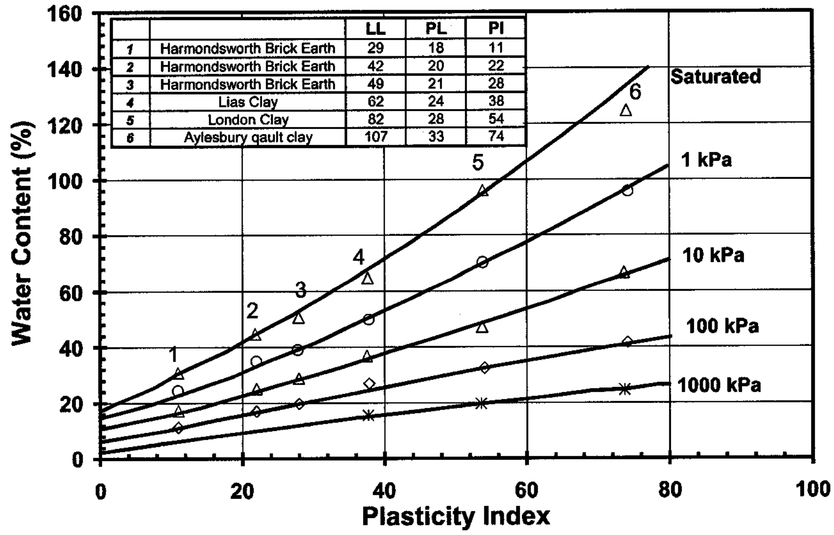

Figure 5.5: Moisture content and plasticity index relationship for various matric suction values and for various plastic soils (modified after Black, 1962)

soils are summarized in Table 5.1. The plasticity information of the soils gathered is also shown in plasticity chart (Fig. 5.6).

The relationship between the suction capacity, C and liquid limit, w_L is plotted using the database including clay fraction as an additional parameter (Fig. 5.7). The suction capacity, C versus liquid limit along with clay fraction graph for sixteen different soils in Fig. 5.7 shows a better correlation in comparison to the suction capacity versus liquid limit proposed by other investigators (Jucá, 1993; Marinho & Chandler, 1993). This can be attributed to the introduction of clay fraction as an additional parameter. The above relationship can be used as a valuable tool to estimate the SWRC of a compacted plastic soils.

Figure 5.8 shows all the measured SWRCs in terms of gravimetric water content versus suction in the experimental part of this study. The SWRCs (gravimetric water content versus suction) of the plastic compacted specimens fall in a narrow range. This result shows that the initial compaction water content, dry density, compaction effort or volume change have only arginal influence on the gravimetric water content versus suction relationship. The parameter that predominantly controls the gravimetric water content change due to suction is the physico-chemical characteristics of compacted plastic soils. Furhtermore, the SWRCs of the soils in the database also support that approach

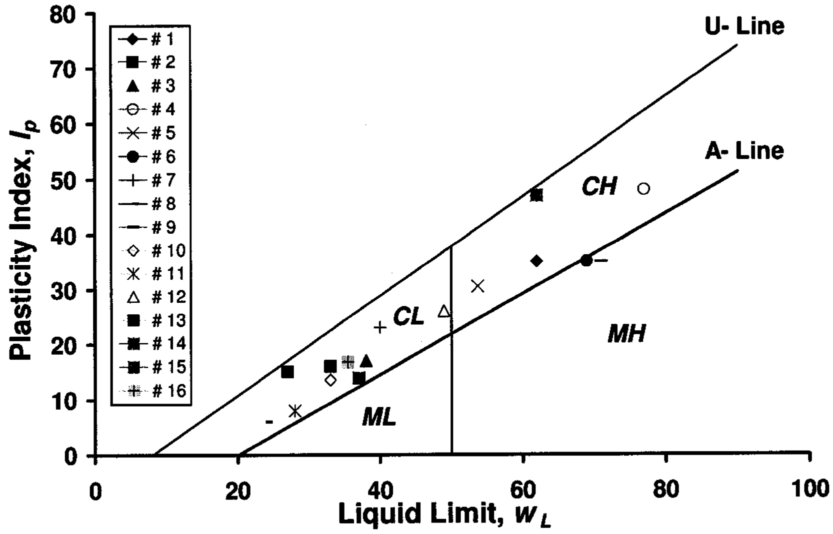

Figure 5.6: Plasticity chart for the soils gathered from the literature

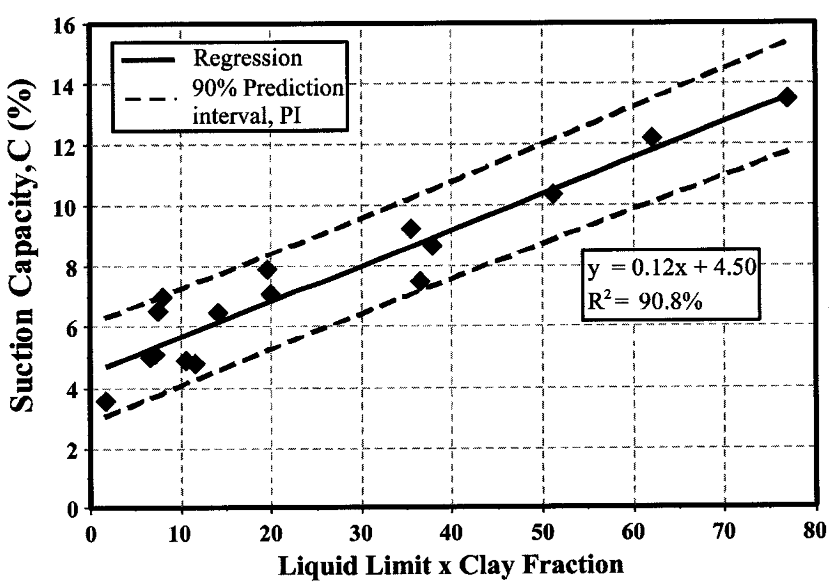

Figure 5.7: Suction capacity, C versus (liquid limit x clay fraction), for the soils studied in this research

(Fig. 5.9).

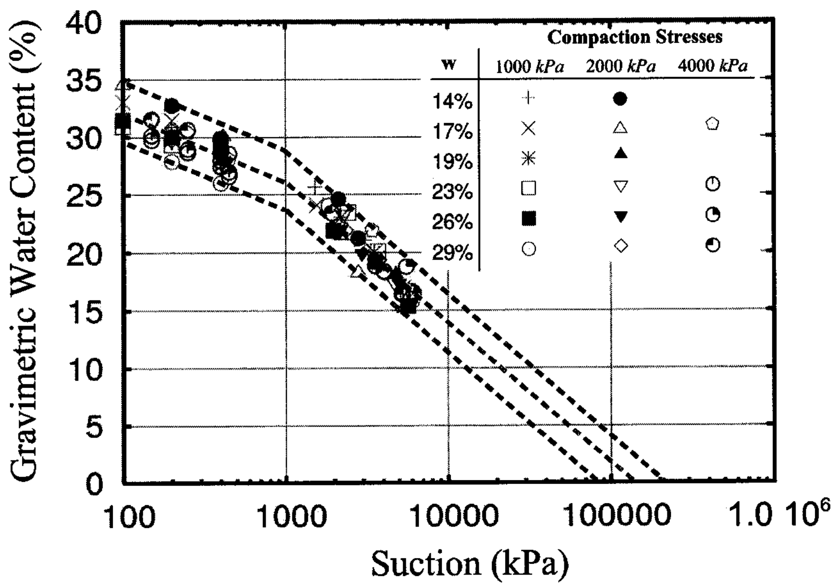

Figure 5.8: SWRCs of all the specimens studied in the research program

5.3.2 Estimation Technique

One method to estimate the entire SWRC would be to obtain several points (at least two points) of gravimetric water content versus suction data, and apply one of the fitting models presented in the literature review chapter. However, measuring suction beyond 500 kPa becomes difficult with conventional apparatus using axis-translation technique.

Another approach to obtain the SWRC is to use one point measurement of gravimetric water content in the matric suction range of 100 - 500 kPa which will provide an estimation of the first part of the bilinear curve. From the present study, it has been shown that the slope of desorption line can be obtained using the information based on liquid limit and clay fraction. Furthermore, desorption line can be located if a point on desorption line is known. The ψ_p, which is the intercept of the desorption line on the suction axis (Fig. 5.10) can be estimated and used as one required point.

The value, ψ_p lies in a narrow band of suction for typical fine-grained compacted soils. For the data on Champlain sea clay and database shown in Table 1, an average value of 100000 kPa may be used for ψ_p. After locating desorption line, a corresponding

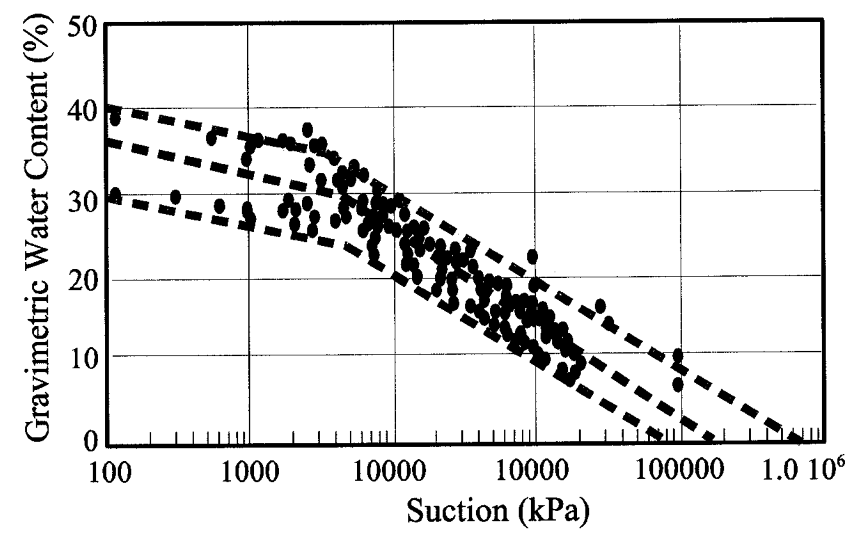

Figure 5.9: The gravimetric water content versus suction relationship for the soils in the database

gravimetric water content point for a suction value between 1000 - 3000 kPa is determined. This range is chosen since most of the compacted fine-grained soils exhibit linear desorption characteristics within that suction range.

It is proposed that the SWRC of a statically compacted plastic soil can be estimated using the procedure explained below.

- Step 1: The suction capacity, C is determined from liquid limit and clay fraction (Fig. 8);
- Step 2: The suction capacity, C and ψ_p are used to estimate the water content at a suction value of 1000 - 3000 kPa (Fig. 5.10);
- Step 3: One data point of suction versus water content is now determined using, say, the axis translation technique or any other measurement techniques. In addition, the saturated water content, w_sat, is also easily determined.

This information on two data points, one estimated point on the desorption curve (i.e. 1000-3000 kPa) and the other measured point in the range of 50 to 500 kPa are then fitted using Brutsaert's (1966) equation;

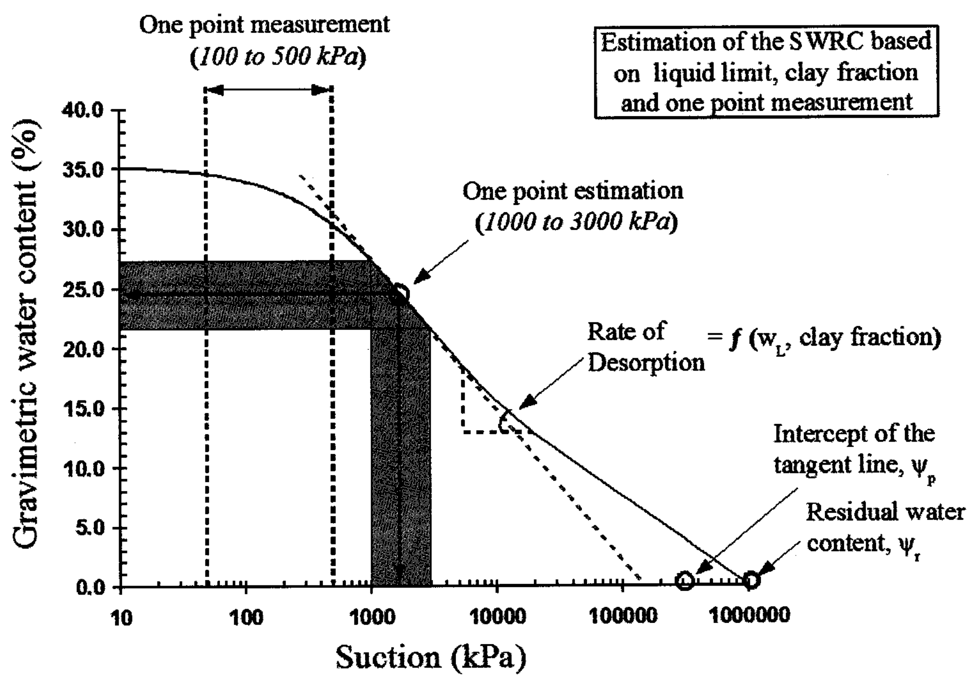

Figure 5.10: The essential features for estimating the SWRC using the proposed method

$$\mathrm{w_w} = w_r + \frac{(w_s - w_r)}{\left[1 + \left[\frac{\psi}{a_b}\right]^{n_b}\right]} \tag{5.3}$$

where: w_w: the gravimetric water content; w_s: the saturated gravimetric water content; w_r: is the residual gravimetric water content; a_b is the first fitting parameter; n_b is the second fitting parameter, and ψ: is the suction in kPa.

Brutsaert (1966) model is used in this estimation technique as it requires only two parameters to fit the SWRC. Thus, the entire SWRC can be estimated using this model with the information of only two data points (i.e., one measured point in the matric suction range of 100 and 500 kPa) and one estimated point in the suction range of 1000 to 3000 kPa).

5.4 Verification of the Proposed Technique

Figures 5.11, 5.12 and 5.13 show the SWRCs predicted using proposed method. For specimens compacted at dry of optimum (Figs. 5.12 and 5.13) the prediction is more succesful when compared to the prediction for the specimens compacted at dry of optimum (Fig. 5.11).

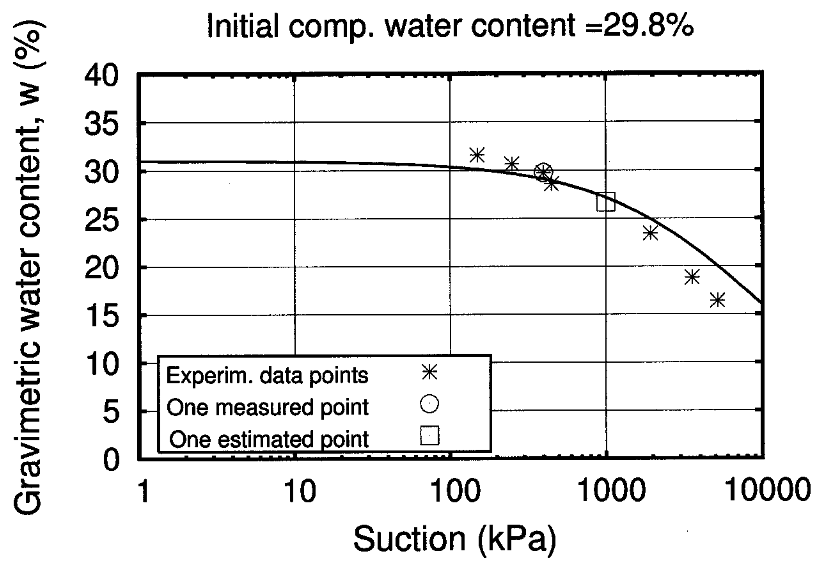

Figure 5.11: The estimated SWRC for the specimen compacted to 4000 kPa with an initial compaction water content 29.8%

Figures 5.14 and 5.15 show the comparisons between the experimental data and the one point estimation technique for the Indian Head Till (soil #16) and for the highly plastic clay from the databank of University of Wisconsin (soil #14). In each case, there was a satisfactory comparison between the measured and the estimated SWRC for all the compacted soils summarized in Table 5.1.

The performance of the proposed method was also verified using the soils in the database. Figures 5.14 and 5.15 show the SWRCs for Indian Head till (Vanapalli *et al.* , 1999) and a plastic clay (Tinjum *et al.* , 1997). The comparisons between the predicted SWRC and the experimental data point looks satisfactory.

In the experimental results section, it was shown that the dry density has a marginal influence on the water retention characteristics on the compacted Champlain sea clay studied in this research. Similar observations were reported in the literature (Wan *et al.* , 1995; Delage *et al.* , 1996). This can be attributed to the fact that water sorption-desorption phenomena occur within the intra-aggregate porosity, which is mainly controlled by physico-chemical forces exerted by clay minerals present in the soil. Simms & Yan-

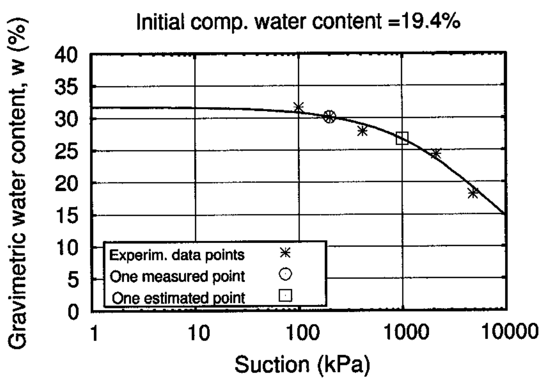

Figure 5.12: The estimated SWRC for the specimen compacted to 1000 kPa with an initial compaction water content 19.5%

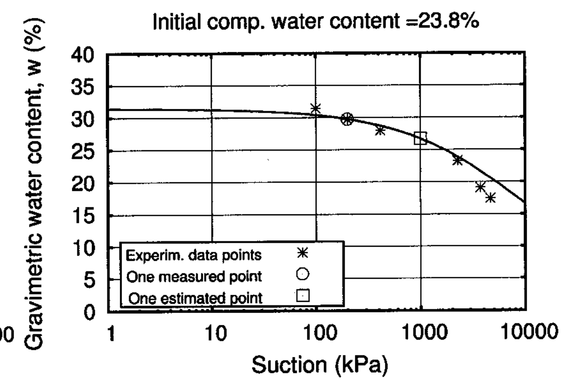

Figure 5.13: The estimated SWRC for the specimen compacted to 1000 kPa with an initial compaction water content 23.8%

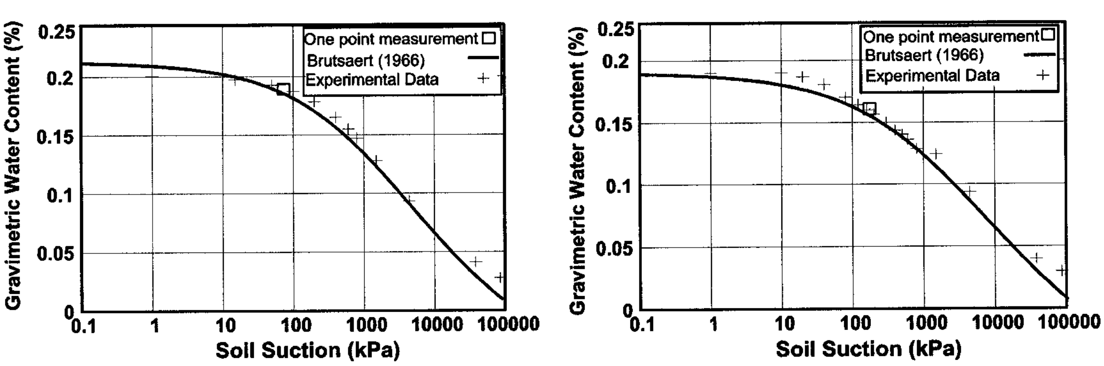

(a) (b)

Figure 5.14: Comparisons for Indian Head till Soil #16 (w_i= 19.2%, wet of optimum) (b) (w_i= 16%, optimum) (Vanapalli *et al.* , 1999)

ful (2002) also observed that the pore size distributions of the micropores are similar, regardless of the compaction water content.

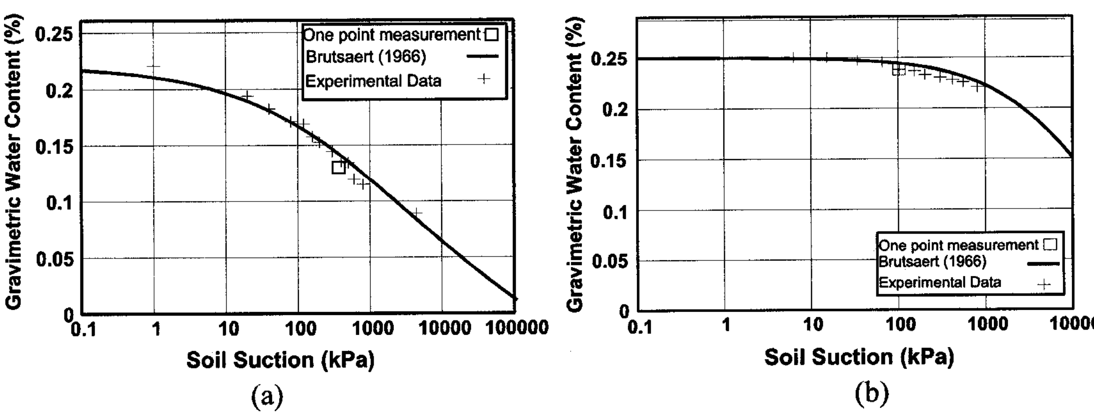

Figure 5.15: Comparisons for Indian Head till (a) Indian Head till, soil #16 (w_i= 13.2%, dry of optimum) (b) Highly plastic clay, soil #14 (w_i= 23%, Wet of optimum)

This intra-aggregate porosity is not influenced by the compaction process and there is no substantial influence of the dry density. Contrary to sand and low plastic clay, for which SWRC is mainly controlled by capillary effects, the rate of desorption of highly plastic soils predominantly controlled by the physico-chemical effects. This explains the unique relationship between the liquid limit, w_L, clay fraction and the suction capacity, C.

5.5 Limitation of the Proposed Model

The proposed equation gives succesful predictions for the compacted Champlain sea clay specimens and the soils available in the database. However, the relationship that one can obtain from this prediction method is gravimetric water content versus suction relationship (See Chapter 4: Experimental Results and Discussions). Therefore, this relationship can only be converted to degree of saturation versus suction relationship if the soil has a rigid pore structure. In other words, the volume change should be negligible for the proposed method to be applied.

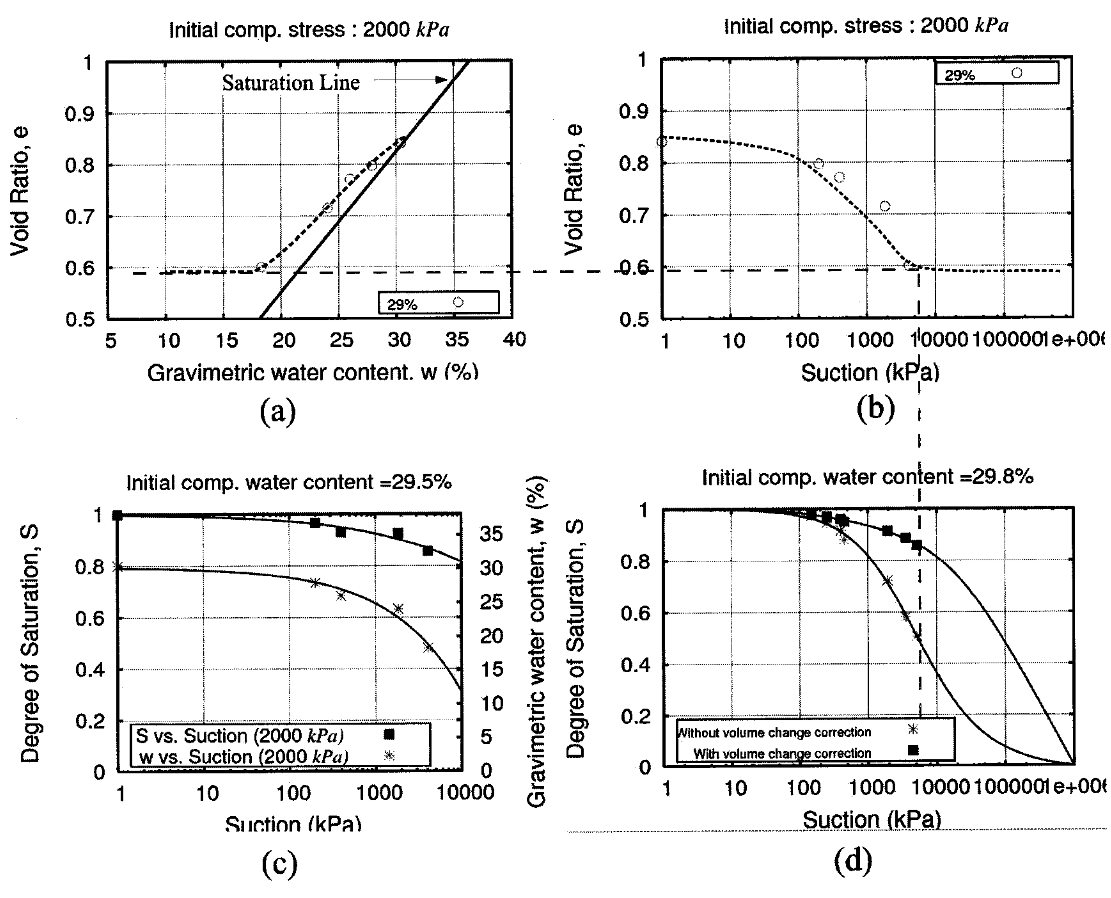

Figure 5.16: The drying path for the specimen compacted to 2000 kPa with an initial compaction water content 29.8%

Table 5.1: Effective stress equations for unsaturated soils

	Soil Type	G_s	CF^* (%)	w_L (%)	w_L (%)	Reference	USCS
1	Champlain sea clay	2.75	58	63	27	Author's results	CH
2	Selset clay	2.70	20	33	37	Bishop et al., (1964)	CL
3	Mangla Shale	2.79	21	38	21	"	CH
4	London clay	2.75	100	77	29	Marinho et al.,(1993)	CH
5	Clay/Sand mix.(1)	2.74	90	69	24	"	CH
6	Clay/Sand mix.(2)	2.72	70	54	19	"	MH
7	Clay/Sand mix.(3)	2.70	50	40	17	"	CL
8	Clay/Sand mix.(4)	2.69	30	24	18	"	CL
9	Grey clay	2.71	72	71	36	Jucá (1993)	MH
10	Gaudalix clay	2.66	35	33	19.4	"	CL
11	Clayey sand	2.64	6	28	20	"	CL
12	Soil B	n/a	40	49	26	Tinjum et al. (1997)	CL
13	Soil C	n/a	28	27	15	"	CL
14	Soil F	n/a	53	67	21	"	CH
15	Soil M	n/a	44	32	14	"	CL
16	Indian Head Till	2.72	30	35.5	16.68	Vanapalli et al. (1999)	CL

CF : Clay Fraction

Chapter 6

Conclusions and Recommendations

6.1 Conclusions

The following conclusions may be derived from the test results on the compacted Champlain sea clay:

- The type of compaction (i.e., static or dynamic compaction) has a considerable influence on the measured post-compaction suction values and the SWRC behavior of the compacted Champlain sea clay regardless of the initial compaction water content or the dry unit weight.

- The compaction effort is found to have marginal influence on the SWRC behavior the compacted Champlain sea clay as compared to the influence of initial compaction water content.

- The compaction curve along with the post-compaction suction contours provides valuable information about the stress state of the soil. The suction contours have negative slopes for the specimens compacted with water content values that are dry of optimum. The slope of the contours increases with an increase in the initial compaction water content. These contours may even possess positive slopes for the specimens compacted close to optimum or wet of optimum water contents based on the compressibility characteristics of the soil.

- The volume change (i.e., shrinkage) of the compacted specimens influences the SWRCs depending on the initial compaction water content. For the specimens compacted with water content values dry of optimum, the volume change with respect to suction has only a marginal effect. Whereas, for the specimens compacted at the wet of optimum, the volume change has a substantial effect on the SWRC behavior. As a result, the prediction or estimation of the engineering properties (i.e., for example unsaturated hydraulic conductivity function) should be conducted using the appropriate SWRC.

- It is found that the gravimetric water content versus suction relationship is predominantly governed by the clay hydration. Accordingly, the rate of desorption for compacted plastic soils can be estimated using liquid limit, w_L, and clay fraction CF.

- The technique proposed for estimating the drying portion of SWRC of compacted plastic soils using liquid limit, w_L, and clay fraction CF provided good comparisons between the measured and estimated SWRC for the soil studied in this research program and the soils present in the database.

- The psychrometer is found to give meaningful results for suction values starting from 400 kPa. The maximum suction value that was measured using this equipment 8541 kPa.

6.2 Recommendations for Further Research

Further research on the following topics related to the engineering behavior of compacted clay soils and the prediction methods are suggested:

- The compaction curve obtained by (static compaction method) along with the post-compaction suction values should also be determined for other types of compaction procedures (i.e., dynamic compaction and kneading).

- The estimation technique should be extended to incorporate additional factors such as stress history of the soil. The database should be expanded and categorized with respect to the compaction procedure and plasticity information.

- The SWRC relationship should be estimated in terms of degree of saturation versus suction taking account of volume change behavior using conventional properties and one measured data point of suction and degree of saturation.

Appendix A

Appendix

A.1 SWRCs of All the Compacted Specimens

This section includes the soil-water retention curves in terms of degree of saturation-gravimetric water content-suction.

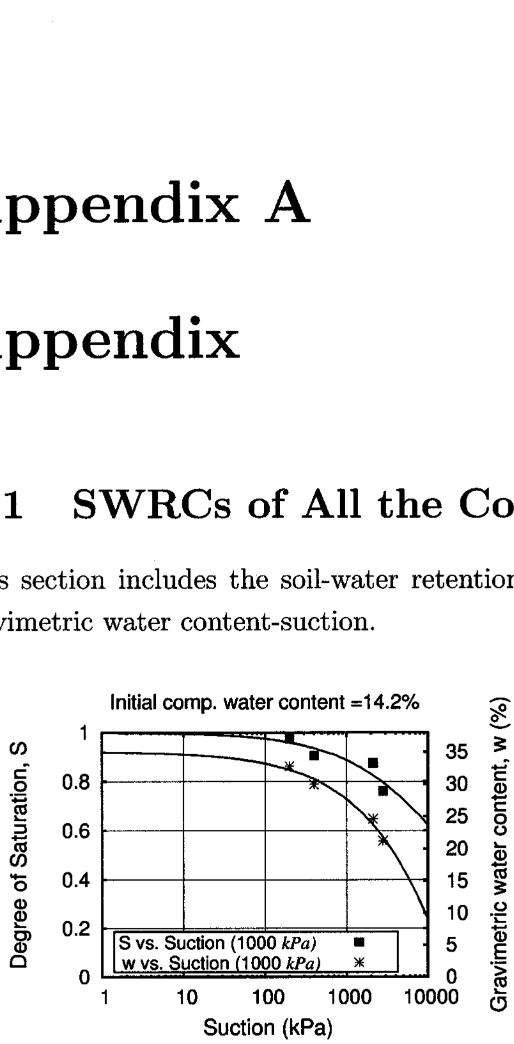

Figure A.1: SWRCs of the specimen compacted to 1000 kPa with an initial comp. water content 14.2%

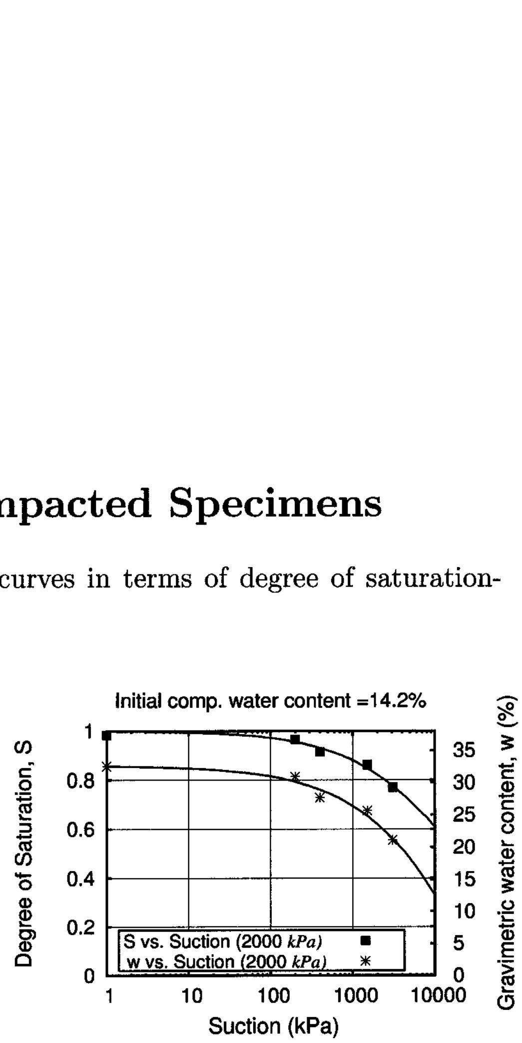

Figure A.2: SWRCs of the specimen compacted to 2000 kPa with an initial comp. water content 14.2%

A.2 Hydraulic Conductivity Test Results

This section includes the saturated and unsaturated hydraulic conductivity graphs.

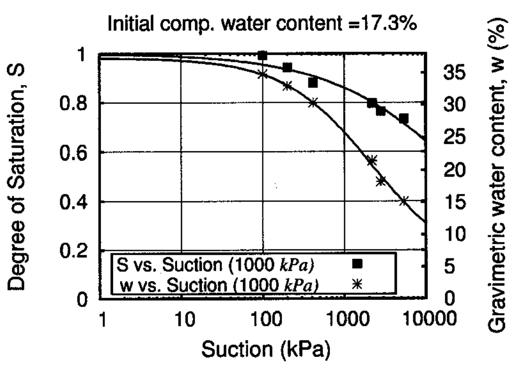

Figure A.3: SWRCs of the specimen compacted to 1000 kPa with an initial comp. water content 17.3%

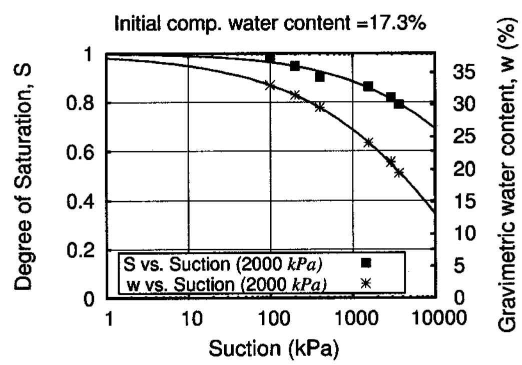

Figure A.4: SWRCs of the specimen compacted to 2000 kPa with an initial comp. water content 17.3%

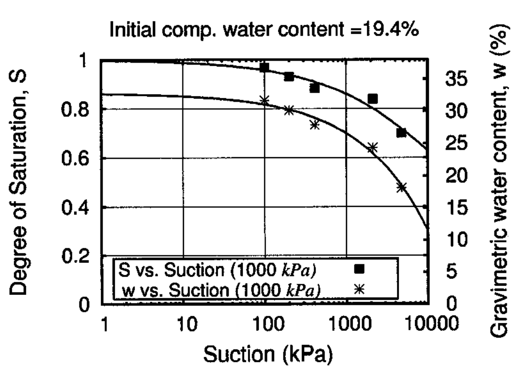

Figure A.5: SWRCs of the specimen compacted to 1000 kPa with an initial comp. water content 19.4%

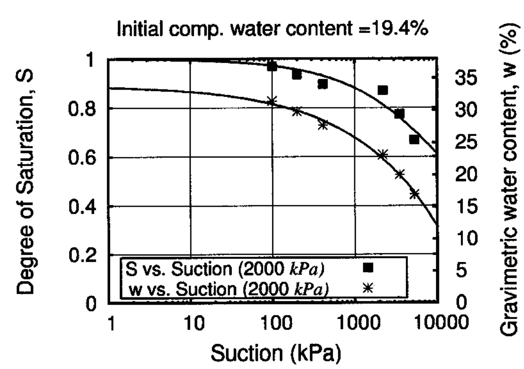

Figure A.6: SWRCs of the specimen compacted to 2000 kPa with an initial comp. water content 19.4%

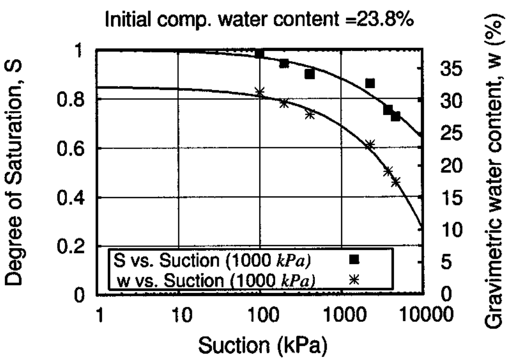

Figure A.7: SWRCs of the specimen compacted to 1000 kPa with an initial comp. water content 23.8%

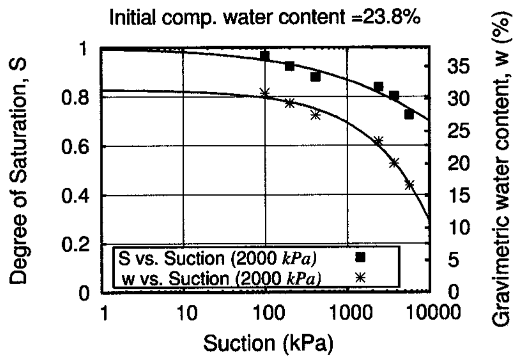

Figure A.8: SWRCs of the specimen compacted to 2000 kPa with an initial comp. water content 23.8%

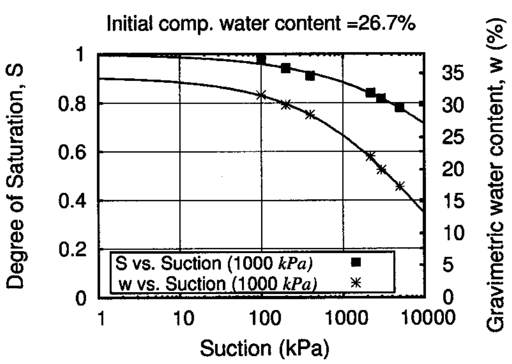

Figure A.9: SWRCs of the specimen compacted to 1000 kPa with an initial comp. water content 26.7%

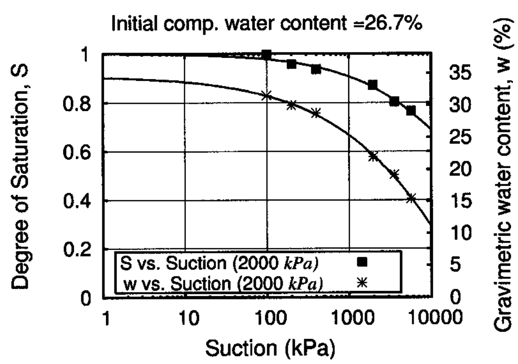

Figure A.10: SWRCs of the specimen compacted to 2000 kPa with an initial comp. water content 26.7%

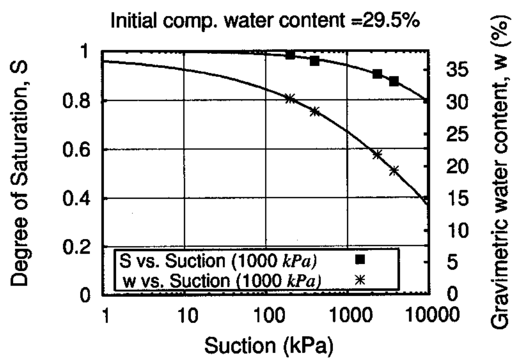

Figure A.11: SWRCs of the specimen compacted to 1000 kPa with an initial comp. water content 29.5%

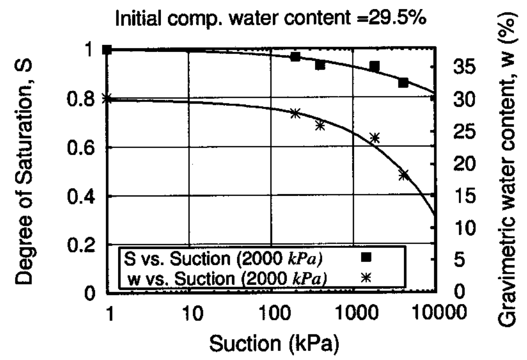

Figure A.12: SWRCs of the specimen compacted to 2000 kPa with an initial comp. water content 29.5%

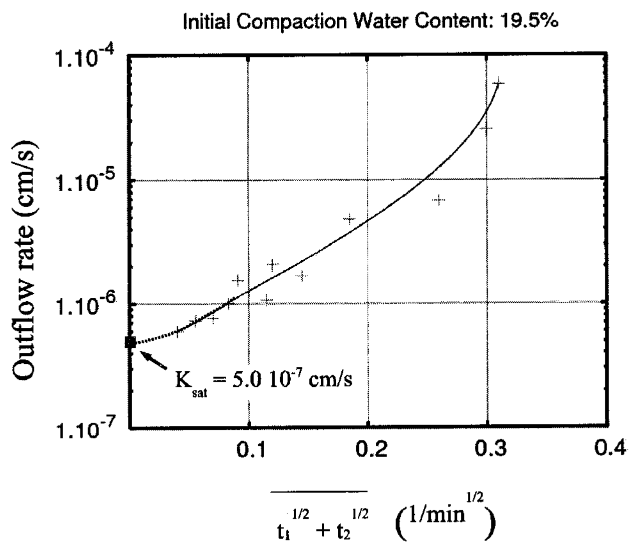

Figure A.13: The outflow data for the dry of optimum specimen

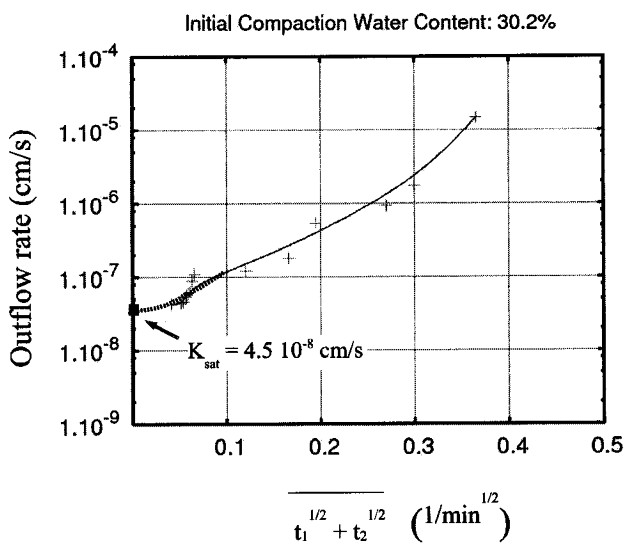

Figure A.14: The outflow data for the wet of optimum specimen

A.3 X-ray Diffraction Results

References

Abramento, M., & Carvalho, C.S. 1989. Geotechnical parameters for the study of natural slopes instabilization at Serra do Mar-Brazilian southeast. *Proceedings of the Twelfth International Conference on Soil Mechanics and Foundation Engineering*, 1599–1602.

Aitchison, D. G. 1961. Relationships of moisture stress and effective stress functions in unsaturated soils. *Pages 44–52 of: In Proceedings of the Conference on Pore Pressure and Suction in Soils, Butterworths, London.*

Al-Dhahir, Z.A., & Morgenstern, N.R. 1969. Intake factors for cylindrical piezometer tips. *Soil Science*, **107(1)**, 7–21.

Allam, M.M., & Sridharan, A. 1987. Stresses present in unsaturated soils. *Journal of Geotechnical Engineering*, **113**(11), 1395–1399.

Alonso, E.E., Gens, A., & Hight, D.W. 1987. Special problem soils. General Report. *In Proceedings of the 9th European Conference on Soil Mechanics and Foundation Engineering, Dublin, 31 August - 3 September. E.T. Hanrahan, T.L.L. Orr and T.F. Widdis (ed.). A.A. Balkema, Rotterdam.*, **3**, 1087–1146.

Arya, L.M., & Paris, J.F. 1981. A phsyico-empirical model to predict the soil moisture-characteristic from particle size distribution and bulk density data. *Soil Science Society of America Journal*, **45**, 1023–1030.

ASTM, D2216. 1994a. Laboratory determination of water (moisture) content of soil and rock by mass. *In Annual Book of ASTM Standards, American Society of Testing Material, Philadelphia, PA*, **4.08**, 177–180.

ASTM, D422. 1994b. Standard test method for particle size analysis of soils. *In Annual*

Book of ASTM Standards, American Society of Testing Material, Philadelphia, PA, **4.08**, 10–16.

ASTM, D698. 1994c. Test method for laboratory compaction characteristics of soils using standard effort. *In Annual Book of ASTM Standards, American Society of Testing Material, Philadelphia, PA*, **4.08**, 69–76.

ASTM, D854. 1994d. Standard test method for specific gravity of soils. *In Annual Book of ASTM Standards, American Society of Testing Material, Philadelphia, PA*, **4.08**, 80–83.

Attom, M. F. 1997. The effect of compactive energy level on some soil properties. *Applied Clay Science*, **12**, 61–72.

Aubertin, M., Mbonimba, M., Bussière, B., & Chapuis, R.P. 2003. A model to predict the water retention curve from the basic geotechnical properties. *Canadian Geotechnical Journal*, **40(6)**, 1104–1122.

Barbosa, P.S.A., de Lima, C.H.C. Silva D.C., & de Lima, L.C. 2002. A study of some factors influencing the soil-water retention curve. *Proceedings of the Third International Conference on Unsaturated Soils, UNSAT2002, Recife, Brazil.*

Barbour, S.L. 1998. The soil-water characteristic curve: a historical perspective. Nineteenth Canadian Geotechnical Colloquium. *Canadian Geotechnical Journal*, **35**, 873–894.

Basheer, I.A. 2000. Empirical modeling of the compaction curve of cohesive soils. *Canadian Geotechnical Journal*, **38**, 29–45.

Bell, J. R. 1977. Compaction energy relationships of cohesive soils. *Transportation Research Record*, **641**, 29–34.

Benson, C.H., & Gribb, M. 1997. Measuring unsaturated hydraulic conductivity in the laboratory and field. *Unsaturated Soil Engineering Practice, GSP No.68, S. Houston and D. Fredlund (eds.) ASCE, Reston, VA*, 113–168.

Bentley, S.P. 1979. Viscometric assessment of remoulded sensitive clays. *Canadian Geotechnical Journal*, **16**, 414–419.

Bishop, A. W., & Donald, I.B. 1961. The experimental study of partly saturated soil in triaxial apparatus. *In Proceedings of the Fifth International Conference on Soil Mechanics and Foundation Engineering, Paris*, **1**, 13–21.

Bishop, A.W. 1959. The principle of effective stress. *Teknisk Ukeblaud*, **106(39)**, 859–863.

Black, W.P.M. 1962. A method of estimating the California bearing ratio of cohesive soils from plasticity data. *Géotechnique*, **12(4)**, 271–282.

Blatz, J., & Graham, J. 2000. A system for controlled suction in triaxial tests. *Géotechnique*, **40**(4), 465–469.

Blight, G.E. 1967. Effective stress evaluation for unsaturated soils. *Journal of Soil Mech. & Fdns. Div., ASCE Proceedings*, **193**, 135–148.

Bouabdallah, A. 1998. *Contribution a l'etude du comportment mecanique des sols fortement desatures.* Ph.D. thesis, Ecole Centrale de Paris, Paris, France.

Bouma, J. 1982. Measuring the hydraulic conductivity of soil horizons with continous macropores. *Soil Sci, Soc. Am. J.*, **46**, 438–441.

Bouma, J., Hole, D. I., & Amerman, C.R. 1971. Field measurement of unsaturated soil hydraulic conductivity by infiltration through artificial crusts. *Soil Sci. Soc. Am. Proc.*, **35**, 362–364.

Boussinesq, M. J. 1876. Theoretical Essay on The Equilibrium of Elasticity of Pulverulent Masses and on The Pressure of Earths Without Cohesion. *Memoires Couronnes, Acad. R. Sci. Belg.*, **40(4)**.

Bozozuk, M. 1962. Soil shrinkage damages shallow foundations at Ottawa Canada. *The Engineering Journal*, 33–37.

Brackley, L.J.A. 1975. Model of unsaturated clay structure and its application to swell behavior. *Proceedings of 6th Reg. Conf. for Afr. on Soil Mech. and Found. Eng., Steel Times, Durban, South Africa.*, 71–79.

Brady, K. C. 1988. Soil suction and the critical state. *Géotechnique*, **38**(1), 117–120.

Brooks, R. H., & Corey, A. T. 1964. Hydraulic properties of porous media. *Colorado State University, Fort Collins, Colo. Hydrology Paper*, **3**.

Brown, R.W. 1970. Measurement of water potential with thermocouple psychrometers: Construction and applications. *Res. Paper INT-293. USDA Forest Serv., Ogden, UT.*

Brutsaert, W. 1966. Probability laws for pore size distributions. *Soil Science*, **101**, 85–92.

Buckingham, E. 1907. Studies on the movement soil moisture. *U.S. Department of Agriculture, Bureau of Soils-Bulletin, No.38.*

Bulut, R., Lytton, & Wray. 2001. Soil suction measurements by filter paper. *Proceedings of Geotechnical Special Publications. Expansive Clay Soils and Vegetative Influence on Shallow Foundations, ASCE*, **115**, 243–261.

Campbell, E. C., Campbell, G. S., & Barlow, W. K. 1973. A dewpoint hygrometer for water potential measurement. *Agric. Meteorol.*, **12**, 113–121.

Campbell, G. S. 1979. Improved Thermocouple psychrometers for measurement of soil water potential in a temperature gradient. *Journal of Phys. E: Sci. Instrum.*, **12**, 739–743.

Campbell, G.S., & Gardner, W. H. 1971. Pscyhrometric measurement of soil water potential: Temperature and bulk density effects. *Soil Sci. Soc. of Am. Proc.*, **35(1)**, 8–12.

Caruso, A., & Tarantino, A. 2004. A shearbox for testing soils from medium to high degrees of saturation. *Géotechnique*, **54(4)**(4), 281–284.

Côté, J., & Konrad, J.M. 2002. Assessment of the hydraulic characteristics of unsaturated base-course materials: a practical method for pavement engineers. *Canadian Geotechnical Journal*, **40(1)**, 121–136.

Chiasson, P. 2005. Methods of interpretation of borehole falling-head tests performed in compacted clay liners. *Canadian Geotechnical Journal*, **42**, 79–90.

Childs, E.C., & Collis-George, N. 1950. The permeability of porous materials. *Proceedings, Royal Society, London, Series A*, **210**, 392–405.

Croney, D., & Coleman, J.D. 1954. Soil structure in relation to soil suction (pF). *Journal of Soil Science*, **5(1)**, 75–84.

Croney, D., Coleman, J. D., & W.P.M.Black. 1958. Movement and distribution of water in relation to highway design and performance. *Highway Research Board Special Report*, **40**, 226–252.

Cui, Y.J. 1993. *Etude du comportement d'un limon compacté non saturé et de sa modélisation dans un cadre élastoplastique.* Ph.D. thesis, Ecole Nationale des Ponts et Chaussees, Paris, France.

Cui, Y.J., & Delage, P. 1996. Yielding and plastic behavior of an unsaturated compacted silt. *Géotechnique*, **46(2)**, 291–311.

Delage, P., & Lefebvre, G. 1983. Study of the structure of a sensitive Champlain clay and of its evolution during consolidation. *Canadian Geotechnical Journal*, **21**, 21–35.

Delage, P., Audiguier, M., Cui, Y.J., & Howat, M. 1996. Microstructure of a compacted silty clay. *Canadian Geotechnical Journal*, **33**, 150–158.

Delage, P., Howat, M.D., & Cui, Y.J. 1997. The relationship between suction and swelling properties in a heavily compacted unsaturated clay. *Engineering Geology*, **50**, 31–48.

Dineen, K. 1999. Evaporation from clay soils - Laboratory study. *12th African Regional Conference on Soil Mechanics & Geotechnical Engineering*, **1**, 88–93.

Donald, I.B. 1956. Shear strength measurements in unsaturated non-cohesive soils with negative pore pressures. *Proceedings of the Second Australia-New Zealand Conference on Soil Mechanics and Foundation Engineering*, 200–204.

Edil, T.B., & Motan, E.S. 1987. Laboratory evaluation of soil suction components. *Geot. Test. J.*, **7(4)**, 173–181.

Elsbury, B.R., Daniel, D.E., Sraders, G.A., & Anderson, D.C. 1990. Lessons learned from compacted clay liners. *Journal of Geotechnical Engineering*, **116(11)**, 1641–1660.

Fleureau, J.M., Verbrugge, J.C., Huergo, P.J., Correia, A.G., & Saoud, S.K. 2002. Aspects of the behavior of the compacted clayey soils on drying and wetting paths. *Canadian Geotechnical Journal*, **39**, 1341–1357.

Fredlund, D.G. 2000. The implementation of unsaturated soil mechanics into geotechnical engineering. The 1999 R.M. Hardy Lecture, 52nd Canadian Geotechnical Conference. *Canadian Geotechnical Journal*, **37(5)**, 963–986.

Fredlund, D.G. 2004. Use of soil-water characteristic curves in the implementation of unsaturated soil mechanics. *Proceedings of the Third International Conference on Unsaturated Soils, UNSAT2002, Recife, Brazil*, **3**, 887–901.

Fredlund, D.G., & Rahardjo, H. 1993. *Soil Mechanics for Unsaturated Soils.* John Wiley & Sons.

Fredlund, D.G., & Xing, A. 1994. Equation for the soil-water characteristic curve. *Canadian Geotechnical Journal*, **31**, 521–532.

Fredlund, D.G., Fredlund, M.G., & Wilson, G. W. 1997. Prediction of the soil-water characteristic curve from grain-size distribution and volume-mass properties. *3rd Brazilian symp. on unsaturated soils, Rio de Janeiro, Brazil*, 22–25.

Gallipoli, D., Gens, A., Sharma, R.S., & Vaunat, J. 2003. An elasto-plastic model for unsaturated soil incorporation the effect of suction and degree of saturation on mechanical behavior. *Géotechnique*, **53(1)**(4), 123–135.

Garga, V. K., & Zhang, H. 1997. Volume change in undrained triaxial tests on sands. *Canadian Geotechnical Journal*, **34**, 762–772.

Gee, G., Campbell, M., Campbell, G., & Campbell, J. 1992. Rapid measurement of low soil potentials using a water activity meter. *Soil Sci. Soc. of Am. Journal*, **56**, 1068–1070.

Gersovich, D.M.S., & Sayao, A.S.F.J. 2002. Evaluation of soil-water characteristic curve equations for soils from Brazil. *Proceedings of the Third International Conference on Unsaturated Soils, UNSAT2002, Recife, Brazil*, **1**, 295–301.

Gitirana, G.F.N. 2005. *Weather-related geo-hazard assessment model for railway embankment stability.* Ph.D. thesis, University of Saskatchewan.

Gupta, S.C., & Larson, W.E. 1979. Estimating soil water retention characteristics from particle size distribution, organic matter content, and bulk density. *Water Resources Research*, **15(6)**, 1633–1635.

Harrison, B.A., & Blight, G.E. 2000. The use of indicator tests to estimate the drying leg of the soil-water characteristic curve. *Proc. Asia Conf. on Unsaturated Soils, H. Rahardjo, D.G. Toll, and E.C. Leong (eds.), Singapore, Balkema, Rotterdam, The Netherlands*, 323–328.

Harvey, E. N., Barnes, D.K., McElroy, W. D., Whitely, A.H., Pease, D.C., & Cooper, K. W. 1944. *J. Cell. Comp. Physiol.*, **24**, 1–18.

Haverkamp, R., & Parlange, J.Y. 1986. Predicting the water retention curve from particle size distribution: 1.Sandy soils without organic matter. *Soil Science*, **142**, 325–339.

Hilf, J. W. 1956. *An investigation of pore-water pressure in compacted cohesive soils.* Ph.D. thesis, Technical Memorandum No.654, U.S. Department of the Interior, Bureau of Reclamation, Design and Construction Division, Denver, CO.

Houston, S., Houston, C., & Wagner. 1994. Laboratory filter paper suction measurements. *Geotechnical Testing Journal*, **17(2)**, 185–194.

Jennings, J. E. 1961. A revised effective stress law for use in the prediction of the behavior of unsaturated soils. *In Proceedings of the Conference on Pore Pressure and Suction in Soils, Butterworths, London*, 26–30.

Jucá, J.F.T. 1993. Flow properties of unsaturated soils under controlled suction. *Pages 151–162 of: Proceedings of the 1993 ASCE National Convention and Exposition, Dallas, TX, USA.*

Khalili, N., & Khabbaz, M.H. 1998. A unique relationship for the determination of the shear strength of unsaturated soils. *Géotechnique*, **48(5)**, 681–687.

Klute, A. 1986. Water retention: Laboratory methods. *In A. Klute (ed.) Methods of soil analysis. Part 1. 2nd ed. Agron. Monogr. 9. ASA and SSSA, Madison, WI.*

Krahn, J., & Fredlund, D.G. 1972. On total, matric and osmotic suction. *Journal of Soil Science*, **114(5)**, 339–448.

Lambe, T. W. 1958. The Engineering Behavior of Compacted Clays. *Journal of the Soil Mechanics and Foundation Division*, **84(1655)**, 1–35.

Lambe, T.W., & Whitman, R.V. 1979. *Soil Mechanics.* John Wiley & Sons.

Lee, H. C., & Wray, W. K. 1995. Techniques to evaluate soil suction - A vital unsaturated soil water variable. *Proceedings of the First International Conference on Unsaturated Soils, UNSAT95, Paris, France*, 615–622.

Leong, E. C., & Rahardjo, H. 2002. Factors affecting the filter paper method for total and matric suction measurements. *Geotechnical Testing Journal*, **123**, 321–332.

Leong, E.C., & Rahardjo, H. 1997. Review of soil-water characteristic curve equations. *Journal of Geotechnical and Geoenvionmental Engineering, ASCE*, **123(12)**, 1106–1117.

Likos, W. J., & Lu, N. 2002. Filter paper technique for measuring total soil suction. *Transportation Research Record: Journal of the Transportation Research Board*, **No. 1786, TRB Washington, DC**, 83–89.

Lu, N., & Likos, W. J. 2004. *Unsaturated soil mechanics.* John Wiley & Sons.

Luckner, L., van Genuchten, & Nielsen, D.R. 1989. A consistent set of parametric models for the two-phase flow of immiscible fluids in the subsurface. *Water Resources Research*, **25**, 2187–2193.

Maatouk, A., Leroueil, S., & Rochelle, P. La. 1995. Yielding and critical state of a collapsible silty soil. *Géotechnique*, **45(3)**(4), 465–477.

Marinho, F. 2005. Nature of soil-water characteristic curve for plastic soils. *Journal of Geotechnical and Geoenvironmental Engineering*, **131**, 654–661.

Marinho, F.A.M., & Chandler, R.J. 1993. Aspects of the behavior of clays on drying. *In: In Proceedings of ASCE National Convention.*

Marinho, F.A.M., & Chandler, R.J. 1995. Cavitation and direct measurement of soil suction, in unsaturated soils. *Proceedings of the First International Conference on Unsaturated Soils, UNSAT95, Paris, France*, 623–630.

Marshall, R. J. 1979. Analysis of fundamentals of compacted soils. *In Proceedings of 6th Pan-American Conference on Soil Mech. and Found. Eng, Lima, Peru.*, **3**, 328–338.

Marshall, T.J. 1958. A relation between permeability and size distribution of pores. *Journal of Soil Science*, **9**, 1–8.

Matyas, E.L., & Radhakrishna, H.S. 1968. Volume change characteristic of partially saturated soils. *Géotechnique*, **18(4)**, 432–448.

McCann, I.R., Kincaid, D.C., & Wang, D. 1992. Operational characteristics of the watermark model-200 soil water potential sensor for irrigation management. *Applied Engineering in Agriculture*, **8(5)**, 603–609.

McQueen, S.I., & Miller, R.F. 1974. Approximating soil moisture characteristics from limited data: Empirical evidence and tentative model. *Water Resour. Res.*, **10(3)**, 521–527.

Meerdink, J.S., Benson, C.H., & Khire, M.V. 1996. Unsaturated hydraulic conductivity of two compacted barrier soils. *Journal of Geotechnical Engineering*, **122(7)**, 565–576.

Millar, B.D. 1971. Improved thermocouple psychrometer for the measurement of plant and soil water potential. *Journal. Exp. Bot.*, **22**, 875–890.

Mitchell, J.K. 1993. *Fundamentals of soil behavior.* John Wiley & Sons.

Mitchell, P.W., & Avalle, D.L. 1984. A technique to predict expansive soil movement. *Proc. 5th Int. Conf. on Expansive Soils, Adelaide*, 124–130.

Mualem, Y. 1976. A new model predicting then hydraulic conductivity of unsaturated porous media. *Water Resources Research*, **12**, 513–522.

Neumann, H.H., & Thurtell, G.W. 1972. A Peltier cooled thermocouple dewpoint hygrometer for in situ measurement of water potentials. *In R.W. Brown and B.P. Van Haveren (ed.) Psycrometry in water relations research. Utah Agric. Exp. Stn., Utah State Univ., Logan, UT.*

Newland, P.L. 1965. The behavior of soils in terms of two kinds of effective stress. *Proceedings of the Conference on Expansive Clay Soils*, 78–92.

Ng, C.W.W., & Pang, Y.W. 2000. Influence of stress state on soil-water characteristics and slope stability. *Journal of Geotechnical and Geo-environmental En-gineering*, **126(2)**, 157–166.

Olson, R. E., & Langfelder, L. 1965. Pore water pressures in unsaturated soils. *Journal of the soil mechanics and foundations division*, **91**, 127–150.

Plagge, R., Roth, C. H., & Renger, M. 1992. A new laboratory method to rapidly determine the unsaturated soil hydraulic properties. *Proceedings of the International Workshop on Indirect Methods for Estimating the Hydraulic Properties of Unsaturated Soils, Riverside, CA, University of California*, 653–663.

Power, K. 2005. *The compressibility and suction characteristics of Indian Head till.* M.Phil. thesis, Univeristy of Ottawa.

Quigley, R.M. 1980. Geology, mineralogy and geochemistry of Canadian soft soils: a geotechnical perspective. *Canadian Geotechnical Journal*, **17**, 261–285.

Rahardjo, H., Chang, M. F., & Lim, T.T. 1995. Shear strength and in situ matric suction of a residual soil. *Pages 637–643 of: Proceedings of the first international conference on unsaturated soils*, vol. 2.

Rawlins, S.L., & Campbell, G.S. 1986. Water potential: Thermocouple psychrometry. *In A. Klute (ed.) Methods of Soil Analysis. Part 1. 2nd ed. Agron. Monogr. 9. ASA and SSSA, Madison, WI.*, 597–618.

Reddi, L.N., & Poduri, R. 1997. Use of liquid limit state to generalize water retention properties of fine-grained soils. *Géotechnique*, **47(5)**, 1043–1049.

Reynolds, W.D. 1993. Saturated hydraulic conductivity: Laboratory measurement. *In M.R. Carter (ed.) Soil sampling and methods of analysis. Lewis Publsihers, Boca Raton, FL.*, 589–598.

Richards, S. J. 1965. Soil suction measurements with tensiometers. *Methods of Soil Analysis, Part 1: Physical and Mineralogical Properties, Including Statistics of Measurement and Sampling*, 153–163.

Ridley, A. M., & Wray, W. K. 1995. Suction measurement: A review of current theory and practice. *Proceedings of the First International Conference on Unsaturated Soils, UNSAT95, Paris, France*, **3**, 1293–1322.

Romero, E., Gens, A., & Lloret, A. 1999. Water permeability, water retention and microstructure of unsaturated compacted Boom clay. *Engineering Geology*, **54**, 117–127.

Sanchez-Leal, F.J. 2002. Correlation of maximum density and optimum water content with index properties. *Proceedings of the Third International Conference on Unsaturated Soils, UNSAT2002, Recife, Brazil*, **2**, 647–652.

Schofield, R.K. 1935. The pF of water in soil. *Trans. of the 3rd international congress on soil science*, **2**, 37–48.

Sedano, Infante. 2006. *A modified ring shear test device for determining the hydro-mechanical behavior of unsaturated soils.* Ph.D. thesis, University of Ottawa.

Shuai, F., & Fredlund, D. G. 2000. Use of a new thermal conductivity sensor to measure soil suction. *ASCE GSP No.99*, 1–12.

Sibley, & Williams. 1990b. A new filter material for measuring soil suction. *Geotechnical Testing Journal*, **13(4)**, 381–384.

Sibley, J. W., Smyth, G. K., & Williams, D. J. 1990. Suction-moisture content calibration of filter papers from different boxes. *Geotechnical Testing Journal*, **13(3)**, 257–262.

Sillers, W.S., Fredlund, D.G., & Zakerzadeh, N. 2001. Mathematical attributes of some soil-water characteristic models. *Geotechnical and Geological Engineering*, **19**, 243–283.

Simms, P.H., & Yanful, E.K. 2002. Predicting soil-water characteristic curves of compacted plastic soils from measured pore-size distribution. *Geotechique*, **52(4)**, 269–278.

Simms, P.H., & Yanful, E.K. 2005. A pore-network model for hydromechanical coupling in unsaturated compacted clayey soils. *Canadian Geotechnical Journal*, **42**, 499–514.

Spanner, D. C. 1951. The peltier effect and its use in the measurement of suction pressure. *Journal of Experimental Botany*, **11**, 145–168.

Sridharan, A. 1968. *Some studies on the strength of partly saturated clays.* Ph.D. thesis, Purdue University.

Stormont, J.C., & Anderson, C.E. 1999. Capillary barrier effect of underlying coarse soil layer. *Journal of Geotechnical and Geoenvionmental Engineering, ASCE*, **125(8)**, 641–648.

Sugii, T., Yamada, K., & Condou, H. 2003. Evaluation of soil water characteristic curve of sandy soil using compaction energy. *In Proceedings of 2nd Asian Conference on Unsaturated Soils*, 445–450.

Tadepalli, R., & Fredlund, D.G. 1991. The collapse behavior of a compacted soil during inundation. *Canadian Geotechnical Journal*, **28**, 477–488.

Take, W. A., & Bolton, M.D. 2003. Tensiometer saturation and the reliable measurement of soil suction. *Géotechnique*, **53**, 159–172.

Tarantino, A., & Mongiovi, L. 2003. Calibration of tensiometer for direct measurement of matric suction. *Géotechnique*, **53(1)**, 137–141.

Tarantino, A., & Tombolato, S. 2005. Coupling of hydraulic and mechanical behaviour in unsaturated compacted clay. *Géotechnique*, **55**(4), 307–317.

Tarantino, A., Mongiovi, L., & Bosco, G. 2000. An experimental investigation on the independent isotropic stress variables for unsaturated soils. *Géotechnique*, **50(3)**, 275–282.

Tavenas, F., Chapeau, C., & nad M. Roy, P. La Rochelle. 1974. Immediate settlements of three embankments on Champlain clay. *Canadian Geotechnical Journal*, **11**, 109–141.

Tinjum, J.M., Benson, C.H., & Blotz, L.R. 1997. Soil-water characteristic curves for compacted clays. *Journal of Geotechnical and Geoenvironmental Engineering*, **123(11)**, 1060–1069.

Toll, D. G. 2000. Influence of fabric on the shear behavior of unsaturated compacted soil. *Geotechnical Special Publication*, **99**, 222–234.

Torrance, J.K. 1999. Physical, chemical and mineralogical influences on the rheology of remoulded low-activity sensitive marine clay. *Applied Clay Science*, **14**, 199–223.

Tyler, S.W., & Wheatcraft, S.W. 1990. Fractal processes in soil water retention. *Water Resources Research*, **26(5)**, 1047–1054.

van Genuchten, M. T. 1980. A closed-form equation for predicting the hydraulic conductivity of unsaturated soils. *Soil Science Society of America Journal*, **44**, 892–898.

van Genuchten, M. Th., & Nielsen, D.R. 1985. On describing and predicting the hydraulic properties of unsaturated soils. *Annual Geophsyicae*, **3**, 615–628.

Vanapalli, S. K., Fredlund, D. G., & Pufahl, D. E. 1999. The influence of soil structure and stress history on the soil-water characteristic curve of a compacted till. *Géotechnique*, **49(2)**, 143–159.

Vanapalli, S.K., & Catana, M.C. 2005. Estimation of the soil-water characteristic curves of coarse-grained soils using one point measurement and simple properties. *Pages 401–410 of: Proceedings of an International Symposium on Advanced Experimental Unsaturated Soil Mechnanics.*

Vanapalli, S.K., Fredlund, D.G., & Pufahl, D.E. 2001. Influence of soil structure and stress history on the soil-water characteristics of a compacted till. *Géotechnique*, **LI(6)**, 573–576.

Vanapalli, S.K., Salinas, L.M., Avila, D., & Karube, D. 2004. Suction and storage characteristics of unsaturated soils. *Proceedings of the Third International Conference on Unsaturated Soils, UNSAT2002, Recife, Brazil*, **3**, 1045–1070.

Vereecken, H., Diels, J., van Orshoven, J., Feyen, J., & Bouma, J. 1992. Functional evaluation of pedotransfer functions for the estimation of soil hydraulic propertie. *Soil Science Society of America Journal*, **56**, 1371–1378.

Wan, A.W.L., Gray, M.N., & Grahan, J. 1995. On the relations of suction, moisture content, and soil structure in compacted clays. *Proceedings of the First International Conference on Unsaturated Soils, UNSAT95, Paris, France*, **1**, 215–222.

Wang, X., & Benson, C.H. 2003. Leak-free pressure plate extractor for measuring the soil water characteristic curve. *Geotechnical Journal*, **27(2)**, 1–10.

Warren, B.E. 1969. *X-ray Diffraction.* Addison-Wesley, Reading, MA.

Wescor, Inc. 1998. Water potential systems. *Wescor, Logan, UT.*

Wheeler, S.J., & Karube, D. 1995. State of the art report. Constitutive modelling. *Proceedings of the First International Conference on Unsaturated Soils, UNSAT95, Paris, France*, **3**, 1323–1356.

Wheeler, S.J., & Sivakumar, V. 1995. An elastoplastic critical state framework for unsaturated soils. *Géotechnique*, **45(1)**, 35–53.

Wiebe, H. H. 1981. Measuring water potential (activity) from free water oven dryness. *Plant Physiol.*, **68**, 1218–1221.

Wiebe, H.H., Campbell, G.S., Gardner, W.H., Rawlins, S.L., Cary, J.W., & Brown, R. W. 1971. Measurement of plant and soil water status. *Utah Agric. Exp. Stn. Bull. 484, Utah State Univ. Logan, UT.*

Williams, Thomas, Kelley, Collin, & many others. 2004. Gnuplot: An open source plotting program. *Open Source.*